Synthesis, Processing and Characterization of Nanostructured Conducting Materials

by

Zhen Liu

A dissertation submitted to the Graduate Faculty of
Auburn University
in partial fulfillment of the
requirements for the Degree of
Doctor of Philosophy

Auburn, Alabama
May 7th, 2012

Keywords: Conducting polymers, nanocarbons, microwave, nanocomposites

Approved by

Xinyu Zhang, Committee Chair, Assistant Professor of Polymer and Fiber Engineering
Peter Schwartz, Professor and Head of Polymer and Fiber Engineering
Sabit Adanur, Professor of Polymer and Fiber Engineering
Wei Zhan, Assistant Professor of Chemistry and Biochemistry

Abstract

Several novel synthesis approaches target to precisely control the nano-structures of electric organic polymers have been studied and these methods can afford to yield nanostructured electric organic polymers, (i) conducting polymer nanoclips by using reactive template method, i.e., “oxidative template” approach; (ii) conducting polymer/transition metal nanocomposites by “seeding approach”. Usually conducting polymers like polyaniline, polypyrrole, poly-3, 4-ethylenedioxythiophene (PEDOT) are oxidative polymerized by corresponding monomers using $(NH_4)_2S_2O_8$ (APS) as the oxidant. It is of technological importance to construct “oxidative template” by oxidant APS and surfactant chemical to form nano-precipitation templates which can confine the lattice oriented growth while offering oxidization property for further polymerization. Furthermore, after examining the oxidation potential of different reaction media, i.e., metal salts’ aqueous electrolyte solutions, it is found a novel, facile, one-step and seed-assisted oxidative polymerization reactions can help produce one dimensional conducting polymer with decoration of transitional metal nanoparticles.

Microwave irradiation approach “Poptube” has been emerged as a novel approach and used as a robust tool to promote ultrafast carbon nanotube (CNT) growth by using conducting polymer as heating source and metallocene as precursors. This solid state microwave reaction of great engineering importance, does not require any additional inert

gas protection while can yield only CNTs growth at room temperature in air with only 15–30 seconds.

Acknowledgments

I would like to express all my sincere gratitude to my supervisor, Prof. Xinyu Zhang. He has been providing great guidance and support throughout the whole period of my Ph.D. study in all aspects. His enthusiasm, his inspiration as well as his deep thinking have been of great value for me. His encouragement, his good teaching and his sound advice have enabled me to carry on the research smoothly and rewardingly. With his support, I had numerous opportunities to present my works in conferences or collaborate research groups, which benefit me a lot.

I am very grateful to Prof. Sabit Adanur. He was the instructor of my two core courses and one of the best teachers that I have ever seen. In addition, as my preliminary examination and defense committee member, his valuable insights played a very important role in solidifying my research focus. I also deeply appreciate the enlightening guidance from Prof. Peter Schwartz for many fruitful discussions during my visits to him. Special thanks to Prof. Wei Zhan for serving as my committee and providing so many insightful ideas and suggestions.

I spent a wonderful time during my Ph.D. study in Auburn. Appreciation is expressed to all my Auburn advisors and colleagues.

Finally, I would like to address my deepest gratitude to my beloved parents Mrs Lanling Meng and Dr. Mingzhu Liu, and my dear fiancée Ms. Chenzi Wang for their continuous support and sincere love throughout my study.

Table of Contents

List of Tables

List of Figures

Chapter 1.

INTRODUCTION and LITERATURE REVIEW

1.1. Introduction

The early definition of nano-scale materials is originated from ancient Greek prefix "nano-" which means one-billionth. Nanometer is described as one-billionth of one meter. People start to realize "There's Plenty of Room at the Bottom" by 1959 under the scientific prediction of Dr. Richard P. Feynman, a "virtual design" of an instrumentation that would allow the writing of small image on a tiny pinhead, which has already been achieved by 1984 after the invention of first scanning probe microscope.

In recent advances and development of materials science and engineering, great attentions and endeavors have been devoted to the concept of "nanomaterials", i.e., new materials with ultra small dimensions lead to the novel properties like ultra precise catalytic behaviors and enhanced functionalities. As is motivated by the emerging superior performances of nanomaterials to its bulk counterpart, e.g. electrical, mechanical, catalytic and optical, current nanomaterials based research are centered with the processing and fabrication of various substances that structured within 1 to 100 nm size range by chemical and physical methods. Due to the quantum effects such as finite size effect, quantum effect and filler-size effect, etc., the miniaturized metallic, carbon allotrope and electric organic polymer materials as nano-building blocks have potential to strategically control crystal

defects, band gap, energy states and surface behavior. In historical aspect, the transition has been seen over last three decades that the production of electric materials, such as conducting polymers, carbon allotrope and metal particles, from the originally as-discovered bulky features under micrometer scale to ultra-small textures in the nanoscale regime. newly These emerged nanostructures of these conventional materials with novel properties and functions have undebatably initiated greater and greater technological advances in science, engineering and technology, which benefit human society in many aspects, such as medical science, electrical industry, civil engineering, etc. [1]

Considerable development of metallic nanocrystal, semiconducting inorganic nanomaterials and magnetic nanoparticles have lead to the exciting industrialization of metallic based nanomaterials production, which have being advanced the current chemical and environmental engineering in much deeper and broader level. However, the exploration of electric organic polymer materials, appears comparatively not as satisfactory as the other materials. Actually past industry development experience has already foreseen that polymer nanomaterials can afford to serve as a much broader platform with a variety of advantages over all other materials, e.g., wide accessibility, ease of process, high surface area and band gap tunability which will lead to advanced functionalities. [1]

Among all synthetic polymer nanomaterials, conducting polymers have become the leading actor ever since the discovery of high conductivity polyacetylene in 1976. Chemist Hideki Shirakawa, physicist Alan J. Heeger and chemist Alan G MacDiarmid, discovered in 1976 that oxidation of acetylene by iodine results in a 10^8

Figure 1.1. Nobel laureates: Alan J. Heeger, Alan G. MacDiarmid and Hideki Shirakawa (Year 2000)

fold increment in polyacetylene conductivity. Iodine doped polyacetylene is able to reach the conductivity of silver, which is one of the best readily available conductor. Based on this revolutionary discovery, the three were awarded the Nobel Prize in Chemistry in 2000 and therefore open new doors to the exploration of electric organic polymers development.

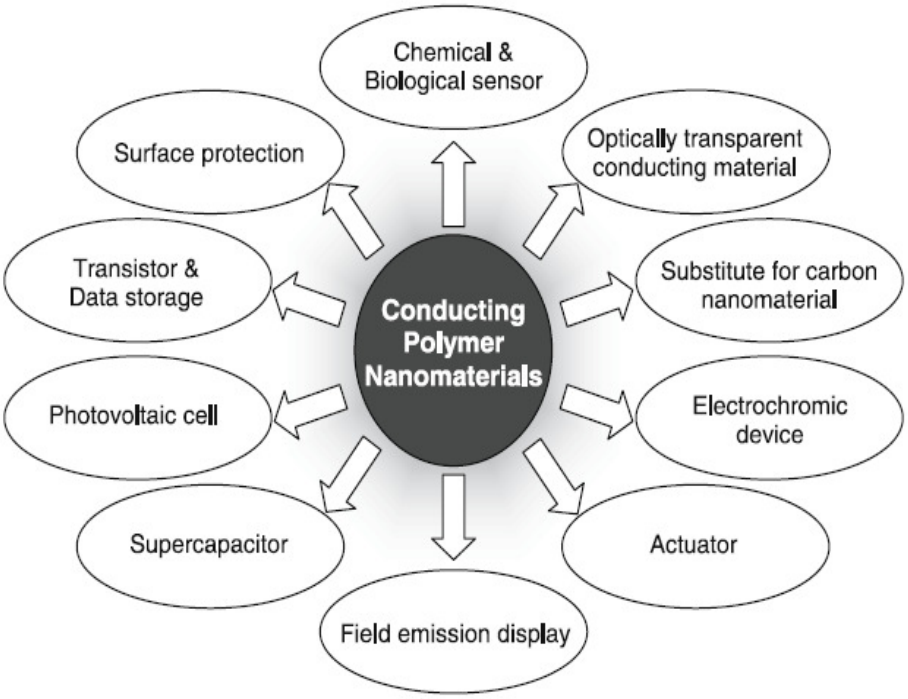

Figure 1.2. Applications of conducting polymer nanomaterials[1]

There is a number of conducting polymers, from which, this dissertation has selected and focused on three major members, namely, polyaniline (PANI), polypyrrole (PPy), poly-3, 4-ethylenedioxythiophene (PEDOT). The generic synthetic approach has been adopted is chemical oxidation polymerization, extensive research have been conducted on the physical and chemical properties with precisely engineered on molecular and atomic dimensions. They are able to serve as nano-building blocks for new generation chemical and biological sensors, due to the inherent reversible doping-dedoping mechanism, leading to the particular transition of conductivities, colors and specific capacitance. Newly emerging sensors, in forms of PANI nanofiber, PPy nanotube and PEDOT nanfiber, etc. have fallen into the category of humidity sensor,[2] gas senor,[3] enzymatic sensor[4] and toxic chemical noses.[5]

1.2. Objectives

The goal of this dissertation targets on the main synthesis strategies and characterization approaches of (i) nanostructured conducting polymer nanoclips including polyaniline, polypyrrole, poly-3, 4-ethylenedioxythiophene (PEDOT) nanoclips; (ii) green nano approach to polypyrrole nanofibers; (iii) nanostructured polymer-transition metallic fiber nanocomposites by polypyrrole and a number of transition metals: Pt, Au, Ag and Cu; meanwhile introducing the recently established novel approach of (iv) microwave initiated ultrafast carbon nanotube growth, in great details.

1.3. Chapter Arrangement

This dissertation consists of six chapters. Chapter 1 is the introduction of the topic background, objectives and literature review about electric conducting nanomaterials including conducting polymer nanoclips, nanofibers and conducting polymer/transition metal nanocomposites and carbon nanotubes that grown from microwave chemistry. Chapters 2 to 4, introduce and explain in details about four projects: (i) "oxidative template assembly" approach to nanostructured conducting polymer nanoclips including polyaniline, polypyrrole, poly-3, 4-ethylenedioxythiophene (PEDOT) nanoclips; (ii) green nano approach to polypyrrole nanofibers; (iii) nanostructured polymer-transition metallic fiber composites by polypyrrole and a number of transition metals: Pt, Au, Ag and Cu; (iv) microwave initiated ultrafast carbon nanotube growth. Each chapter includes introduction, experimental, results and discussion, and conclusion parts. Chapter 5 is the conclusions and future works.

1.4. Literature Review

1.4.1. Nanostructured conducting polymers

Conducting polymers, such as polyaniline, polypyrrole, poly(3,4-ethylenedioxythiophene (PEDOT), and polythiophene etc., have drawn many new technological applications, e.g., organic light-emitting devices,[6] rechargeable batteries,[7-10] electrochromic displays,[11-13] plastic electronic circuits.[14-16] These polymers are commonly prepared by chemical oxidative polymerization of the monomer (aniline, pyrrole, etc.) in aqueous solution containing an oxidant such as ammonium peroxydisulfate.[17,18] The reaction belongs to a class of precipitation polymerization reactions, where the bulk of the polymer

precipitates out of the aqueous phase over a very short period of time. This results in the polymers having anirregular-shaped particulate morphology.[17-19]

We have recently described the synthesis of bulk quantities of nanostructured conducting polymers in one step, directly from the monomer with control of bulk nanoscale polymer morphologies. The techniques include "nanofiber seeding" and "sacrificial template" approaches to synthesize nanofiber and nanotubes of conducting polymers. Nanofiber seeding method provides precise control of the morphology of the product, e.g., we can synthesize bulk quantities of nanofibers of polyaniline,[19] polypyrrole,[20] poly-(3,4-ethylene dioxythiophene) (PEDOT),[21] etc., in one step without requiring large organic dopants, surfactants, and/or bulk quantities of insoluble templates.Seeding a conventional chemical oxidative polymerization of the monomers with even very small amounts of nanofiber seeds (usually <1%) dramatically changes the morphology of the resulting doped conducting polymers powders from non-fibrillar (particulate) to almost exclusively nanofibers. As to the sacrificial template method,[22] V_2O_5 sol-gel nanofibers were used as the template toward synthesis of conducting polypyrrole nanotubes. In this process, stoichiometric amount of V_2O_5 sol-gel nanofibers were used to guide the growth of polypyrrole as coating on the template, which will be removed by post-synthesis step, such as rinse with 1M HCl.

1.4.2. Microwave initiated ultrafast carbon nanotube growth

Carbon materials have a long history ever since human started using charcoal. Nanocarbons are a group of carbon materials with one of the dimensions less than 100 nm. The discovery of novel nanocarbon materials, including fullerene, carbon nanotubes (CNT), single layer graphene (SLG) sheet and other nanocarbons has greatly stimulated the interest

of scientists and engineers in carbon materials during the last two decades. As a rapidly growing class of soft electronic materials, different synthetic approaches were applied to nano-sized carbon fibers using pitch-based precursors,[23]and tubular structured nanocarbons using inorganic templates.[24] Among different type of nanocarbons, the fullerene family has received the most attentions.

Graphene is now the rising star in this family. Especially after the announcement of the Nobel Prize in physics in year 2010, SLG sheet made from scotch tape approach has become the center focus in nanocarbon materials,[25] which was one of the strongest materials ever tested as of 2009.[26] SLG also possesses even better thermal and electrical conductivities than CNTs, because of the unique flat structures. There are many different ways to produce SLG such as drawing method,[25] epitaxial growth on silicon carbide,[27] and graphite oxide reduction.[28] However, the research in this SLG is still in its early stage.

Comparing to SLG, CNT has already been developed for the last two decades, since Iijima discovered multi-walled CNTs, a new class of allotrope of carbon.[29] CNT related research has been one of the most popular fields, due to the superior mechanical, thermal and electrical properties. CNT has demonstrated a wide selection of applications in composite materials,[30] smart structures,[31] chemical sensors,[32] energy storage[33] and nano-electronic devices.[34] There are three major techniques to produce CNTs, including arc-discharge,[35] laser ablation[36] and chemical vapor deposition (CVD)[37]. These techniques normally require vacuum or inert gas protection, high temperature and/or high atmospheric pressure. Among the three, CVD has the most derivatives such as the conventional thermal CVD, microwave plasma assisted CVD (MPCVD), and Plasma-Enhanced CVD (PECVD). The sophisticated procedures and instruments needed for CNT production make the cost of as-produced CNT

remains high. In addition, the poor solubility/dispersibility is another factor that limits the application of CNT.[38]

1.4.2.1. Microwave Chemistry

Microwaves are defined as electromagnetic waves with wavelengths ranging from 1 mm to 1 m, or frequencies between 0.3 GHz and 300 GHz. Microwave heating has been widely recognized and used for industrial, scientific and medical purposes, since it possesses higher energy efficiency comparing to conventional thermal heating. The most popular frequencies for microwave ovens are 0.915 GHz, 2.45 GHz, and 5.8 GHz, etc., out of which 2.45 GHz (corresponds to a wavelength of 12.24 cm) is available worldwide, to avoid interference with wireless communications and cell phone frequencies.

1.4.2.2 Microwave Heating Insulators

When microwave irradiation is applied to materials, a corresponding electric field interacts with these materials, and various responses may take place, depending upon the electrical conductivity and the nature of the materials. For an insulator, electrons do not move easily, but electronic reorientation or distortions of induced or permanent dipoles can cause heating of the materials.[39] For example, in most of our daily applications in households and the research laboratories, the microwave is used to heat the insulators, such as the water molecules in food, or organic solvents and reagent molecules, which are called dielectric heating. Water molecule is a typical example with permanent dipoles due to its asymmetrical molecular structure. If there is no external electric field, the dipoles in water molecules are randomly oriented, and the net macroscopic polarization vector is zero.[39] The

dipoles of water molecules will align with the field in the presence of a static electric field, and the macroscopic polarization vector is maximized. These dipoles of the water molecules can rotate, but these rotationsare against a friction force. As the frequency of the electric field increases, e.g., 2.45 GHz for microwave, the dipoles are undergoing a rapid switching electric field, which results in rearrangements of the molecular dipoles in the field and quick rotations of the molecules, but not precisely following the alternating field.[40,41] As the water molecules rotate, they bump other molecules in the food to make them move randomly. The process is similar to frictional heating caused by collisions of molecules and atoms. The same thing happened to the organic synthesis, due to the similarity of water to many other organic solvents and reagents in terms of polarity and insulation.

1.4.2.3 Microwave Heating Conductors

The microwave and conductor interaction is more complicated. In a conductor, electrons will move with much more freedom in the materials comparing to an insulator in the presence of the external electric field. The moving electrons, or the current flow through the conductors, will generate heat in material through resistive heating, if the material is not a superconductor.[39]

Meanwhile, there are several parameters that affect the microwave heating of conductors. Electronic conductivity is one of the most important factors in metallic and semiconducting materials.[39] Experimental data demonstrated that the materials with moderate conductivity (10^{-5}~10Ω•m) heat more efficiently than insulating or highly conducting materials.[39,42,43] Dimension is another important factor. For a thick metallic conductor, the microwave irradiation can be reflected in most of the cases due to the skin

effects, while the thin conductors have a lot less reflection than the thick ones, since the skin depth is larger than the dimension of the sample, thickness or diameter etc.[44]

1.4.2.4 Microwave Chemistry in Nanomaterials

There is a wide selection of techniques to produce nanomaterials, such as self-assembly,[45,46]electro-spinning for nanofibers and nanotubes,[47,48] electro-spraying for nanoparticles,[49]templated growth using track-etched membranes,[50] surfactants,[18] polymers[51] and zeolites[52].Some of the reactions can be carried out at room temperature, but some of those need to be performed under elevated temperatures to initiate the reactions, which can be achieved by conventional volumetric heating, or microwave heating. The conventional volumetric heating was suffering with target-less, low efficient heat transfer from the heating sources to the reagents. However, microwave irradiation is working on each of the individual molecules, and providing more homogeneous but selective heating process.

A variety of nanomaterials with different morphologies have been synthesized through microwave heating approach, such as nanorods,[53] nanowires, nanofibers,[54,55] nanotubes,[44] nanosheets[56] and nanoparticles.[57-59] The function of the microwave irradiation in these processes is mainly to initiate dielectric heating of the reaction media. For example, Zhu *et al*has successfully demonstrated tellurium nanorods can be synthesized using ionic liquid or water as the solvent.[53]Nanorods, nanoparticles or nanowires may be produced depending on different experimental conditions, e.g.,different solvents, reaction periods, and temperatures. And Gerbec*et al* reported microwave dielectric heating can be used to enhance the rate of nanoparticle formation, the quality of the product and the size distributions, through a selection of solvents, such asoctadecene and decane.[60]

1.4.2.5 Microwave Initiated Synthesis of Nanocarbon Materials

The production of nanostructured carbon materials often requires high temperature,[61,62] high pressure[63] and high current[64]density processes, or in another words, it is an energy intensive process. The process temperature can be as high as 800-900ºC[61] in a thermal CVD approach, when producing sea urchin-like nanocarbons. Sometimes even higher temperature (> 1000ºC[62])can be used to produce iron filled nanocarbon spheres. In HiPCo and arc discharge approaches to single walled carbon nanotubes, high pressure[65] and high current density[64] are always required. As a common practice, at this level of energy intensity, inert gas protection is always a must to prevent carbon elements being oxidized by the harsh experimental conditions. It's not very usual to see nanocarbon production under standard condition for temperature (20°C) and pressure (101.325 KPa, 1 atm), which is defined by National Institute of Standards and Technology (US).Due to its uniqueness of the heating process, microwave offers the opportunity to initiate the nanocarbonization process at room temperature, in the air with atmospheric pressure. Since microwave chemistry in dielectric heating to produce organic compounds[66] and inorganic nanomaterials[67] has been extensively reviewed and discussed, we will focus more in the studies about microwave initiated carbonization process by irradiating conducting materials, instead of insulating materials. Although the methodologies in this direction are still under investigation, with much fewer published reports, there is great opportunity and potential in leading to newly designed advanced materials, and novel manufacturing systems.

1.5. References

(1) Jang, J. *Adv Polym Sci* **2006**, *199*, 189.

(2) Mahadeva, S. K.; Yun, S.; Kim, J. *Sensor Actuat a-Phys* **2011**, *165*, 194.

(3) Park, E.; Kwon, O. S.; Park, S. J.; Lee, J. S.; You, S.; Jang, J. *J Mater Chem* **2012**, *22*, 1521.

(4) Kausaite-Minkstimiene, A.; Mazeiko, V.; Ramanaviciene, A.; Ramanavicius, A. *Biosens Bioelectron* **2010**, *26*, 790.

(5) Gursoy, S. S.; Uygun, A.; Tilki, T. *J Macromol Sci A* **2010**, *47*, 681.

(6) Choi, J. H.; Kim, J. Y.; Kim, M.; Kim, H. M.; Joo, J. *Opt Mater* **2003**, *21*, 147.

(7) Chen, R. J.; Wu, F.; Chen, J. Z.; Wu, S. X.; Li, L.; Chen, S.; Zhao, T. *J. Phys. Chem. C* **2011**, *115*, 6057.

(8) Posudievsky, O. Y.; Kozarenko, O. A.; Dyadyun, V. S.; Jorgensen, S. W.; Spearot, J. A.; Koshechko, V. G.; Pokhodenko, V. D. *J. Power Sources* **2011**, *196*, 3331.

(9) Suresh, G. S.; Manjunatha, H.; Venkatesha, T. V. *J. Solid State Electrochem.* **2011**, *15*, 431.

(10) Huang, Y. H.; Chen, W. M.; Qie, L.; Yuan, L. X.; Xia, S. A.; Hu, X. L.; Zhang, W. X. *Electrochimica Acta* **2011**, *56*, 2689.

(11) Dyer, A. L.; Amb, C. M.; Reynolds, J. R. *Chem. Mater.* **2011**, *23*, 397.

(12) Andersson, P.; Forchheimer, R.; Tehrani, P.; Berggren, M. *Adv. Funct. Mater.* **2007**, *17*, 3074.

(13) Reynolds, J. R.; Witker, D. *Macromolecules* **2005**, *38*, 7636.

(14) Son, Y.; Hwang, Y. S.; Lee, Y. *Mol. Cryst. Liq. Cryst.* **2007**, *472*, 503.

(15) Parashkov, R.; Becker, E.; Riedl, T.; Johannes, H. H.; Kowalsky, W. *P Ieee* **2005**, *93*, 1321.

(16) Forrest, S. R.; Moller, S.; Perlov, C.; Jackson, W.; Taussig, C. *Nature* **2003**, *426*, 166.

(17) Zhang, X.; Chan-Yu-King, R.; Jose, A.; Manohar, S. K. *Synthetic Met* **2004**, *145*, 23.

(18) Zhang, X.; Manohar, S. K. *Chem Commun* **2004**, *20,*, 2360.

(19) Zhang, X.; Goux, W. J.; Manohar, S. K. *Journal of the American Chemical Society* **2004**, *126*, 4502.

(20) Zhang, X.; Manohar, S. K. *Journal of the American Chemical Society* **2004**, *126*, 12714.

(21) Zhang, X.; MacDiarmid, A. G.; Manohar, S. K. *Chem Commun* **2005**, *42*, 5328.

(22) Zhang, X.; Manohar, S. K. *Journal of the American Chemical Society* **2005**, *127*, 14156.

(23) Park, S. H.; Kim, C.; Jeong, Y. I.; Lim, D. Y.; Lee, Y. E.; Yang, K. S. *Synthetic Met* **2004**, *146*, 207.

(24) Kruk, M.; Dufour, B.; Celer, E. B.; Kowalewski, T.; Jaroniec, M.; Matyjaszewski, K. *Journal of Physical Chemistry B* **2005**, *109*, 9216.

(25) Novoselov, K. S.; Geim, A. K.; Morozov, S. V.; Jiang, D.; Zhang, Y.; Dubonos, S. V.; Grigorieva, I. V.; Firsov, A. A. *Science* **2004**, *306*, 666.

(26) Lee, C.; Wei, X.; Kysar, J. W.; Hone, J. *Science* **2008**, *321*, 385.

(27) Sutter, P. *Nature Materials* **2009**, *8*, 171.

(28) Eswaraiah, V.; Jyothirmayee Aravind, S. S.; Ramaprabhu, S. *Journal of Materials Chemistry* **2011**, *21*, 6800.

(29) Iijima, S. *Nature (London, United Kingdom)* **1991**, *354*, 56.

(30) Gorga, R. E.; Cohen, R. E. *Journal of Polymer Science Part B-Polymer Physics* **2004**, *42*, 2690.

(31) Polshettiwar, V.; Baruwati, B.; Varma, R. S. *Acs Nano* **2009**, *3*, 728.

(32) Kong, J.; Franklin, N. R.; Zhou, C.; Chapline, M. G.; Peng, S.; Cho, K.; Dailt, H. *Science (Washington, D. C.)* **2000**, *287*, 622.

(33) Baughman, R. H.; Zakhidov, A. A.; de Heer, W. A. *Science* **2002**, *297*, 787.

(34) Tao, Y.; Gong, F. H.; Wang, H.; Wu, H. P.; Tao, G. L. *Mater Chem Phys* **2008**, *112*, 973.

(35) Journet, C.; Maser, W. K.; Bernier, P.; Loiseau, A.; Lamy de la Chapells, M.; Lefrant, S.; Deniard, P.; Lee, R.; Fischer, J. E. *Nature (London) FIELD Full Journal Title:Nature (London)* **1997**, *388*, 756.

(36) Fischer, J. E.; Dai, H.; Thess, A.; Lee, R.; Hanjani, N. M.; Dehaas, D. L.; Smalley, R. E. *Physical Review B: Condensed Matter* **1997**, *55*, R4921.

(37) Baykal, B.; Ibrahimova, V.; Er, G.; Bengue, E.; Tuncel, D. *Chem. Commun. (Cambridge, U. K.)* **2010**, *46*, 6762.

(38) Abusch-Magder, D.; Someya, T.; Wang, J.; Laskowski, E.; Dodabalapur, A.; Bao, Z.; Tennant, D. M. *Los Alamos National Laboratory, Preprint Archive, Condensed Matter* **2002**, 1.

(39) *Microwave Processing of Materials*; The National Academies Press, 1994.

(40) Mingos, D. M. P.; Baghurst, D. R. *Chem. Soc. Rev.* **1991**, *20*, 1.

(41) Gabriel, C.; Gabriel, S.; Grant, E. H.; Halstead, B. S. J.; Mingos, D. M. P. *Chemical Society Reviews* **1998**, *27*, 213.

(42) Hua, Y. X.; Liu, C. P. *T Nonferr Metal Soc* **1996**, *6*, 35.

(43) Walkiewicz, J. W. K., G.; McGill, S. L. *Minerals and Metallurgical Processing* **1988**, *5*.

(44) Hong, E. H.; Lee, K.-h.; Oh, S. H.; Park, C.-g. *Adv. Funct. Mater. FIELD Full Journal Title:Advanced Functional Materials* **2003**, *13*, 961.

(45) Whitesides, G. M.; Grzybowski, B. *Science* **2002**, *295*, 2418.

(46) Whitesides, G. M.; Mathias, J. P.; Seto, C. T. *Science* **1991**, *254*, 1312.

(47) Li, D.; Wang, Y.; Xia, Y. *Nano Letters* **2003**, *3*, 1167.

(48) Li, D.; Xia, Y. *Advanced Materials (Weinheim, Germany)* **2004**, *16*, 1151.

(49) Hatton, T. A.; Scholten, E.; Dhamankar, H.; Bromberg, L.; Rutledge, G. C. *Langmuir* **2011**, *27*, 6683.

(50) Demoustier-Champagne, S.; Duchet, J.; Legras, R. *Synthetic Met* **1999**, *101*, 20.

(51) Zhao, D. Y.; Feng, J. L.; Huo, Q. S.; Melosh, N.; Fredrickson, G. H.; Chmelka, B. F.; Stucky, G. D. *Science* **1998**, *279*, 548.

(52) Caruso, F.; Wang, Y. J. *Chem. Mater.* **2006**, *18*, 4089.

(53) Zhu, Y.-J.; Wang, W.-W.; Qi, R.-J.; Hu, X.-L. *Angewandte Chemie, International Edition* **2004**, *43*, 1410.

(54) Zhang, X.; Manohar, S. K. *Chem Commun* **2006**, 2477.

(55) Zujovic, Z. D.; Gizdavic-Nikolaidis, M. R.; Stanisavljev, D. R.; Easteal, A. J. *Macromolecular Rapid Communications* **2010**, *31*, 657.

(56) Yu, S. H.; Wu, L. H.; Yao, H. B.; Hu, B. *Chem. Mater.* **2011**, *23*, 3946.

(57) Ziegler, J.; Merkulov, A.; Grabolle, M.; Resch-Genger, U.; Nann, T. *Langmuir* **2007**, *23*, 7751.

(58) Zhu, J.; Palchik, O.; Chen, S.; Gedanken, A. *Journal of Physical Chemistry B* **2000**, *104*, 7344.

(59) Harpeness, R.; Gedanken, A. *Langmuir* **2004**, *20*, 3431.

(60) Gerbec, J. A.; Magana, D.; Washington, A.; Strouse, G. F. *J. Am. Chem. Soc.* **2005**, *127*, 15791.

(61) Ting, J. M.; Chuang, C. M.; Sharma, S. P.; Lin, H. P.; Teng, H. S.; Huang, C. W. *Diamond Relat. Mater.* **2008**, *17*, 606.

(62) Hsin, Y. L.; Lin, C. F.; Liang, Y. C.; Hwang, K. C.; Horng, J. C.; Ho, J. A. A.; Lin, C. C.; Hwu, J. R. *Adv. Funct. Mater.* **2008**, *18*, 2048.

(63) Nikolaev, P.; Bronikowski, M. J.; Bradley, R. K.; Rohmund, F.; Colbert, D. T.; Smith, K. A.; Smalley, R. E. *Chemical Physics Letters* **1999**, *313*, 91.

(64) Ebbesen, T. W.; Ajayan, P. M. *Nature (London, United Kingdom)* **1992**, *358*, 220.

(65) Bronikowski, M. J.; Willis, P. A.; Colbert, D. T.; Smith, K. A.; Smalley, R. E. *Journal of Vacuum Science & Technology a-Vacuum Surfaces and Films* **2001**, *19*, 1800.

(66) Kappe, C. O. *Angewandte Chemie, International Edition* **2004**, *43*, 6250.

(67) Bilecka, I.; Niederberger, M. *Nanoscale*, *2*, 1358.

Chp. 2 Oxidative Template for Making Conducting Polymer Nanoclips

2.1. Introduction

Nanostructured conducting polymers have attracted considerable attention due to their unique chemical, physical properties and potential applications as building blocks of nanoelectronic devices. A variety of approaches have been employed to synthesize nanostructured conducting polymers, including templated polymerization[1-3], interfacial polymerization[4], and seeding polymerization[5, 6]. However, most reports highlight strategies to synthesize 0-D or 1-D nanostructures (nanospheres, wires), with very few on higher order dimensional nanostructures, such as 2-D[7, 8] or even 3-D nanostructures, which can be readily applied in the fabrication of electronic devices[9]. This paper describes the synthesis of 2-D conducting polymer nanoclips using oxidative templates composed of cetrimonium cations and peroxydisulfate anions, $(CTA)_2S_2O_8$, that has potential for use as a "universal" template for all major classes of conducting polymers that are synthesized by precipitation polymerization.

We describe a facile, one-step, general "oxidative template assembly" (OTA) approach to synthesize bulk quantities of electronic conducting polymers such as polyaniline (PANI), polypyrrole (PPy) and poly (3, 4-ethylenedioxythiophene) (PEDOT), having an unusual nanoclip-like morphology. The morphology is orchestrated by an insoluble complex formed between an anionic oxidant ($S_2O_8^{2-}$) and a cationic surfactant. The as-produced conducting

polymers possess 2-dimensional (2-D) nanostructures instead of granular structures without the templates. This OTA approach could be used to control the morphologies and allows large scale production of conducting polymers or other precipitation polymerization systems, e.g., sol-gel technique for metal oxides.

2.2. Experimental

2.2.1. Synthesis of Conductive Polypyrrole Nanoclips

In a typical experiment, 0.01 M cetrimonium bromide ($(C_{16}H_{33})N(CH_3)_3Br$) (CTAB) is dispersed in 60 mL 1M HCl under ice bath. After being magnetically stirred 10 min, 0.03 M ammonium peroxydisulfate (APS) was added into the above solution and keep stirring for 10 min resulting in reactive template in the form of white precipitates. All solutions are cooled to 0-3 ºC. Pyrrole (0.12 M) was added into the as-prepared reactive template solution, self-assembly was conducted at 0-3 ºC for 24 hrs, the resulting black precipitate of polypyrrole was suction filtered, washed with copious amounts of aq. 1 M HCl (3 x 100 mL) and acetone (3 x 100 mL) and dried under freeze dry for 12 hrs. The yield of polypyrrole nanoclips powder was ~130 mg.

2.2.2. Synthesis of Conductive Polyaniline Nanoclips

In a typical experiment, 0.01 M cetrimonium bromide ($(C_{16}H_{33})N(CH_3)_3Br$) (CTAB) is dispersed in 60 mL 1M HCl under ice bath. After being magnetically stirred 10 min, 0.03 M ammonium peroxydisulfate (APS) was added into the above solution and keep stirring for 10 min resulting in reactive template in the form of white precipitates. All solutions are cooled to 0-3 ºC. aniline (0.09 M) was added into the as-prepared reactive template solution,

self-assembly was conducted at 0-3 ºC for 24 hrs, the resulting dark green precipitate of polyaniline was suction filtered, washed with copious amounts of aq. 1 M HCl (3 x 100 mL) and acetone (3 x 100 mL) and dried under freeze dry for 12 hrs. The yield of polyaniline nanoclips powder was ~100 mg.

2.2.3. Synthesis of Conductive PEDOT Nanoclips

In a typical experiment, 0.01 M cetrimonium bromide ($(C_{16}H_{33})N(CH_3)_3Br$) (CTAB) is dispersed in 60 mL 1M HCl under ice bath. After being magnetically stirred 10 min, 0.03 M ammonium peroxydisulfate (APS) was added into the above solution and keep stirring for 10 min resulting in reactive template in the form of white precipitates. All solutions are cooled to 0-3 ºC. EDOT (0.08 M) was added into the as-prepared reactive template solution, self-assembly was conducted at 0-3 ºC for 100 hrs, the resulting naval blue precipitate of PEDOT was suction filtered, washed with copious amounts of aq. 1 M HCl (3 x 100 mL) and acetone (3 x 100 mL) and dried under freeze dry for 12 hrs. The yield of PEDOT nanoclips powder was ~80 mg.

2.2.4. Microwave synthesis of nanocarbons from conductive polymer nanoclips

30 mg as-synthesized conductiong polymer nanoclips were placed in glass vials and then heated in a conventional microwave oven for 6 min, with 3min continuous heating and 1min interval. There was sharp sparking associated with light flame which appeared on conductive polymer nanoclips surface. Microwave heating is associated with 55-60% weight loss in polypyrrole, which is attributed to the loss of backbone nitrogen atoms and dopant

ions (Cl-). The elemental composition of carbon (by elemental analysis) has increased upon microwave heating.

2.2.5. Four probe conductivity measurements

The bulk electrical conductivity of the conducting polymer nanoclips was measured by a linear four probe measurement setup described elsewhere (Scheme S1).[1] The conducting polymer powder was pressed at 3500 psi in a mode to rectangular thin film, and the four probes were connected to Agilent Technologies 34980A multifunctional switch/measure unit. The conductivity σ (S/cm) is the reciprocal of electrical resistivity and can be expressed as:

$$\sigma = \frac{l}{R \times A}$$

R is the electrical resistance of a uniform specimen of the material (Ω), can be directly read from the Agilent system; l is the distance between the inner two probes (cm); A is the

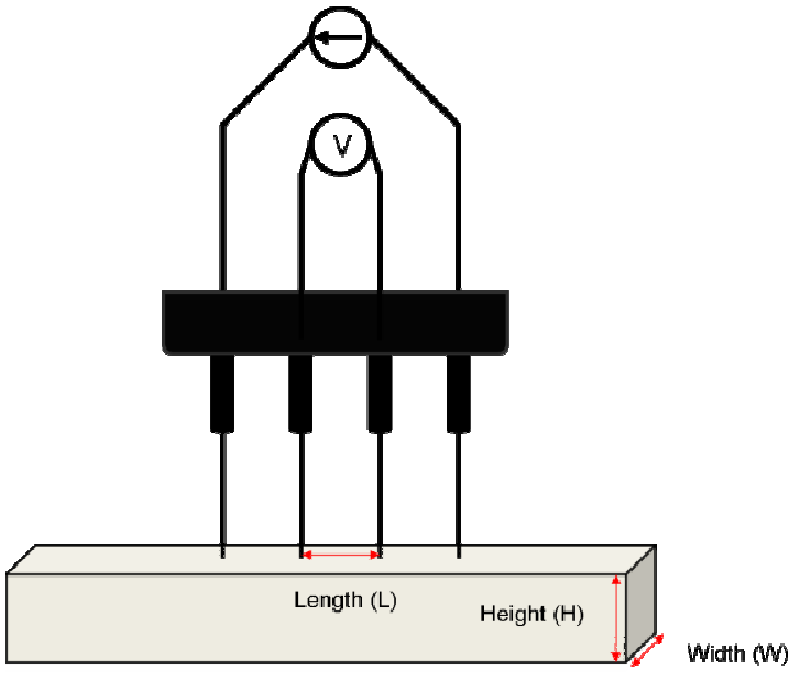

Scheme 2.1. Four probe conductivity measurements

cross-sectional area of the specimen (cm^2). In our test, the parameters for the polypyrrole (PPy) nanoclips sample were: width: 0.2 cm, length: 0.52 cm, thickness: 0.06 cm, resistance from Agilent system: 15.0Ω. The calculated conductivity is 2.89 S/cm.

Please see the experimental data for the conductivity of the conducting polymer nanoclips vs. conventional conducting polymers as control:

Table 2.1: Four probe conductivity (S/cm)

	Conventional samples	Nanoclips
PANI.HCl	2.50	2.15
PPy.Cl	3.28	2.89
PEDOT.Cl	4.23	4.35

2.3. Results and Discussion

The SEM images of the PPy powders obtained above shows a homogeneous nanoclip morphology with average diameter in the range 50-70 nm (Figure 1B), which is to be

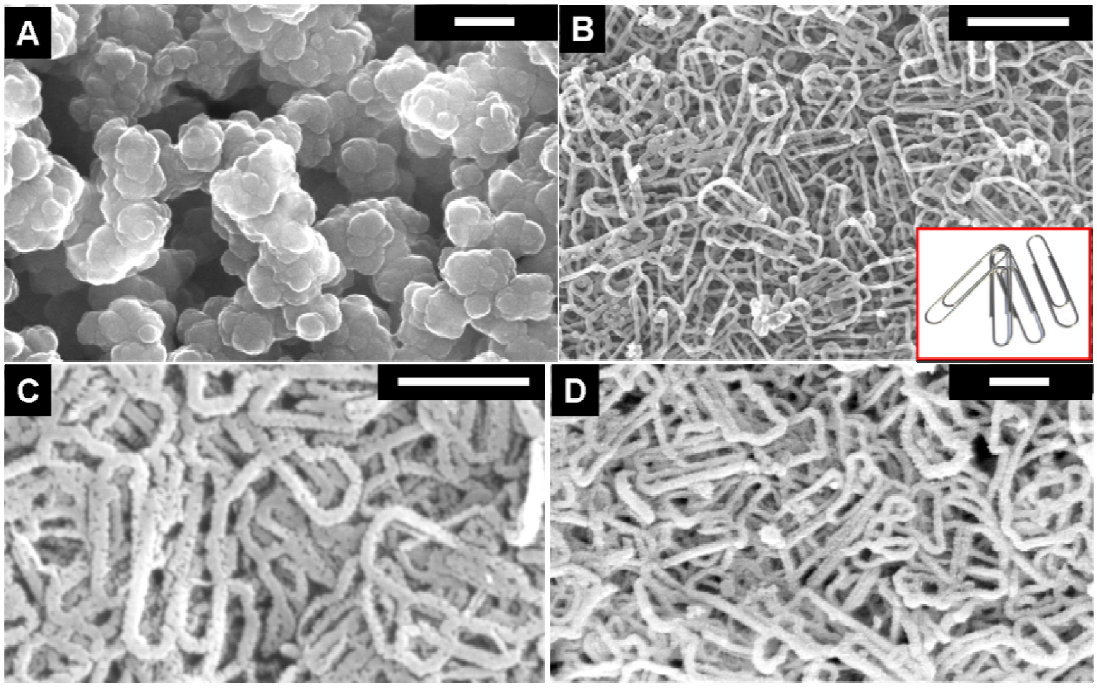

Figure 2.1. SEM images of (A) granular polypyrrole.Cl (scale bar: 200 nm); (B) polypyrrole.Cl nanoclips (scale bar 1 μm, Inset: digital picture of paper clips); (C) polyaniline.HCl nanoclips (scale bar: 1 μm); and (D) PEDOT.Cl nanoclips (scale bar: 1 μm).

contrasted with the granular morphology observed in the absence of CTAB (Figure 2.1A). The OTA method is general and can be used to synthesize other conducting polymers. For example, PANI and PEDOT are synthesized using a very similar procedure. In the case of PEDOT, a longer reaction time is needed presumably because of the larger monomer size and hydrophobic nature of EDOT, which slows the diffusion into the CTAB/APS template complex.

Major classes of conducting polymer powders possess nanoclips morphology (Figure 2.1C, D), with diameter of ~100 nm for PANI, and ~200 nm for PEDOT respectively. The difference in diameters could be explained by the varied size of each individual polymer chain, and the packing patterns of different polymers. The nanoclips are analytically pure and highly conducting, e.g., the elemental analysis of PPy nanoclips has the following composition C: 54.63; H: 4.41; N: 14.71; O: 13.00; Cl: 12.27; Br: 0.89; Total: 99.91. It is consistent with the chemical composition of $(PPy)(CTAB)_{0.01}(Cl^-)_{0.33}(H_2O)_{0.78}$. Although there is trace level surfactant residue in the as-produced polymer, the doping level is 33%, which is consistent with previously published studies[6].

Four-probe pressed-pellet DC conductivities of the conducting polymer nanoclips are in the range of 2-5 S/cm, which is three orders of magnitude higher than the previous report[10]. Spectroscopically, the nanoclips of the conducting polymers are essentially identical to the corresponding granular conventional polymers.

However, there is a significant difference in the capacitance values. Based on Cyclic Voltammetry (CV) study, the specific capacitance values were calculated based on established method[11], and found to be 190 F/g for PPy.Cl nanoclips compared to 35 F/g for granular PPy.Cl. We believe this finding could play an important role in the development of next-generation energy storage devices.

These nanoclips can also be used as precursors for microwave initiated nano-carbonization[12]. In a standardized procedure, 30 mg as-synthesized nanoclips are placed in a glass vial and then heated in a conventional microwave oven, in ambient air, for 5-6 min.

Continuous sparks appear on polymer nanoclips surface owing to the strong absorption of microwave irradiation by conducting polymers. The vials become red hot during the

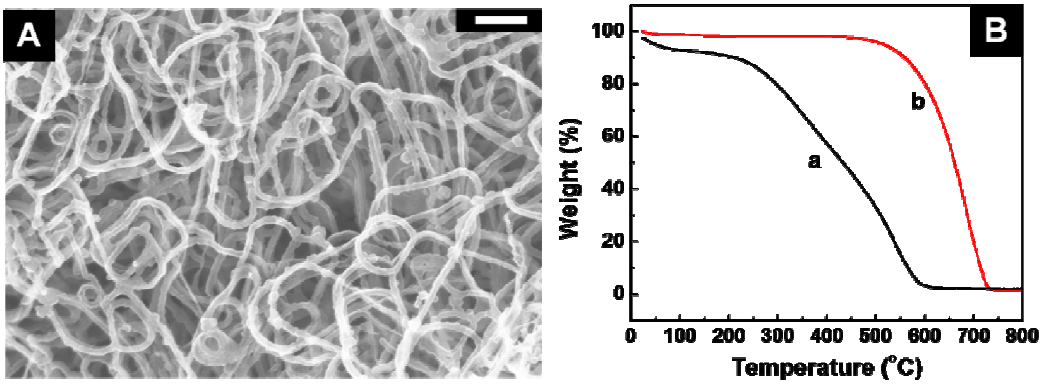

Figure 2.2. (A) SEM image of microwave heated polypyrrole.Cl (scale bar: 300 nm); and (B) TGA of polypyrrole.Cl nanoclips before (a) and after (b) microwave heating.

microwave heating, and the polymer will lose heteroatoms, dopants, etc., from the polymer backbone to produce carbon powder that has retained its nanoclip morphology. The elemental analysis shows that the carbon content increases from 55% to ~80% after microwave heating for 6 min. TGA data (Figure 2.2B) shows a surprisingly large enhancement of the thermal stability after microwave heating, e.g., whereas PPy.Cl nanoclips decompose completely at ~600ºC, nanocarbon clips are very stable with <5% weight loss.

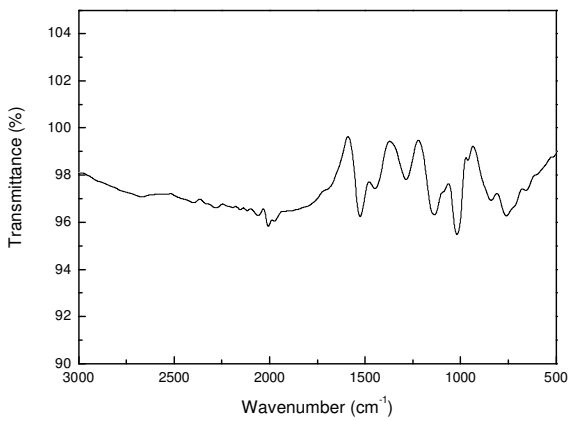

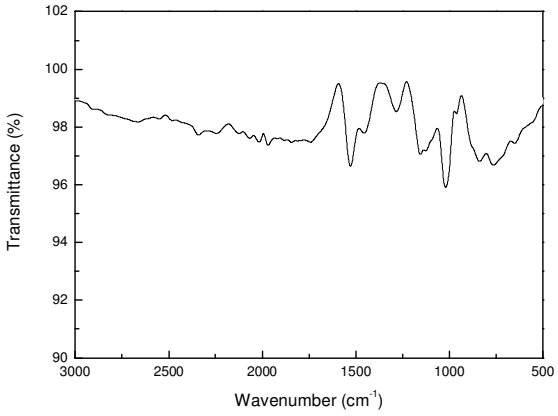

Figure 2.3. FTIR of conventional polypyrrole (left) and polypyrrole nanoclips (right).

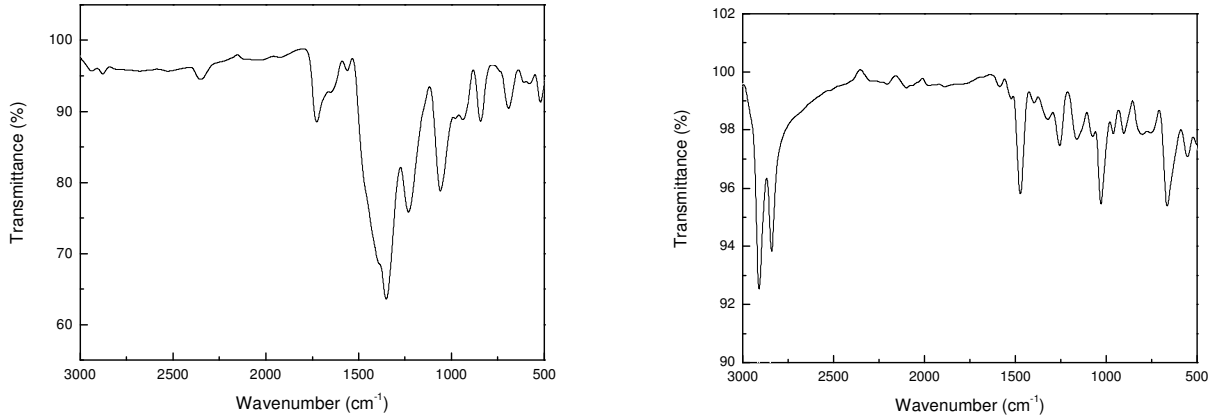

Figure 2.4. FTIR of conventional PEDOT (left) and PEDOT nanoclips (right)

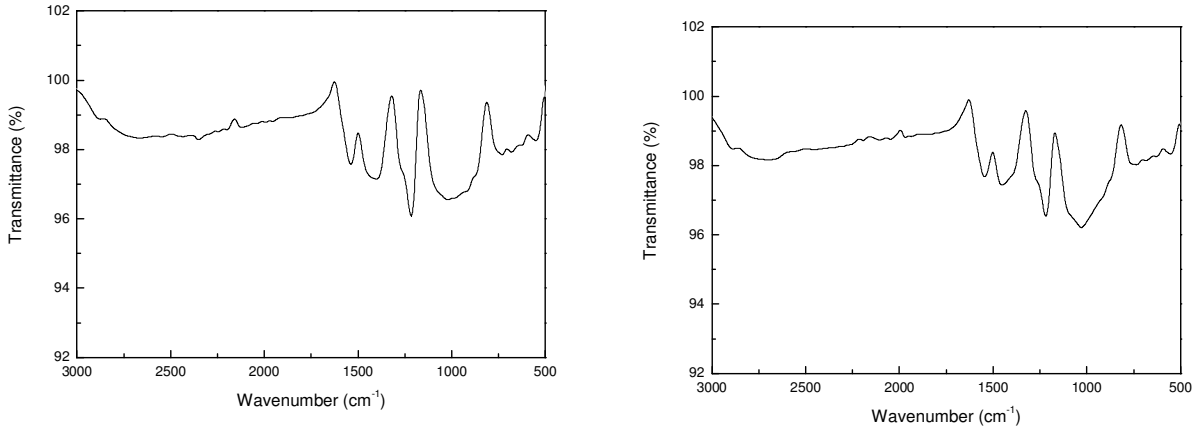

Figure 2.5. FTIR of conventional PANI (left) and PANI nanoclips (right).

The exact mechanism of the micelle packing and leading to the final polymer assembly remain unclear at this point, although a possible rationale is proposed. Based on the XPS investigation of the reactive template, the surface composition of sulphur and

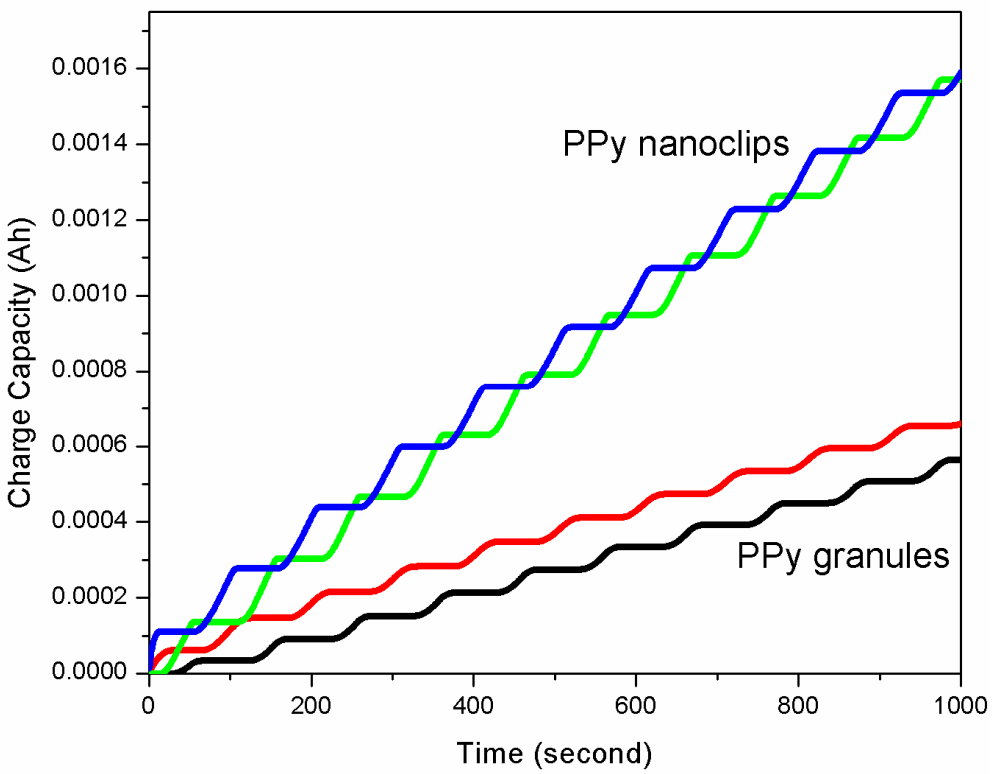

Figure 2.6. Charge/discharge capacity plot of PPy.Cl nanoclips and granules in the range of -0.5V~0.5V (vs. SCE) in aq. 1.0M NaCl electrolyte. Charge (green), discharge (blue) cycles for PPy nanoclips and charge (black), discharge (red) cycles for conventional (granular) PPy.Cl.

nitrogen is found to be 2.5% and 1.1%, which represents 1:2 ratio of peroxydisulfate anions and cetrimonium cations. It is consistent to the chemical structure of $(CTA)_2S_2O_8$. We believe the lamellar micelles are present and are composed of folded, twin-tailed complex of $(CTA)_2S_2O_8$ in the aq. 1M HCl system (Scheme 1), whose formation is favored by high ionic strength of the reaction medium and its affinity to the hydrophilic head group of the complex. Such a finding is different from the previously reported linear structure obtained in a magnetically stirred system using deionized water as reaction medium[2]. The template structure was also discussed elsewhere using distilled water as reaction medium and the

reaction mixture was magnetically stirred as well[7], which yielded different polymer morphologies and relatively low conductivity. The aq. HCl system used in our study has the advantage of (i) promoting higher conductivity of final polymer products; (ii) leading to different assembly mechanism due to enhanced ionic strength, thereby orienting style of the micelles; (iii) protonating amine groups to induce positive charges to the monomers[3]. The positively charged monomers will preferably migrate to the interface between the complex micelles and aq. HCl medium, where the oxidation of the monomers will occur. Due to the excess amount of oxidant used, the template will remain intact until all free oxidants are consumed, i.e., the template will eventually be broken by consumption of the $S_2O_8^{2-}$ ions, which bridges the cetrimonium ions.

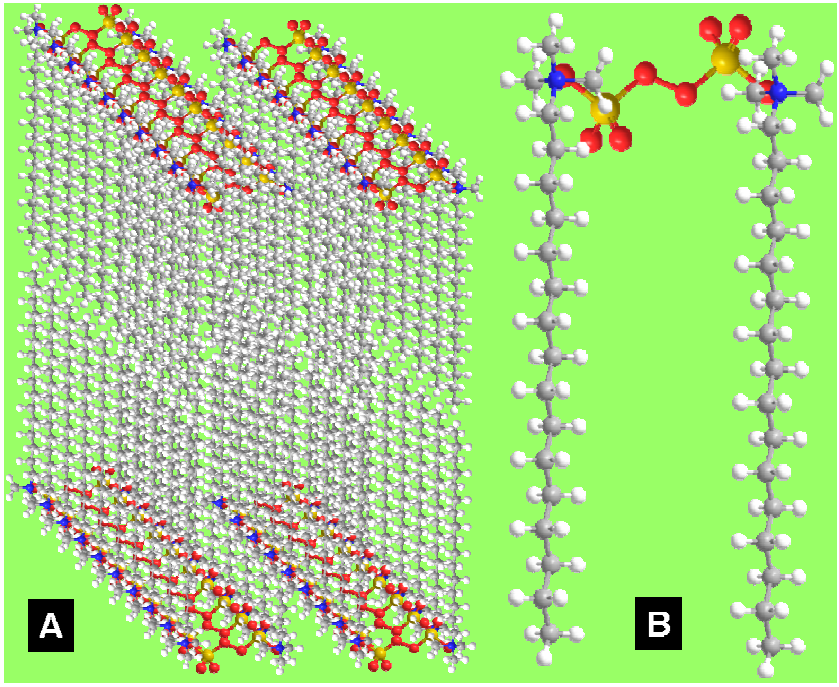

Figure 2.7. (A) lamellar structure of the $(CTA)_2S_2O_8$ complex micelle, and (B) individual $(CTA)_2S_2O_8$ complex with protonated monomer. Red: Oxygen; Yellow: Sulphur; Blue: Nitrogen; Grey: Carbon; White: Hydrogen.

2.4. Conclusions

We demonstrated for the first time the success of OTA approach for preparation of 2-D nanostructure of electronic conducting polymers. Described for the first time are the following: (i) the use of oxidative template as a "universal method" to synthesize in one step, bulk quantity nanoclips of all major classes of conducting polymers, including PANI, PPy and PEDOT, (ii) a convenient method to produce precursors for carbon nanoclips with enhanced thermal stability after microwave heating, and (iii) a folded twin-tailed model for $(CTA)_2S_2O_8$ complex, which lead to lamellar packing and the nanoclips formation.

2.5. References

1. Cepak, V. M.; Martin, C. R., *Chem. Mater.* **1999,** 11, (5), 1363-1367; Misoska, V.; Price, W.; Ralph, S.; Wallace, G., *Synth. Met.* **2001,** 121, (1-3), 1501-1502; Simmons, M. R.; Chaloner, P. A.; Armes, S. P., *Langmuir* **1995,** 11, (11), 4222-4224; Wu, C. G.; Bein, T., *Stud. Surf. Sci. Catal.* **1994,** 84, 2269-2276; Yu, L.; Lee, J.-I.; Shin, K.-W.; Park, C.-E.; Holze, R., *J. Appl. Polym. Sci.* **2003,** 88, (6), 1550-1555; Zhong, W.; Deng, J.; Yang, Y.; Yang, W., *Macromol. Rapid Comm.* **2005,** 26, (5), 395-400; Surwade, S. P.; Agnihotra, S. R.; Dua, V.; Manohar, N.; Jain, S.; Ammu, S.; Manohar, S. K., *J. Am. Chem. Soc.* **2009,** 131, (35), 12528-12529; Surwade, S. P.; Manohar, N.; Manohar, S. K., *Macromolecules* **2009,** 42, (6), 1792-1795.

2. Zhang, X.; Zhang, J.; Liu, Z.; Robinson, C., *Chem. Comm.*. **2004**, (16), 1852-1853.

3. Wu, A.; Kolla, H.; Manohar, S. K., *Macromolecules* **2005,** 38, (19), 7873-7875.

4. Huang, J.; Virji, S.; Weiller, B. H.; Kaner, R. B., *J. Am. Chem. Soc.* **2003,** 125, (2), 314-315.

5. Zhang, X.; Goux, W. J.; Manohar, S. K., *J. Am. Chem. Soc.* **2004,** 126, (14), 4502; Zhang, X.; MacDiarmid, A. G.; Manohar, S. K., *Chem. Commun.* **2005,** 42, 5328-5330.

6. Zhang, X.; Manohar Sanjeev, K., *J. Am. Chem. Soc.* **2004,** 126, (40), 12714-12715.

7. Wang, Y.; Yu, C.; Li, Z.; Zhou, D.; Chen, W.; Xue, G., *Colloid Polym. Sci.* **2009,** 287, (11), 1325-1330.

8. Wang, T.; Zhong, W.; Ning, X.; Wang, Y.; Yang, W., *J. Appl. Polym. Sci.* **2009,** 114, (6), 3855-3862.

9. Ackermann, J.; Videlot, C.; Nguyen, T. N.; Wang, L.; Sarro, P. M.; Crawley, D.; Nikolic, K.; Forshaw, M., *Appl. Surf. Sci.* **2003,** 212-213, 411-416.

10. Zhang, X.; Zhang, J.; Song, W.; Liu, Z., *J. Phys. Chem. B* **2006,** 110, (3), 1158-1165.

11. Wang, Y.-G.; Li, H.-Q.; Xia, Y.-Y., *Adv. Mater.* **2006,** 18, (19), 2619-2623.

12. Zhang, X.; Manohar Sanjeev, K., *Chem. Comm.* **2006**, (23), 2477-2479.

Chp. 3 Green Nano Approach to Nanostructured Polypyrrole

3.1. Introduction

Nanostructured conducting polymers have become a multidisciplinary research area and it has been under continuous investigation ever since 1970s. This trend has been extended for over three decades. Among the conducting polymer family, Polypyrrole (PPy) has been distinguished as one of the major conducting polymers and possesses a broad band of applications in sensors, functional coating, energy storage and optical devices, due to its unique properties, such as easy preparation, tunable conductivity, reversible redox property, environmental stability and biocompatibility.[5-8] A variety of synthetic techniques have been developed towards PPy nanostructures, which can be used as building blocks of nanoelectronic devices. The major synthetic techniques include templated polymerization,[9] interfacial polymerization,[10] and seeding polymerization.[11] PPy is typically synthesized by chemical oxidative polymerization of pyrrole in dilute acids as reaction media and ammonium peroxydisulfate (APS, $(NH_4)_2S_2O_8$), as the oxidant. This chemical oxidative polymerization of pyrrole in aqueous 1M HCl yields black granular powders of PPy·Cl. Although APS is pretty popular in PPy synthesis, other oxidants including $FeCl_3$, KIO_3, $K_2Cr_2O_7$, are also employed in the oxidative polymerization reactions of pyrrole.[12]

Several attempts have been made recently to synthesize conducting polymers with milder and greener oxidant, such as acetic acid/noble metal system,[13] $HCl/NaCl/H_2O_2$ system[14] and

enzyme/H_2O_2 system,[15], aiming to develop greener, milder or even "catalyst-free" approaches. In this study, we report a green approach using two different catalysts respectively: V_2O_5 nanofiber seeds and ferrous chloride ($FeCl_2$), along with the green oxidant H_2O_2. There are several major advantages of using H_2O_2 over APS in pyrrole polymerization, namely, (i) H_2O_2 is a green oxidant since by-product of the reaction is just water, which can be directly recycled without post-purification processes, (ii) different combinations of H_2O_2 with the catalysts will offer varied oxidative powers, which can help to understand the formation mechanisms of nanostructured conducting polymers.

In a typical synthesis, PPy nanofibers was obtained by adding catalytic amount (~2 mg) of V_2O_5 nanofiber seeds into 50 mL DI water, in which 0.5 mL pyrrole has been pre-dispersed. There is no color change observed until the introduction of 5 mL H_2O_2, indicating V_2O_5 seeds itself is not capable of oxidizing the pyrrole monomer; meanwhile, H_2O_2 itself is also considered too weak to oxidize the pyrrole monomers in H_2O, this can be evidenced by experimental observation that there is no color change at room temperature with the addition of H_2O_2 into pyrrole/H_2O mixture. The polymerization is initiated by adding H_2O_2 to the pyrrole/V_2O_5/H_2O system, and after 12 hrs reaction, the dark precipitation of PPy was filtered and washed with copious amounts of DI water (3 × 100 mL) and acetone (3 × 100 mL). The powder was then freeze-dried for another 12 hrs, yielding ~100 mg of PPy nanofibers. We believe that the V_2O_5 nanofiber seeds played key roles in not only controlling the morphology by the seeding effect,[11] but also serving as the catalyst to promote the oxidation of H_2O_2, which could be called "catalytic seeding" effect.

3.2. Experimental

3.2.1. Green Synthesis of Conductive Polypyrrole Nanofibers

In a typical synthesis, PPy nanofibers was obtained by adding catalytic amount (~2 mg) of V_2O_5 seeds into 50 mL DI water, in which 0.5 mL pyrrole has been pre-dispersed. After the addition of 5 mL H_2O_2, the polymerization was initiated and lasted for 12 hrs. The dark precipitation of polypyrrole was filtered and washed with copious amounts of DI water (3 × 100 mL) and acetone (3 × 100 mL). The powder was then freeze-dried for 12 hrs, yielding ~100 mg of PPy nanofibers.

3.2.2. Green Synthesis of Conductive Polypyrrole Nanospheres

In a typical experiment, polypyrrole nanospheres can be synthesized by first adding 0.1 g ferrous chloride ($FeCl_2$) to 60 mL DI water, where 1 mL pyrrole has been pre-dispersed. After the addition of 5 mL H_2O_2 to the pyrrole/$FeCl_2$/H_2O mixture, pyrrole polymerization was initiated and lasted for 12 hrs. The dark precipitated polypyrrole was filtered and washed with copious amounts of DI water (3 × 100 mL) and acetone (3 × 100 mL). The powder was then freeze-dried for 12 hrs, yielding ~100 mg of PPy nanospheres.

3.2.3. Potential-time Profiling Characterization of in-situ Polymerization Process

The reaction mixture was setup for potential-time profiling using previously established procedure [1,2] (Pt wire electrode, saturated calomel electrode (SCE) reference). The potential was monitored continuously with time starting from the very beginning of the polymerization.

3.2.4. Particle Size measurement of the as-prepared polypyrrole nanospheres

The particle sizes of the as-prepared nanospheres were measured by a NICOMP 380 ZLS Particle Sizer in the dispersions of two different surfactants: dioctyl sulfosuccinate sodium (AOT) or Triton X-100 (TX-100). A typical testing process is described as follows: a certain amount of surfactant was added into 50 mL distilled water (0.10g for AOT, 0.50g for TX-100), which was stirred continuously at 80ºC, until the surfactant was fully dissolved and the solution became transparent. Desired amount of polypyrrole nanospheres (e.g. 0.005g, 0.010g) were added into the as-prepared surfactant solution at 60ºC and stirred for around 10 min. And then the dispersions were placed in water bath and ultrasonicated for 30 min. Finally, the obtained dispersions with known concentrations were added to the test cell of NICOMP 380 ZLS Particle Sizer and their particle sizes were measured subsequently.

3.3. Results and Discussion

The scanning electron microscopy (SEM) image of this dark PPy powder showed that the as-prepared PPy is composed of predominantly nanofibers having diameters in the range of 80-100 nm (Fig. 1B). It is noteworthy that changing the reaction medium from DI water to HCl will lead to the change of the initial PPy nanofibers into irregular shaped granules (Fig. 1A). To investigate the “solvent effect”

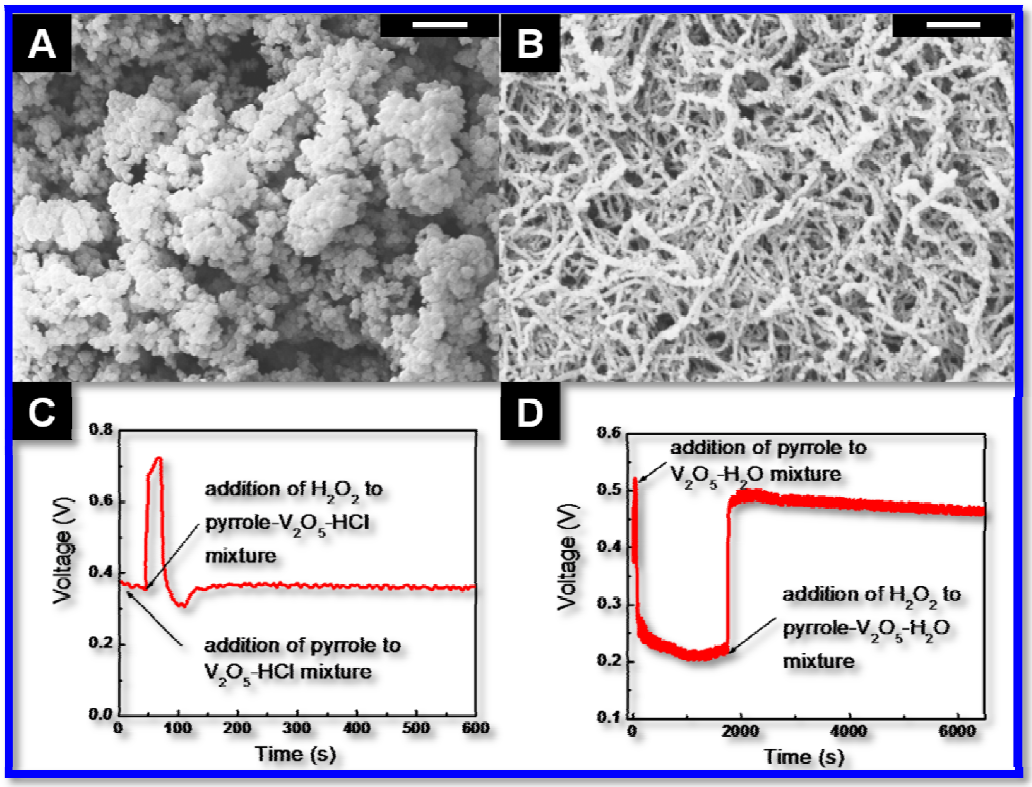

Figure 3.1. (A, C) SEM image of PPy granules and potential-time profile of pyrrole polymerization using $V_2O_5/H_2O_2/HCl$ system; (B, D) SEM image of PPy nanofibers and potential-time profile of pyrrole polymerization using V_2O_5/ H_2O_2/H_2O system. Scale bar: 2 μm

in these two systems, potential-time profiling was carried out to understand the reaction kinetics and thermodynamics.[2] It is found that the initial potential of V_2O_5/H_2O mixture was 0.53 V, upon adding pyrrole, the potential dropped to 0.27 V in a very short period of time, and stabilized around 0.25 V (Fig. 1D). The V_2O_5/H_2O/PPy solution was basically in light yellowish color due to the intrinsic color of V_2O_5. The solution turned into opaque after

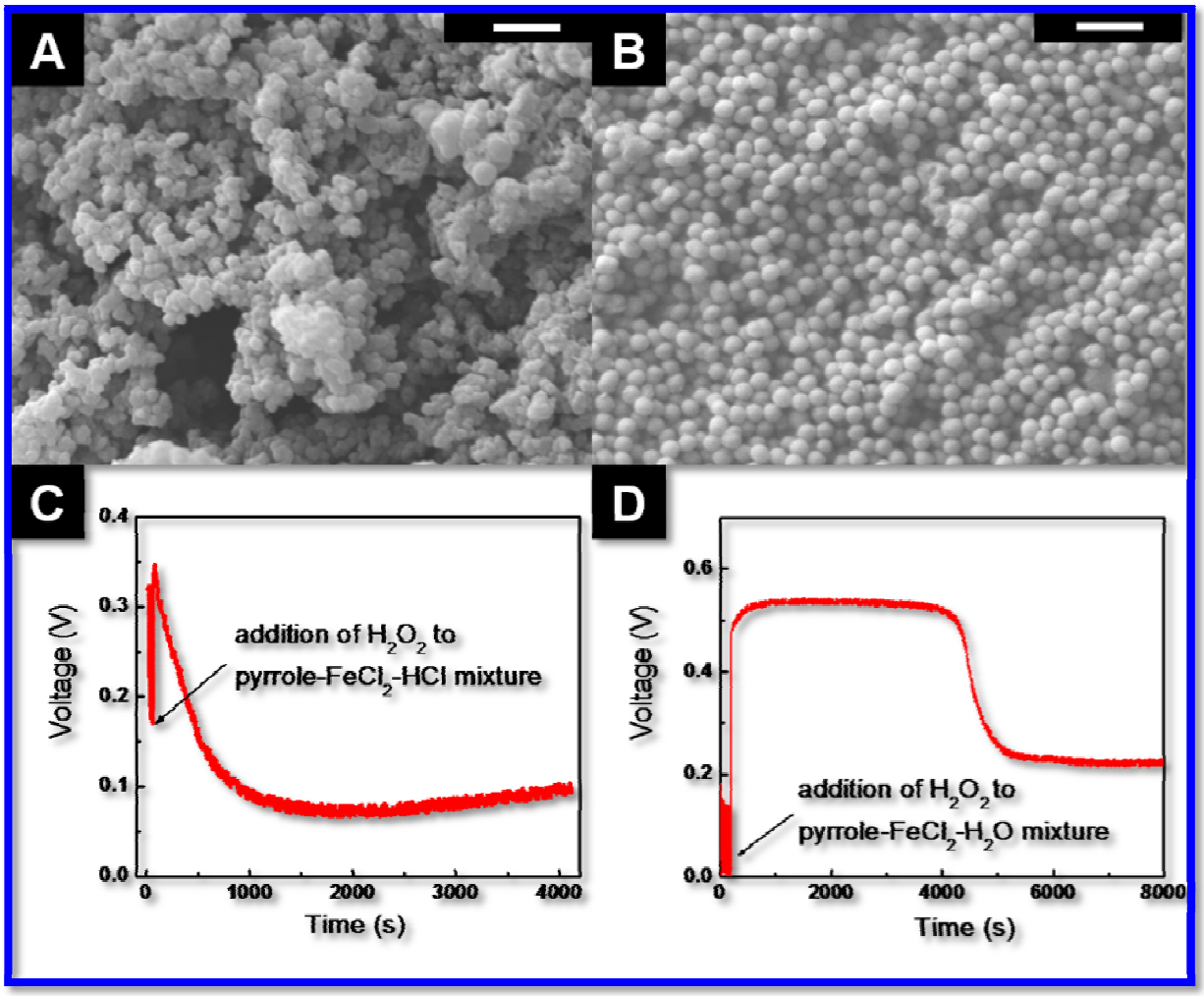

Figure 3.2. (A, C) SEM image of PPy granules and potential-time profile of pyrrole polymerization using $FeCl_2/H_2O_2/HCl$ system; and (B, D) SEM image of PPy nanospheres and potential-time profile of pyrrole polymerization using $FeCl_2/H_2O_2/H_2O$ system. Scale bar: 2 μm

introducing the oxidant H_2O_2, and the potential increased to 0.51 V to initiate the pyrrole polymerization (Fig. 1D). In a control experiment, the potential of pyrrole/HCl aqueous solution was found to be 0.37 V, upon adding V_2O_5, the potential rose rapidly up to 0.74V

and dropped back to 0.3 V within 50 seconds. The V_2O_5/HCl/PPy mixture was in light yellowish color and turned into opaque immediately after introducing H_2O_2, and the potential stabilized at 0.36 V to oxidize the pyrrole monomers (Fig. 1C). Since V_2O_5 nanofiber seeds can be dissolved in HCl to form VO_2^+ ions,[11] one can consider that the combination of solid state V_2O_5 and H_2O_2 in DI water gives a higher potential than the combination of VO_2^+ ion and H_2O_2 in HCl. And the survival of V_2O_5 seeds in DI water helped the fibrillar growth of PPy.[11]

If the catalyst is replaced by $FeCl_2$, nanospheres of PPy were obtained instead of nano-fibrillar morphology when V_2O_5 nanofiber seeds were used. Similar synthetic approach was carried out by adding 0.1 g $FeCl_2$ to 60 mL DI water, where 1 mL of pyrrole has already been pre-dispersed. After the addition of H_2O_2 to the pyrrole/$FeCl_2$/H_2O mixture, pyrrole polymerization was initiated. The dark precipitated PPy is filtered and washed with copious amounts of DI water (3 × 100 mL) and acetone (3 × 100 mL) after 12 hrs reactions. The powder was then freeze-dried for another 12 hrs, yielding ~100 mg of PPy nanospheres.

Very interestingly, the as-prepared PPy is composed of predominantly nanospheres with ~400 nm in diameter (Fig. 2B). It is notable that the nanosphere morphology will be changed to irregular shaped granules once the reaction medium is switched from DI water to HCl (Fig. 2A). The potential-time profiling was again applied to compare these two systems. The pyrrole/$FeCl_2$/H_2O mixture was transparent, light-green coloured solution, with an initial potential of ~0 V, which turned into opaque right after the introduction of H_2O_2, and the potential increased from 0 V to 0.53 V. During the polymerization of pyrrole, a potential plateau was formed and lasted for about 1 hr, and then the potential dropped to ~0.23 V, indicating the completion of polymerization (Fig. 2D).[2, 4] However, if 1M aq. HCl was used

instead of DI water, the initial potential of PPy/HCl/$FeCl_2$ mixture was found to be 0.16 V (Fig. 2C). Upon adding H_2O_2, the potential rose up to 0.35V and dropped back to ~0.1 V gradually afterwards, which has relatively lower potential than the DI water system, and no plateau was formed. Although it was not clear what would be the driving force for the formation of nanospheres vs. granules in these two different reaction systems, we do believe

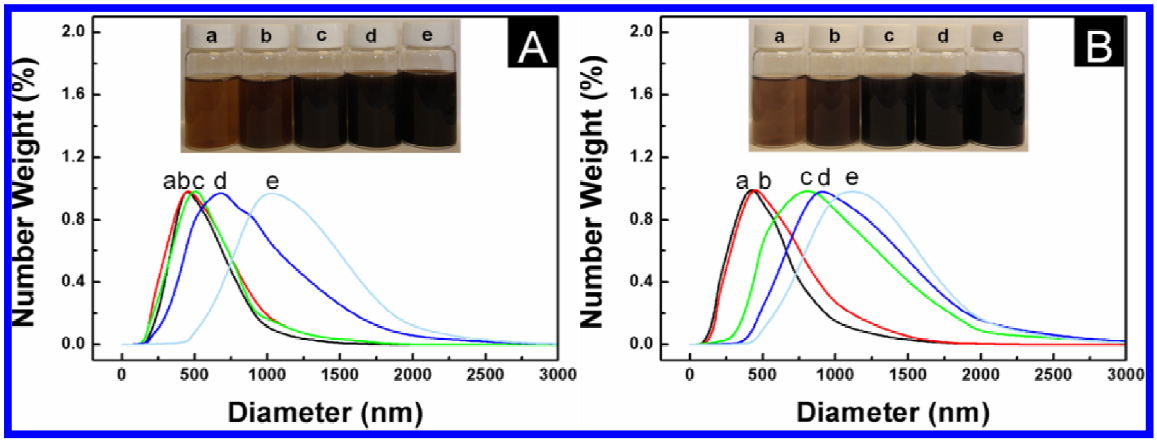

Figure 3.3. Dynamic light scattering test for particle size distribution of PPy nanospheres dispersed in (A) AOT surfactant and (B) Triton X-100 surfactant. Concentrations from a-e: 0.1, 0.2, 0.6, 1, and 2 g/L.

that the protonation of pyrrole monomers, and strong ionic strength in 1M aq. HCl medium could make pyrrole monomers very hydrophilic, comparing to their more hydrophobic nature in DI water system. The surface tension between the hydrophobic pyrrole monomer droplet and DI water could help to form micelle-like structures,[16] and play a key role in the formation of nanospheres. In addition, the values of the oxidative potentials of the polymerization system could also affect the nanostructure formation of PPy.

The dispersibility of the as-prepared PPy nanosphere is of special interest in nanoelectronic device fabrication. Dynamic light scattering (DLS) was used to evaluate the stability and processibility of the nanospheres dispersed in different types of surfactants. Non-ionic surfactant Triton-X 100 (TX-100), and anionic surfactant dioctyl sodium sulfosuccinate (AOT) were selected to disperse the PPy nanospheres, since they are inexpensive and widely used in different fields of application. After dispersing the PPy nanospheres in aq. solutions of these two surfactants, DLS measurements were carried out to test these nanosphere dispersions with a series of different concentrations, and the resulting particle size distributions are shown in Fig. 3.3.

PPy nanospheres with five different concentrations from 0.1 g/L to 2 g/L were prepared by using ultra-sonication bath. The DLS particle size of the dispersions revealed narrower distribution curves for AOT surfactant, in the range of 450 to 1000 nm, comparing to TX-100 system, which is in the range of 400 to 1120 nm. It could be explained by the ionic vs. non-ionic nature of these two surfactants. Nanospheres, stabilized by the dioctyl sulfosuccinate anions, will repel each other to prevent the formation of agglomerates, due to the same negative surface charges. However, it will be easier to form agglomerate since there is no charge on TX-100 surfactants to generate a repelling force between nanospheres.

According to the DLS results for the particle size distribution of the PPy nanosphere, we could readily disperse the as-prepared nanospheres in aqueous surfactant solutions, forming stable dispersions with high sample loads. And this result indicates the great potential of using the nanospheres to fabricate the next generation nanoelectronic devices in the ease of its dispersion form. For example, spin-coating of this PPy nanosphere dispersion to make conducting films, anti-static layers or transparent electrode for applications such as anti-static

coatings or electroluminescent lamps. These nanofibers and nanosphere structures can also be used as precursors for microwave initiated nanocarbonization,[17] which is a rapid and facile approach to convert conducting polymer nanostructures to nanocarbons.

3.4. Conclusions

In summary, we demonstrated for the first time: (i) a "green-nano" approach for one-step synthesis of bulk quantities of PPy nanofibers and nanospheres using different catalysts, i.e., V_2O_5 nanofibers and $FeCl_2$; (ii) a convenient method to achieve the goal of morphological control of PPy nanostructures by simply changing reaction media, e.g., 1M HCl to DI water; and (iii) the potential-time profiling technique was adopted in this "green-nano" approach for PPy system, which could provide insights for probing the mechanism of the nanostructure formation.

3.4. References

1. X. Zhang, H. S. Kolla, X. Wang, K. Raja and S. K. Manohar, *Adv. Funct. Mater.*, 2006, **16**, 1145.
2. H. S. Kolla, S. P. Surwade, X. Zhang, A. G. MacDiarmid and S. K. Manohar, *J. Am. Chem. Soc.*, 2005, **127**, 16770.
3. S. K. Manohar, A. G. MacDiarmid and A. J. Epstein, *Synth. Met.*, 1991, **41**, 711.
4. Y. Wei, K. F. Hsueh and G. W. Jang, *Polymer*, 1994, **35**, 3572.
5. K. J. Gilmore, M. Kita, Y. Han, A. Gelmi, M. J. Higgins, S. E. Moulton, G. M. Clark, R. Kapsa and G. G. Wallace, *Biomaterials*, 2009, **30**, 5292.
6. N. K. Guimard, N. Gomez and C. E. Schmidt, *Prog. Polym. Sci.*, 2007, **32**, 876.

7. Y. Kudoh, *Synth. Met.*, 1996, **79**, 17.

8. A. Ramanaviciene, A. Kausaite, S. Tautkus and A. Ramanavicius, *J. Pharm. Pharmacol.*, 2007, **59**, 311.

9. A. M. Wu, H. Kolla and S. K. Manohar, *Macromolecules*, 2005, **38**, 7873.

10. J. X. Huang, S. Virji, B. H. Weiller and R. B. Kaner, *J. Am. Chem. Soc.*, 2003, **125**, 314.

11. X. Zhang and K. Manohar Sanjeev, *J. Am. Chem. Soc.*, 2004, **126**, 12714.

12. S. Jain, S. P. Surwade, S. R. Agnihotra, V. Dua, P. A. Eliason, G. J. Morose and S. K. Manohar, *Green Chem.,* 2010, **12**, 585.

13. H. V. R. Dias, X. Y. Wang, R. M. G. Rajapakse and R. L. Elsenbaumer, *Chem. Comm.*, 2006, 976.

14. S. P. Surwade, S. R. Agnihotra, V. Dua, N. Manohar, S. Jain, S. Ammu and S. K. Manohar, *J. Am. Chem. Soc.*, 2009, **131**, 12528.

15. M. S. Ram and S. Palaniappan, *J. Mol. Catal. A-Chem.*, 2003, **201**, 289.

16. Z. Liu, X. Zhang, S. Poyraz, S. P. Surwade and S. K. Manohar, *J. Am. Chem. Soc.*, 2010, **132**, 13158.

17. X. Y. Zhang and S. K. Manohar, *Chem. Comm.*, 2006, 2477.

Chp. 4 Seeding Approach to Metal Nanoparticles Decorated Conducting Polymer Nanofiber Network

4.1. Introduction

A novel metal displacement reaction occurred between "synthetic metals" (conducting polymers) and different metals salt aqueous electrolytes, namely noble metals: gold (Au), platinum (Pt), and transition metals: silver (Ag), and copper (Cu) by inviting "nanofiber seeding"[1] approach to synthesize, in one step, bulk quantities of Au, Pt, Ag or Cu nanoparticles decorated conducting polymer nanofiber network. Pyrrole was seeded by vanadium pentoxide (V_2O_5) sol-gel nanofibers[2] and polymerized under different metal salt aqueous solutions, such as AuCl, $HAuCl_4 \cdot 3H_2O$, $PtCl_2$, $PtCl_4$, AgCl and $CuCl_2$. The implementation of V_2O_5 nanofiber seeds in the metal salt solutions can afford to drastically change the morphology of the as-produced polypyrrole (PPy) from irregular shaped granules to almost exclusively nanofibers. The formation of these PPy Nanofiber-Noble Metal Nanoparticle (PNNMN) composites can be attributed to the seeding effect of V_2O_5 which could promote the formation of one dimensional conducting polymer nanofiber growth. The polymerization induction stage, monitored by open circuit potential, was discovered to play a critical role in determining the morphology of the as-precipitated polymers.[3] Due to the seeding and catalytic dual functions, V_2O_5 nanofibers can be defined as catalytic seeds, which not only involves in orchestrating the nanofiber formation of polymer nanostructure as a seeding agent, but also able to exhibit the catalytic capability by raising the overall oxidative potential in metal salts with relatively low oxidation potentials, such as $Pt(II)Cl_2$ and $CuCl_2$.

Organic/inorganic hybrid nanomaterials span a broadband of researches and applications, ranging from novel synthesis, such as polymer and metal nanofiber composites,[4,5] ultrathin free-standing films of metal oxide-polymer composite,[6] unique functional nanodevices, e.g., mesoporous separation membranes of polymer-coated copper hydroxide nanostrands,[7] to highly advanced biological sensors[6] and chemical sensors.[8,9] Among those, dispersed nanostructured noble metals, e.g., both Au and Pt exhibit excellent properties in magnetism,[10] plasma resonance,[11] and catalysis.[12,13] On the other hand, nanostructured conducting polymers such as PPy nanofibers,[1] nanotubes[14] and nanoclips,[15]possess both superior electronic and mechanical properties,[16] which make them ideal candidates for the fabrication of next-generation nano-electronic devices. Meanwhile, Continuous endeavours have been devoted to polypyrrole/silver or copper based nanocomposites due to the ubiquitous applications in chemical sensing,[7] surface enhanced Raman scattering,[8] and catalysis,[9] anisotropic silver and polypyrrole nanocomposites can offer; whilst nanostructured copper can be electrodeposited and directly immobilized on deeply reduced polypyrrole to form nanocomposite film,[10] it can also be electrochemically incorporated with polypyrrole film and been used for application of modification of glassy carbon electrode for advanced chemical sensor fabrication.[11]

There are a number of endeavours to immobilize the nanostructured noble metal nanoparticles onto conducting polymers matrix, i.e., the utilization of ionic liquid for PPy/Au and PPy/Ag nanocomposites;[17] the use of poly(vinyl pyrrolidone) (PVP) to achieve PPy/Au core-shell nanostructure by interfacial polymerization.[18] Furthermore, conducting polymer precursors, such as polyaniline,[19] polypyrrole[14] and polythiophene nanotubes[20] were utilized as templates to form coaxial nanocables with encapsulated Co, Ag and Au nanostructures.

Porous aluminium oxide was reported as a hard template to assist the formation of Au-capped, protein-modified polypyrrole nanowire through electrochemical polymerization.[21]However the simultaneous control of both morphologies of conducting polymers and transition metals remains a challenge. Our previous discovery of seeding polymerization technique, among the myriad of others, can offer a facile, and one-step approach to achieve concurrent control of both morphologies of conducting polymer and transition metals, without the assistance of any other templates or capping agents. In this seeding approach, catalytic amount of nanofibrillar V_2O_5 (1-2 mg) serves as the "seed", which could not only direct the formation of PPy nanofibers, but also promote the polymerization process by oxidizing pyrrole monomer into its nanofibril oligomer form.[22] As the reactive seeds, the V_2O_5 nanofibers will react with pyrrole monomers as the transition metal ions do.[1] And the nanofibrillar oligomers, formed due to the reaction between pyrrole monomers and V_2O_5 nanofibers will further react with the transition metal ions and reduce them to noble metal nanocrystals. This type of reaction can be considered as a novel metal displacement reaction, since the redox reaction is taken place between the synthetic metal (PPy) and its oligomers, and the noble metal ions, which possess high oxidation potential.

In a typical synthesis, 1-2 mg of V_2O_5 nanofibers were introduced to 50 mL of aqueous noble metal salt solutions, i.e., AuCl, $HAuCl_4 \cdot 3H_2O$, $PtCl_2$, $PtCl_4$, AgCl and $CuCl_2$. Pyrrole monomers were then added into the mixture to initiate the polymerization reaction, after 15 min magnetic stirring. Polymerization reaction will last for 24 hrs and then followed by filtration and purification steps. Potential-time profiling was monitored, providing real time monitoring for the oxidative potential change of the reaction mixture, throughout the polymerization process. Since pyrrole monomer can be polymerized by the noble metal salt

ions solely, and as an example, granular PPy was obtained from the oxidation of pyrrole monomer using $PtCl_2$ without V_2O_5 nanofibers. While with the addition of catalytic amount of V_2O_5 nanofibers as reactive seeds, the as-produced PNNMN composites powders exhibit homogeneous nanofibrillar network, on which noble metal nanoparticles were deposited. The diameter of the PPy nanofibers in these PNNMN composites is in the range of15-30 nm, and the size of nanoparticles of the Au or Pt is around 80-100 nm. Spectroscopically, the PPy nanofibers in the composites are similar to the previously published work.[15] Elemental analysis of these composites was carried out by Energy-dispersive X-ray spectroscopy (EDX), which indicates the loading ratio of noble metals is in the range of 35-55 wt.%, depending on different types of metals and the initial concentrations of their cations. These EDX data are also consistent with our Thermogravimetric Analysis (TGA) tests of the nanocomposites. It is to be noted that the PPy nanofibers were shortened in the TEM image, which is probably due to the ultrasonication step during the sample preparation process.

4.2. Experimental

4.2.1. Synthesis of polypyrrole (PPy) and noble metal nanocomposites

In a typical synthesis, 1-2 mg of V_2O_5 sol-gel nanofibers were slowly added into the noble metal salt solutions under magnetic stirring. After the addition of V_2O_5, 0.1mL of pyrrole monomer was added to the reaction media in a 60-second period. The solution color was spontaneously darkened and turned into black with the formation and dispersion of black precipitates of PPy. The reaction solution was magnetically stirred for 24 hours for the completion of polymerization and a better homogenous noble metal nanoparticles distribution into PPy nanofibers. The resulting black precipitate of polypyrrole was suction

filtered, washed with copious amounts of aq. 1M HCl (3×100mL) and acetone (3×100mL) and freeze dried for 12h. The yield of nanocomposites powder was ~50-100 mg depending on different types of metal salts.

4.2.2. *Synthesis of polypyrrole (PPy) and transition metal (Ag, Cu) nanocomposites*

In each typical seeding experiment, 1mL of V_2O_5 sol-gel was prepared and slowly introduced into well-dispersed (0.005M; 0.1M; 0.2M) solutions of $AgNO_3$ or $CuCl_2$ in DI water, under vigorous magnetic stirring for one minute. 1mL of pyrrole monomer was then added to the reaction. The color of the solution then gradually darkened indicates the formation and dispersion of PPy precipitates, which is a typicallytake place during oxidation polymerization of polypyrrole. A further stirring time period of 24 hours has been given in order to obtain a homogenous metal nanoparticle dispersed onto polypyrrole nanofibers. The final precipitates wereeventually suction filtered and washed with copious amounts of DI water (3x100mL) and acetone (3x100mL), respectively. The damp precipitates were allowed to air dry for overnight.The yield of nanocomposites powder was ~35-90 mg caused by different metal salt concentrations.

4.2.3. TEM sample preparation of PPy Nanofiber-Nobel Metal Nanoparticle Composites (PNNMN)

In a typical process, 5 mg of the as-synthesized PNNMN composite was weighted and dispersed in 10 mL ethanol with bath sonication for 20 minutes. The resultant dispersion was drop casted onto the copper grid and dried for TEM characterization.

4.2.4. Potential-time profiling characterization of in-situ polymerization process

The reaction mixture was characterized by potential-time profiling using established methods,[1-3] (Pt wire electrode, saturated calomel electrode (SCE) reference). The electrode configuration was immersed into the reaction solution before starting the polymerization reaction. Each reactant required for the polymerization process was added following the sequence of metal salts, V_2O_5, and finally pyrrole monomer. 10 minutes' interval was allowed between the additions of each reactant, which would give better indication about the potential change according to the potential-time profiling curve. The potential of the reaction solution was monitored and recorded from the beginning of each individual polymerization experiment and the corresponding control experiment without the addition of V_2O_5 nanofibers.

4.2.5. Electrochemical tests for PPy-Pt and PPy-Au catalysts

The electrochemical behaviors of PPy-Pt and PPy-Au catalysts were measured by Cyclic Voltammetry (CV) at room temperature in a three-electrode cell using Arbin electrochemical instrument (Arbin-010 MITS Pro 4-BT 2000). Bare graphite rod was used as counter electrode; PPy (control), PPy-noble metal nanocomposites (1-2 mg) and nanocarbon-noble metal nanocomposites (1-2 mg) were uniformly decorated on the tip of the graphite rod electrode with carbon colloids paste to fabricate three types of working electrode, respectively. Saturated Calomel Electrode (SCE) was used as the reference electrode. Tests were conducted by cycling the potential between -0.8V to 0.4V vs. SCE in 1M aq. KOH solution, 5 vol.% of CH_3OH. The scan rate was set at 20mV/s.

The discharge capacity of the PPy-Pt catalysts was measured by modifying the graphite electrode with these catalysts and subjecting the modified electrode to CV test in the same three-electrode cell configuration. Pt wire was used as the counter electrode and Ag/AgCl electrode was used as the reference. The CV characteristic of the modified electrode was measured in 1M KCl solution with a cyclic range of -0.8V-0.8V at a scan rate of 50 mV/s. The discharge capacity of the PPy-Pt catalysts was measured simultaneously as the CV characteristic of the modified electrode was recorded.

4.2.6. Microwave synthesis of Nanocarbon-Noble Metal Nanoparticle (NCNMN) composites from PPy Nanofiber-Noble Metal Nanoparticle (PNNMN) composites

50 mg of the as-synthesized nanocomposite material were placed in a glass vial and then irradiated in a conventional microwave oven, under ambient condition for 5-6 min. Sparks were observed at nanocomposite surfaces during microwave heating. It is found from the field emission scanning electronic microscopy (FE-SEM) that the morphology of NCNMN is consistent with its microwave precursor PNNMN.

4.2.7. Cyclic Voltammetry Measurement of PPy-Ag/G and C-Ag/G Electrodes

The cyclic voltammetry measurement (CV) was performed on the BT 2000 testing system (Arbins' Instrument). A conventional three electrode cell was constructed to conduct the CV measurement. A PPy-Ag/G or C-Ag/G electrode was used as the working electrode, while a platinum wire was used as the counter and Ag/AgCl as the reference. The CV measurement was performed in 10 mM phosphate buffer solution (PBS) with a cyclic range from -0.8-0.2 V and a scan rate of 20 mV/s. PBS solution without and with the existence of

H_2O_2 at various concentrations (0-3.0 mM) was subject to the CV measurement, and the corresponding electrode responses were recorded subsequently.

4.2.8. Amperometric Measurement of PPy-Ag/G and C-Ag/G Electrodes

The BT 2000 testing system connected with a conventional three electrode cell was utilized to perform the amperometric measurement. A PPy-Ag/G or C-Ag/G electrode was used as the working electrode while a platinum wire was used as the counter and Ag/AgCl as the reference. The cell voltage was kept at -0.45 V and 20 minutes' stabilized time was allowed at the beginning of each amperometric measurement. The measurements were performed in 10 mM PBS solution under constant stirring and H_2O_2 with different concentrations were successively injected into the testing solution at an increment of 0.1 mM (0.1-1.6 mM). The electrode response was taken as the difference between the steady-state and background current.

4.3. Results and Discussion

The initial oxidation potentials of both AuCl and $HAuCl_4.3H_2O$ solution are around 0.9V, which are ready to polymerize pyrrole monomer to PPy granules. With the addition of V_2O_5 nanofibers, there is not much enhancement for the existing potentials of Au cations, but the morphology of PPy is changed from irregular granules to homogeneous nanofibers. As a result, Au cations were reduced to corresponding metal nanoparticles. Regarding to $PtCl_2$ and $PtCl_4$ systems, the situation is different. The initial potentials of $PtCl_2$ and $PtCl_4$ are around 0.3V and 0.6V respectively. The addition of V_2O_5 will enhance both the oxidation potentials (Figure 4.2 C, D) by about 0.1V for $PtCl_2$ system and 0.005V for $PtCl_4$ system, which could assist the polymerization process. Thus it could be concluded that V_2O_5 nanofibers could

direct the formation of the nanofibrillar morphology, possibly due to its oxidizing ability of pyrrole to the formation of nanofibriller oligomers.[1] As a comparison, the sequence of adding reagents can be exchanged and further prove that the addition of V_2O_5 nanofibers at the early

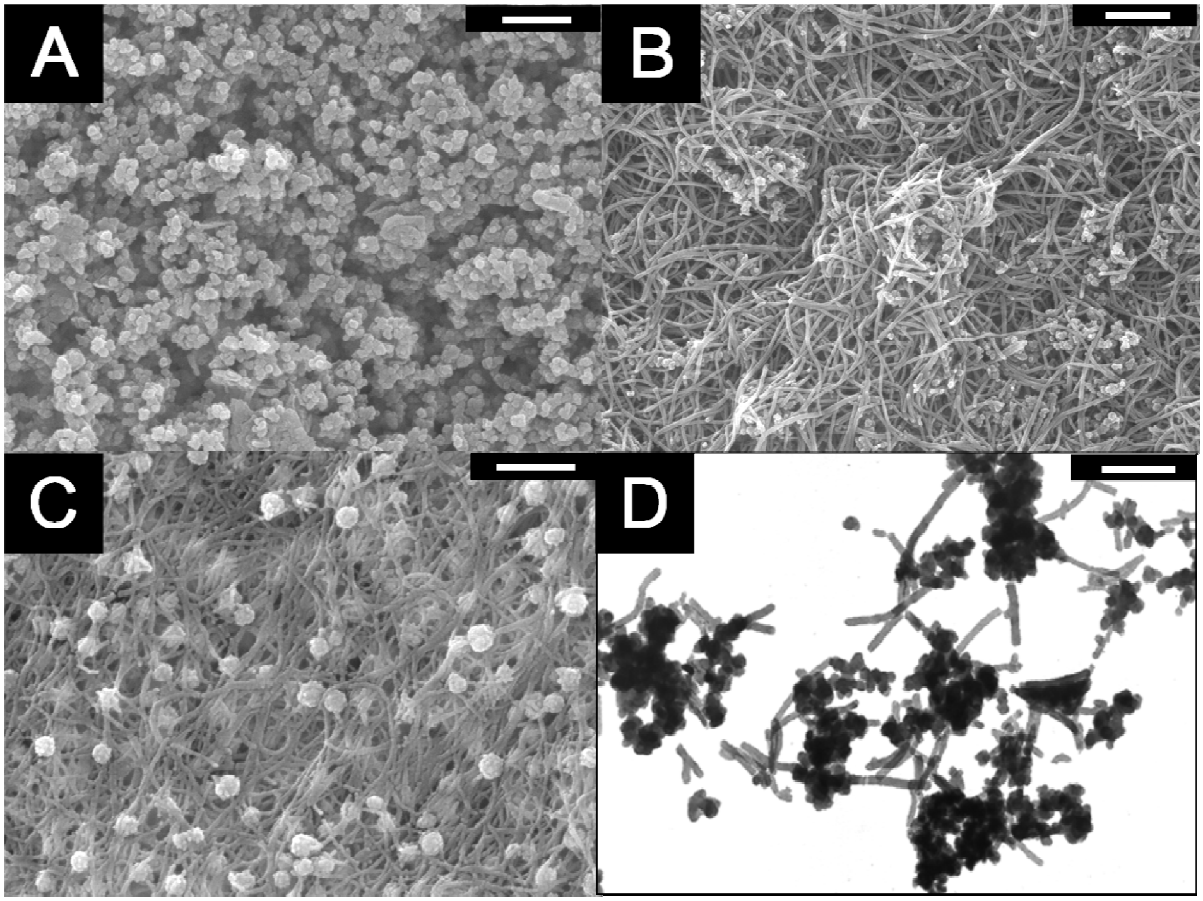

Figure 4.1. SEM images: (A) PPy granules oxidized by $PtCl_2$ without V_2O_5 seeds; (B) PPy/Au nanofiber composites from V_2O_5/pyrrole/AuCl system; (C) PPy/Pt nanofiber composites from V_2O_5/pyrrole/$PtCl_4$ system; and (D) TEM image of PPy/Pt nanofiber composites from V_2O_5/pyrrole/$PtCl_4$, scale bar: 500 nm.

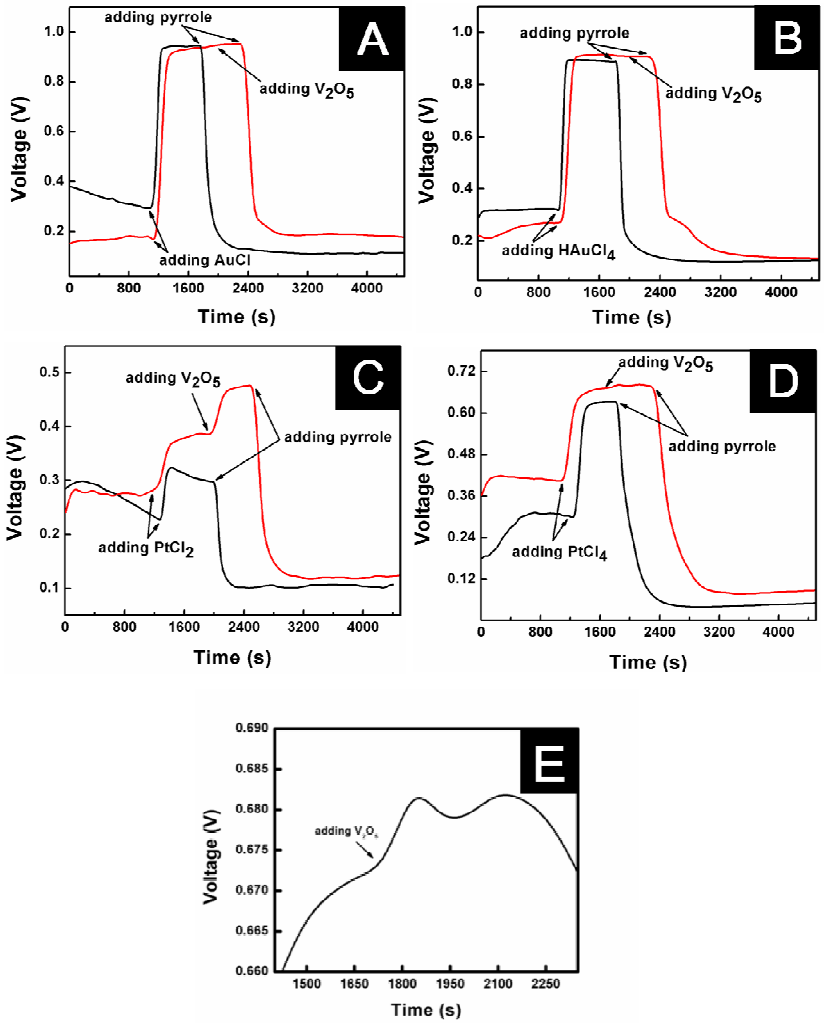

Figure 4.2. Potential-time profiles of pyrrole polymerization via different systems between seeding and non-seeding approach: (A) V_2O_5/pyrrole/AuCl; (B) V_2O_5/pyrrole/$HAuCl_4$; (C) V_2O_5/pyrrole/ $PtCl_2$; and (D) V_2O_5/pyrrole/$PtCl_4$; (E) a zoom-in view of oxidation potential increment by adding V_2O_5 to pyrrole/$PtCl_4$ system

state not only provide sufficient oxidation potential but also orchestrate the nano-fibrillar growth of polypyrrole.

From the SEM and HRTEM images of these PPy-Ag and PPy-Cu nanocomposites in Fig 4.3, the diameter of PPy is in the range of 50 to 80 nm (Figure 4.3A and 4.3C), and the HRTEM images (Figure 4.3B and 4.3D) reveal that the Ag and Cu have been dispersed and encapsulated within the PPy sheath.Energy-dispersive X-ray spectroscopy (EDX) has been conducted to provide the elemental analysis of these composites, it is found that the loading ratio of silver and copper nanoparticles in PPy is in the range of 40-50wt.% (Table 1), which varies with different types of metals and the initial concentrations of each cations.

It is found that other than the main seeding role V_2O_5 usually played in noble metal solution systems,[1-3] the solution oxidation potential of copper or silver aqueous solutions can be actually enhanced well pass the oxidation threshold to expedite oxidation of pyrrole with just catalytic amount of V_2O_5 nanofibers. In-situ monitoring of the polymerization reactions by Open Circuit Potential (OCP) measurement reveals the oxidation profiles throughout the polymerization process.In fact, the oxidation potentials of $AgNO_3$ and $CuCl_2$ solutions are in the range of 0.225 V to 0.300 V, which is impotent to initiate the pyrrole polymerization in an acceptable time manner.[12] However, V_2O_5 nanofibers can play as a critical enhancer, to promote the solution oxidation potential right above 0.450 V, which accelerate the pyrrole polymerization in a big way. Meanwhile, the as-synthesized PPy has homogeneous nanofibrillar morphology, due to the seeding effect of the V_2O_5 nanofibers.

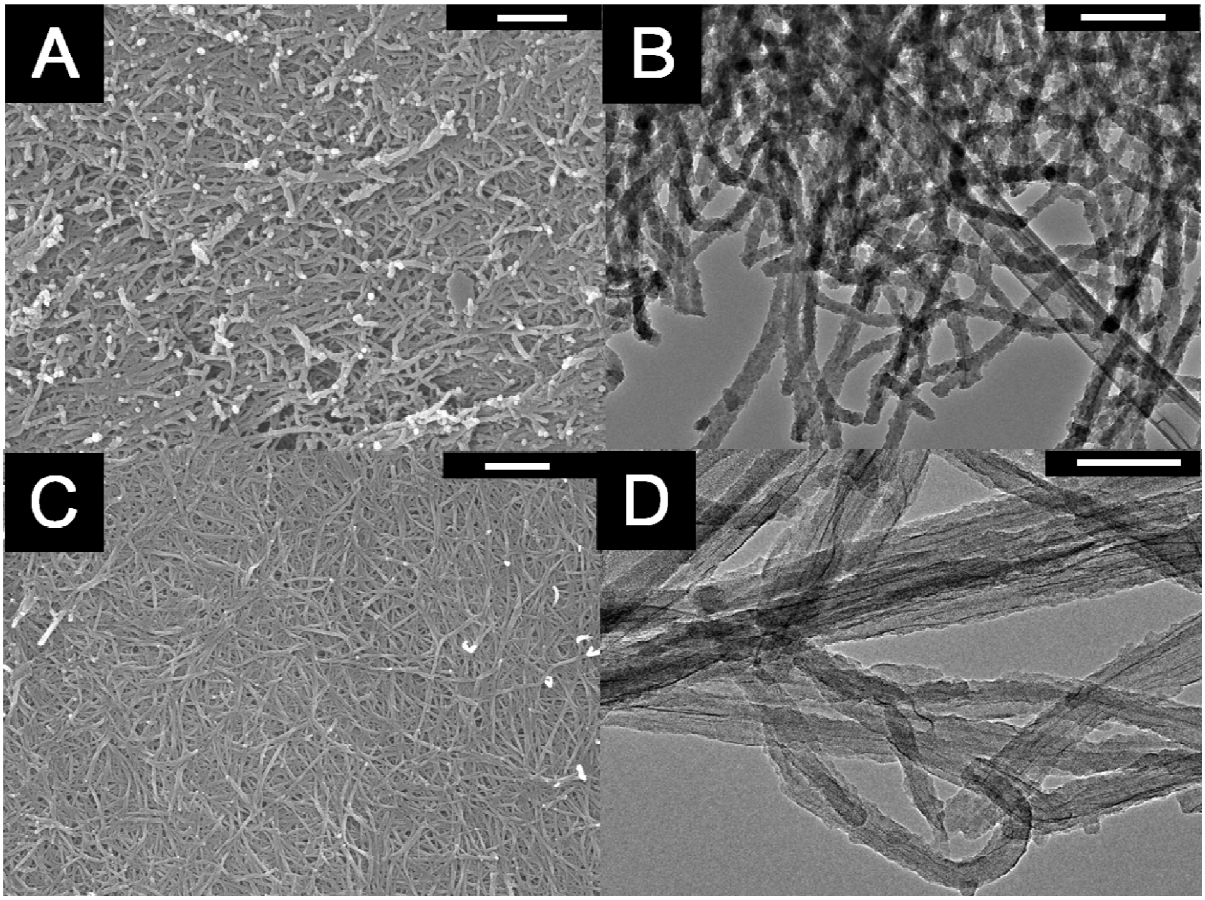

Figure 4.3. SEM images of: (A) PPy/Ag nanofiber composites from V_2O_5/pyrrole/$AgNO_3$ (0.02M); (C) PPy/Cu nanofiber composites from V_2O_5/pyrrole/$CuCl_2$ (0.02M); and TEM images of: (B) PPy/Ag nanofiber composites from V_2O_5/pyrrole/$AgNO_3$ (0.02M); (D) PPy/Cu nanofiber composites from V_2O_5/pyrrole/$CuCl_2$ (0.02M). Scale bar: 500 nm

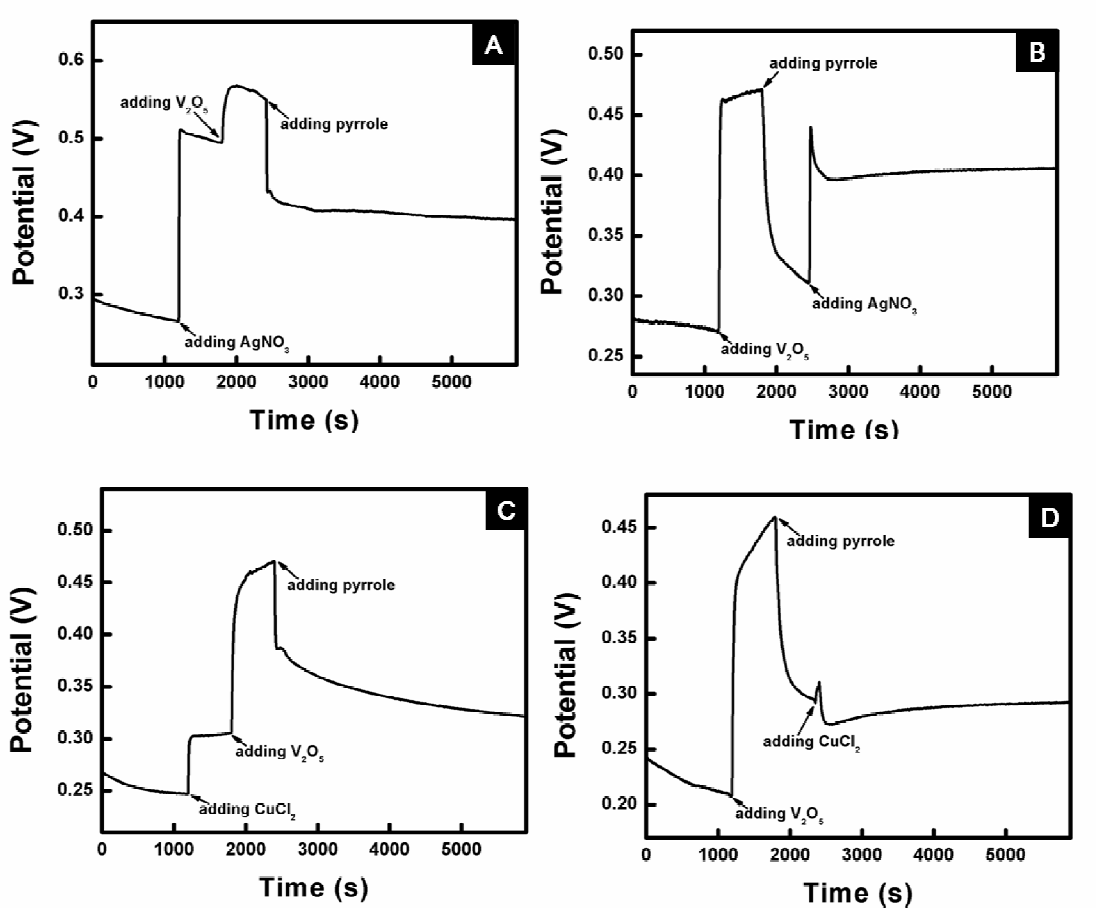

Figure 4.4. Potential-time profiles of pyrrole polymerization via different systems in different reagent addition sequences: (a) $AgNO_3/V_2O_5$/pyrrole (0.02M); (b) V_2O_5/pyrrole/$AgNO_3$ (0.02M); (c) $CuCl_2/V_2O_5$/pyrrole (0.02M); (d) V_2O_5/pyrrole/$CuCl_2$ (0.02M)

These PNNMN composites can be applied as precursors for microwave-assisted nanocarbonization, resulting in nanocarbon-noble metal composites.[23] Aiming to initiate nano-carbonization, the PPy/noble metal nanocomposites were processed by a standardized microwave heating procedure: 50 mg of the as-synthesized nanocomposite material were placed in a glass vial and then irradiated in a conventional microwave oven, under ambient

condition for 5-6 min. Sparks were observed on the surfaces of the nanocomposites, which became red hot as an indication of very high temperature.[23]As a result, the PPy nanofiber network will lose the heteroatoms of the polymer backbones and be converted to carbon nanofiber network.[23] It is also worthy of noting that variation of oxidation potentials offered by different metal ions will affect final products' conductivity,[24] which is directly associated with its microwave activity. For example, the nanocarbon-Pt composite made from the PPy/Pt precursor using microwave heating, did not show significant difference in the FTIR spectra (Figure 4.7) comparing to the original precursor. The low oxidative potential of $PtCl_2$ system may yield PPy with lower conductivity, which results in incomplete nanocarbonization of PPy. This is consistent with the FTIR spectra.

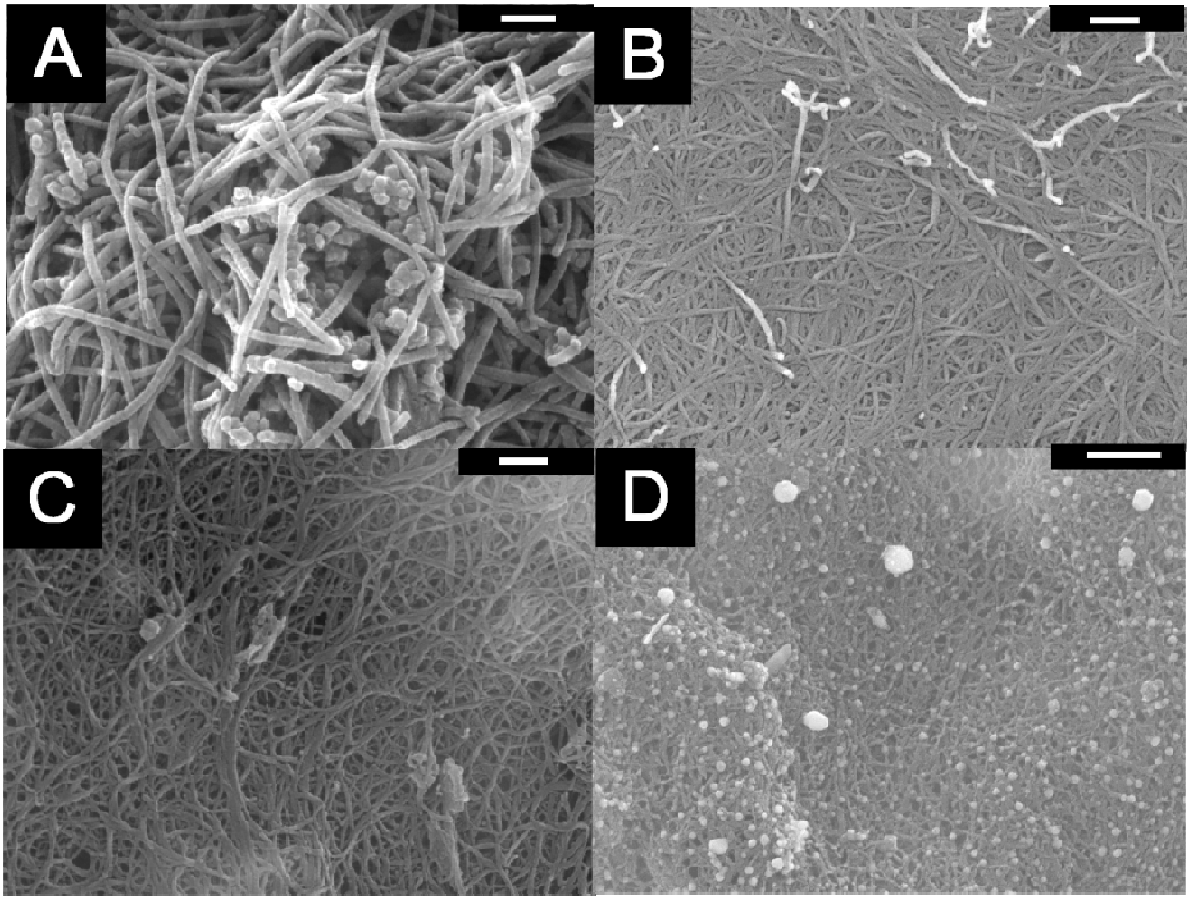

Figure 4.5. Polypyrrole-noble metal nanofiber composites (before and after microwave) SEM images from: (a) V_2O_5/pyrrole/AuCl system before microwave; (b) V_2O_5/pyrrole/AuCl system after microwave; (c) V_2O_5/pyrrole/$HAuCl_4$ system before microwave; and (d) V_2O_5/pyrrole/$HAuCl_4$ system after microwave, scale bar: 500 nm.

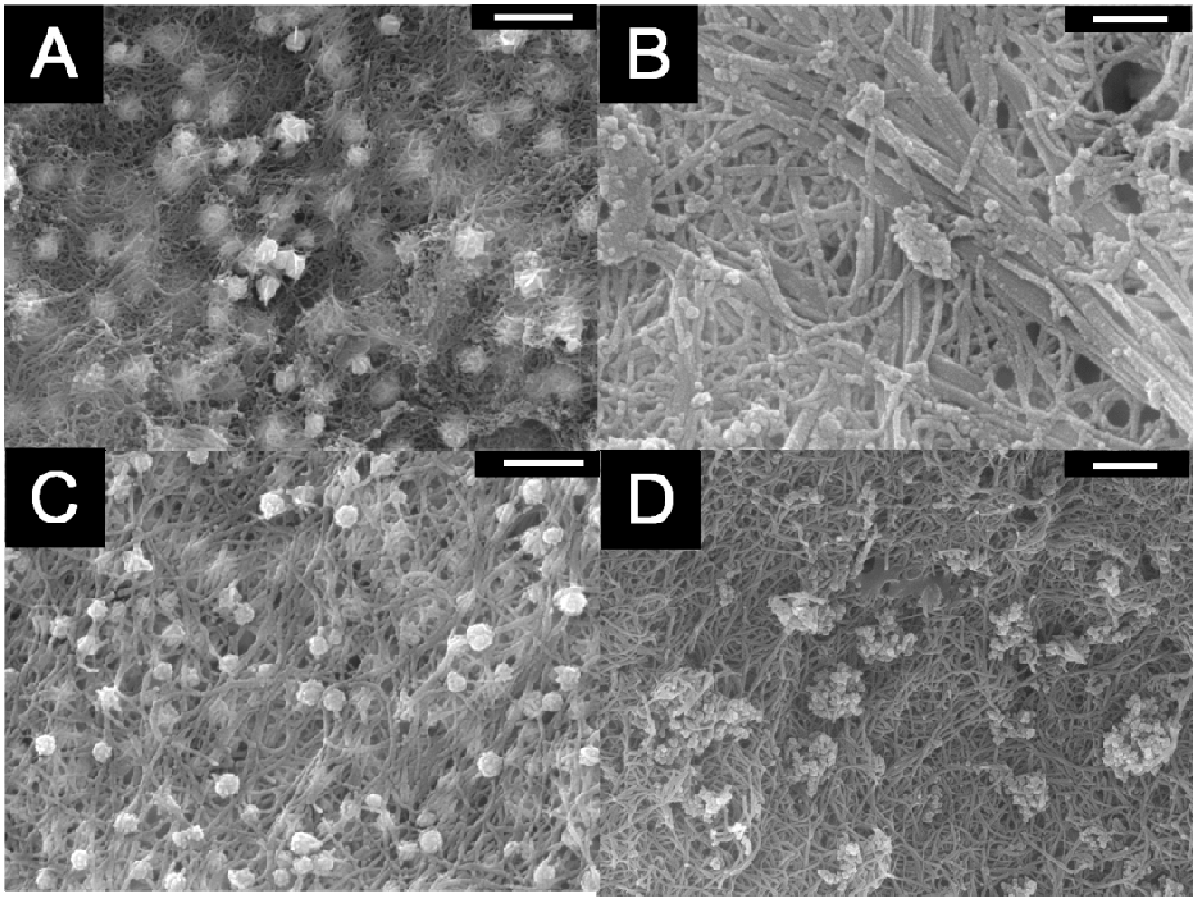

Figure 4.6. Polypyrrole-noble metal nanofiber composites (before and after microwave) SEM images from: (a) V_2O_5/pyrrole/$PtCl_2$ system before microwave; (b) V_2O_5/pyrrole/$PtCl_2$ system after microwave; (c) V_2O_5/pyrrole/$PtCl_2$ system before microwave; and (d) V_2O_5/pyrrole/$PtCl_2$ system after microwave, scale bar: 500 nm.

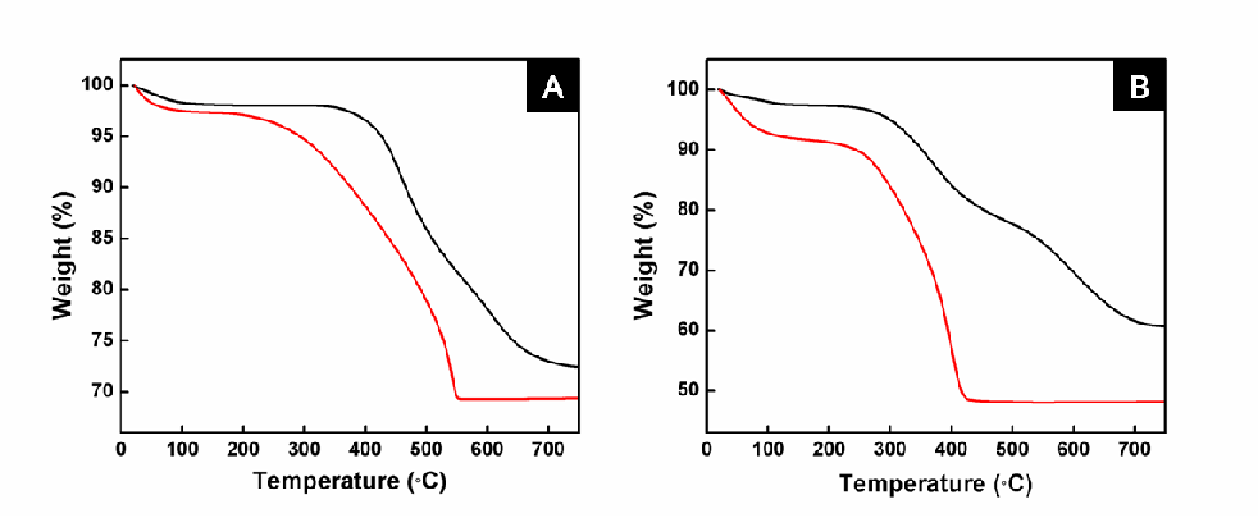

Figure 4.7. Thermogravimetric Analysis (TGA) of (A) PPy-Au nanofiber composites (V_2O_5/pyrrole/AuCl system) before (red) and after (black) microwave heating and (B) PPy-Pt nanofiber composites (V_2O_5/pyrrole/$PtCl_4$ system) before (red) and after (black) microwave heating. Heating rate: 10°C/min, under N_2 flow.

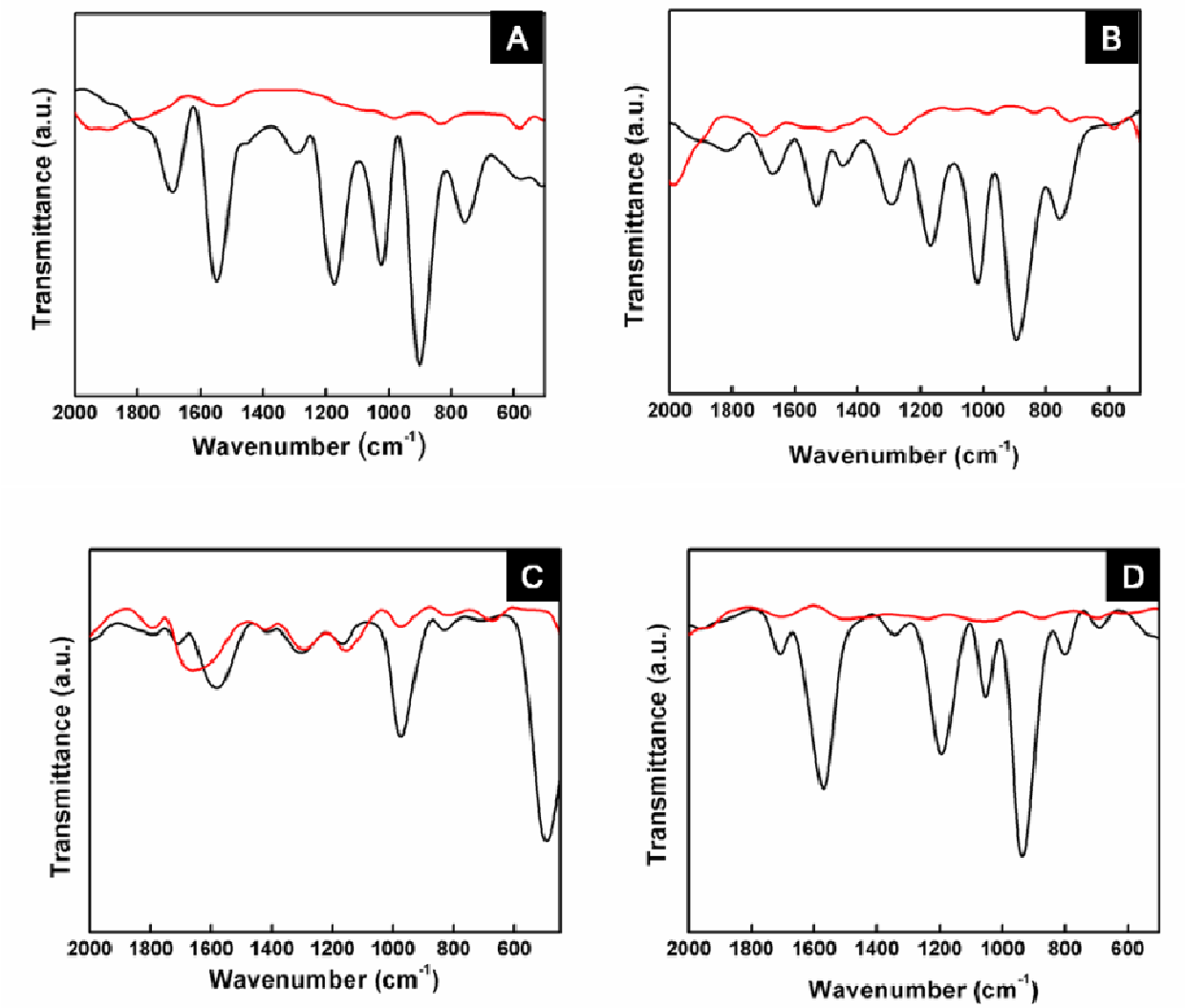

Figure 4.8. FTIR of (A) PPy-Au nanocomposites from V_2O_5/pyrrole/AuCl system, before (black) and after (red) microwave heating; (B) PPy-Au nanocomposites from V_2O_5/pyrrole/$HAuCl_4$ system before (black) and after (red) microwave heating; (C) PPy-Pt nanocomposites from V_2O_5/pyrrole/$PtCl_2$ system before (black) and after (red) microwave heating; (D) PPy-Pt nanocomposites from V_2O_5/pyrrole/$PtCl_4$ system before (black) and after (red) microwave heating

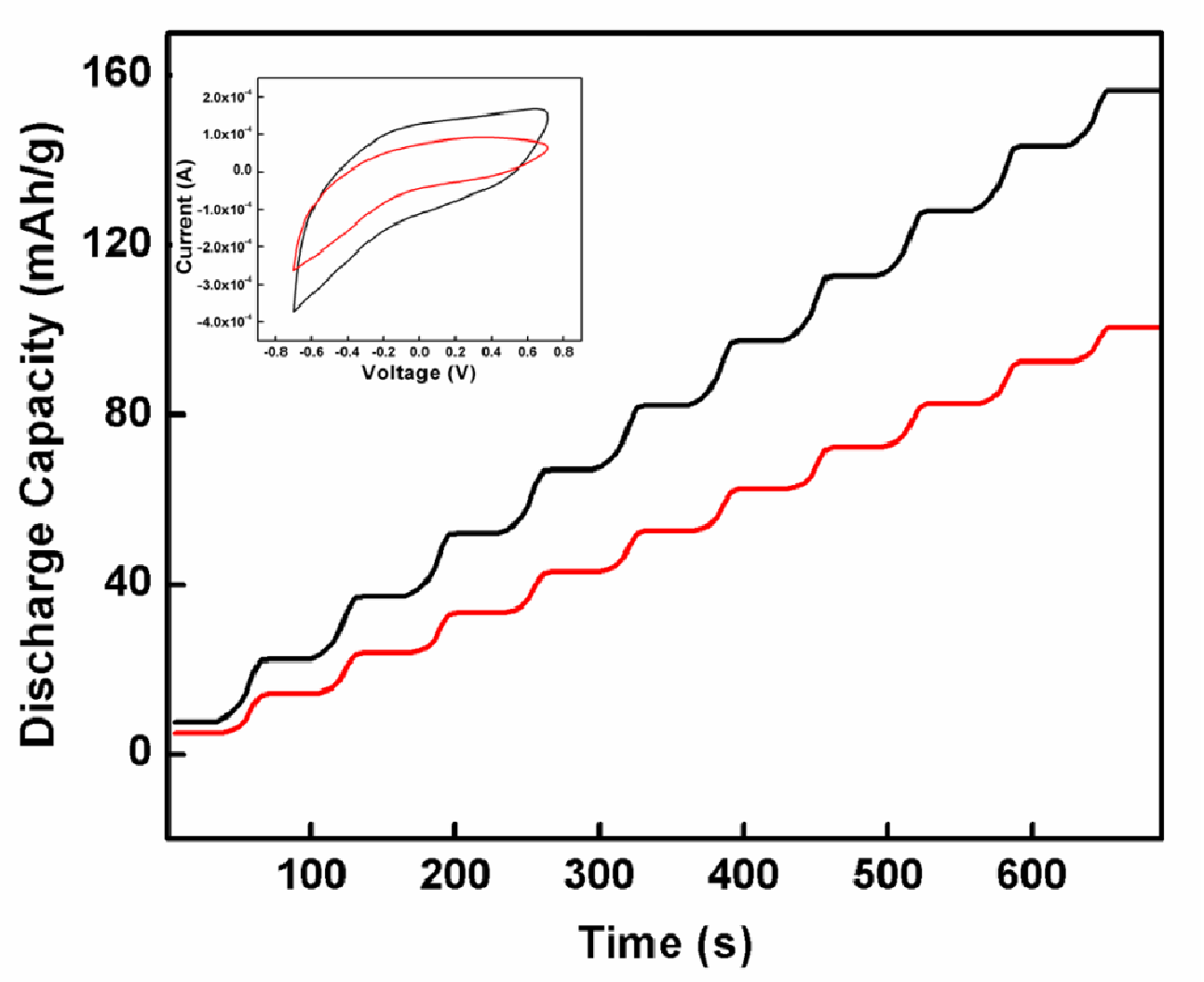

Figure 4.9. Discharge capacity plot of PPy-Pt nanofiber composites before (red) and after (black) microwave heating in the range of -0.8-0.8V (vs. Ag/AgCl) in aqueous 1.0 M KCl electrolyte. Inset: cyclic voltammograms of PPy-Pt nanofiber composite before (red) and after (black) microwave in the range of -0.8-0.8V (vs. Ag/AgCl) in aqueous 1.0 M KCl electrolyte.

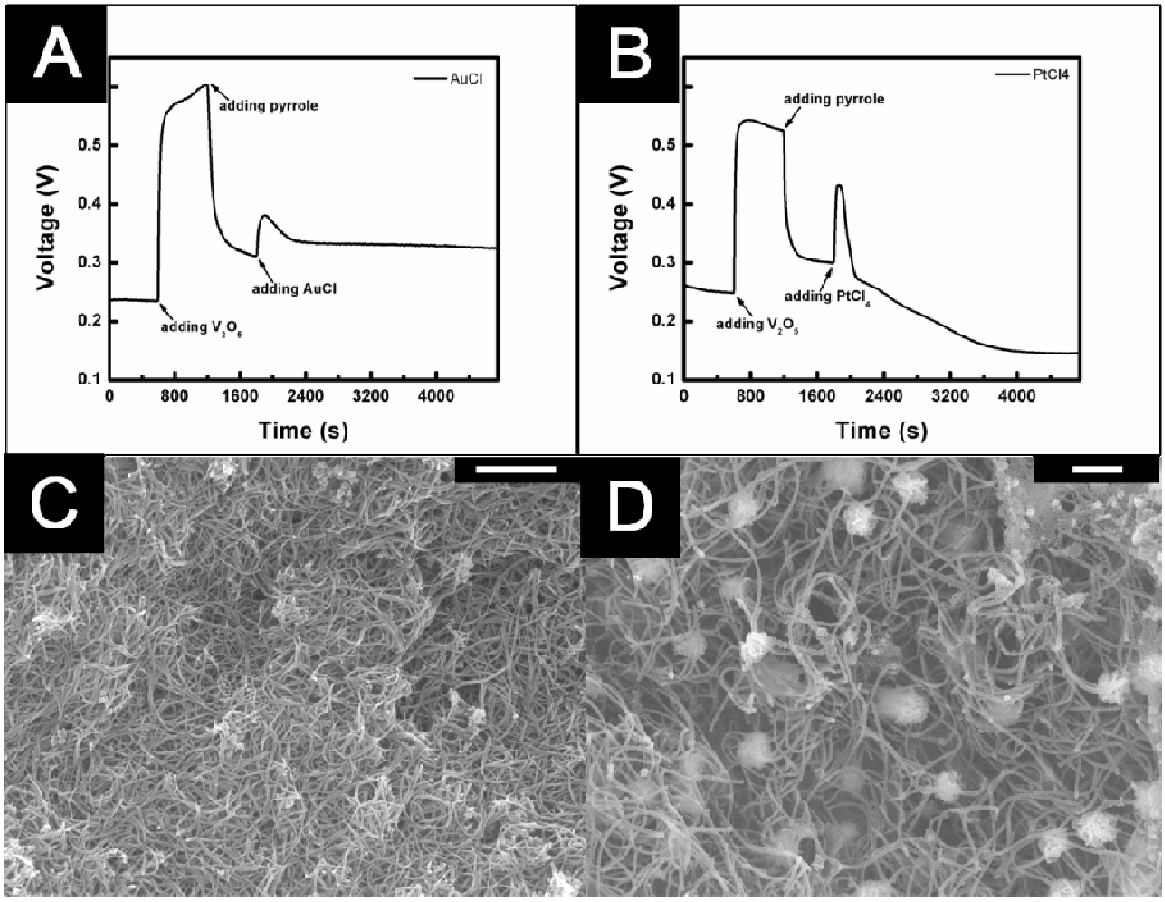

Figure 4.10. Potential-time profiles of pyrrole polymerization via different reagent addition sequences: (a) V_2O_5/pyrrole/AuCl sequence; (b) V_2O_5/pyrrole/$PtCl_4$ sequence; Polypyrrole-noble metal nanofiber composites SEM images from: (c) V_2O_5/pyrrole/AuCl system; (d) V_2O_5/pyrrole/$PtCl_4$ system. Scale bar: 500 nm

Table 4.1. EDX data of the nanocomposites made in noble metal systems

Systems	C	N	O	Cl	V	Au / Pt	Total
V_2O_5/Pyrrole/AuCl 0.005M	34.98	9.93	4.96	0.69	-0.10	49.54	100
V_2O_5/Pyrrole/AuCl 0.01M	36.59	9.17	5.44	0.97	-0.17	47.99	100
V_2O_5/Pyrrole/AuCl 0.02M	30.26	8.69	4.03	1.80	0.07	55.14	100
V_2O_5/Pyrrole/$HAuCl_4$ 0.005M	43.42	14.50	5.08	2.00	0.16	34.83	100
V_2O_5/Pyrrole/$HAuCl_4$ 0.01M	39.26	10.09	2.89	2.35	0.24	45.17	100
V_2O_5/Pyrrole/$HAuCl_4$ 0.02M	43.45	9.05	4.92	4.48	-0.02	38.14	100
V_2O_5/Pyrrole/$PtCl_2$ 0.005M	32.44	6.73	10.78	8.61	6.22	35.21	100
V_2O_5/Pyrrole/$PtCl_2$ 0.01M	29.42	5.91	9.10	11.07	2.75	41.76	100
V_2O_5/Pyrrole/$PtCl_2$ 0.02M	27.79	4.96	5.28	12.86	0.93	48.18	100
V_2O_5/Pyrrole/$PtCl_4$ 0.005M	34.39	6.37	7.19	9.37	0.18	42.50	100
V_2O_5/Pyrrole/$PtCl_4$ 0.01M	38.24	5.38	5.45	9.06	0.20	41.68	100
V_2O_5/Pyrrole/$PtCl_4$ 0.02M	33.34	9.16	5.31	9.99	0.20	41.99	100

We believe this discovery of the novel metal displacement reactions and the consequent process with microwave will play an important role in the development of nano-structured polymer/carbon-noble metal nanoparticles composites, which can be used as next-generation catalyst materials and energy storage devices, such as fuel cell membranes. Nanoparticles of Au and Pt exhibit high specific area of active surfaces, and therefore will improve the catalytic efficiency, which in general, offers promising insights to make low-loading catalyst systems.[25] In return, these systems will be attractive for fuel cell applications due to lowering of the cost.[25] Moreover, nanofibrillar network composed of conducting PPy will make an efficient supporting layer for the noble metal catalysts, largely due to the ease of the electron transfer between the noble metals and the "synthetic metals", which would enhance the

catalytic properties and stability of the nanocomposites by reducing conduction energy loss.[25] Upon microwave treatment, PNNMN composites will be converted into nanocarbon-noble metal composites, which possesses better thermal and electrochemical stability,[23] and this conversion may enhance the overall catalytic performance of the noble metal nanoparticles.

In order to test our hypothesis, methanol (MeOH) sensing was examined using these as-synthesized nanocomposites through a cyclic voltammetry (CV) technique. Graphite rod was used as the bare working electrode (BWE); PPy (control), PNNMN composites and nanocarbon-noble metal nanocomposites (1-2 mg) were uniformly decorated on the tip of the graphite rod electrode with carbon colloids paste to fabricate three types of working electrodes, respectively. The CV measurements were conducted in 1M aq. KOH solution, with 5 vol.% of MeOH. Another bare graphite rod was used as counter electrode and Saturated Calomel Electrode (SCE) was used as reference electrode. As shown in Figure 3, the BWE and PPy decorated BWE have no oxidative peaks of MeOH, while the PPy-Pt nanocomposites decorated BWE have characteristic peaks for MeOH oxidation, e.g., the peak at the forward cycle (-0.082V) represents the oxidation of MeOH, and the second oxidation peak at the reverse cycle (-0.301V) indicates the oxidation of CO. The positions of these oxidation peaks are consistent to the previous reports.[26] Interestingly, after the conversion of

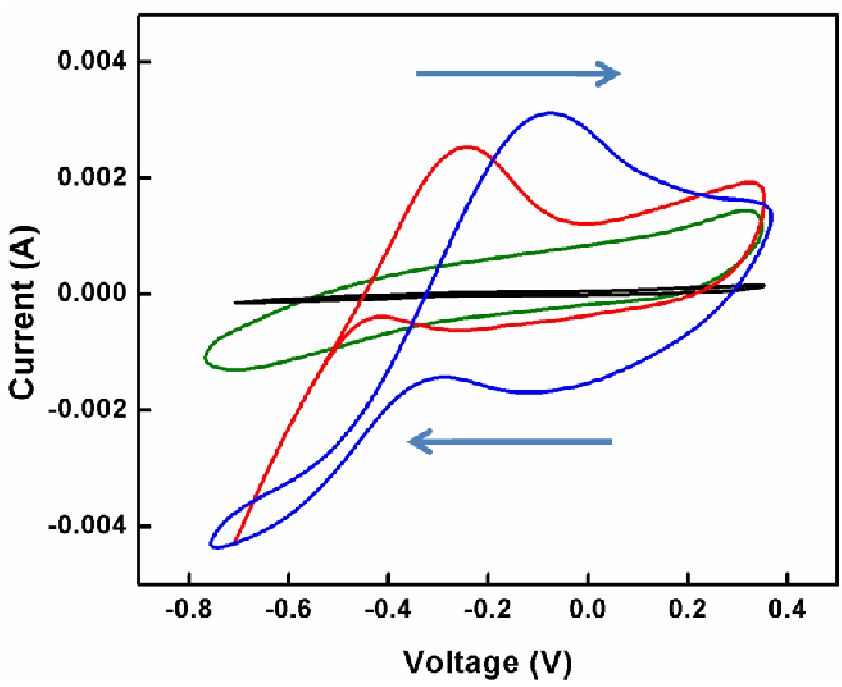

Figur 4.11. Cyclic voltammograms: Black: bare graphite electrode; Green: PPy nanofiber on graphite electrode; Blue: PPy nanofiber-Pt nanoparticles on graphite electrode; Red: microwave heated PPy nanofiber-Pt nanoparticles on graphite electrode.

PPy-Pt to nanocarbons-Pt using microwave, the potentials for the oxidation of MeOH and CO shifted to more negative positions: -0.241V and -0.411V, respectively. The reduced onset potentials could be caused by the enhanced electron donor-acceptor interactions between the noble metal nanoparticles and the microwave-produced nanocarbon supports, which could facilitate easier transfer of the charges within the electrodes and reduce the resistance. The lowered resistance in the electrode will result in reduced onset potential.[27] This lowered resistance or improved conductivity of the nanocarbon-noble metal composite could also be evidenced by its improved discharge capacity (Figure S9), which substantially indicates

better electron transfer efficiency of the hybrid materials, compared to the PPy nanofiber-noble metal composite.[28]In addition, the specific surface area has been increased upon microwave heating,[23] which may improve the contact between the nanocarbons supported Pt catalyst and the MeOH-KOH electrolyte solution. Improved electronic interaction of the nanocarbon support to Pt catalyst could be another reason for the reduced onset oxidative potential for MeOH, which may assist in the enhancement of the fuel cell efficiency.[29,30]

Sensing of hydrogen peroxide (H_2O_2) has been extensively studied due to H_2O_2 has been established and recognized as an essential regulator of eukaryotic signal transduction, which further function as a critical molecule during various biological process studies.[13] Nanostructured silvers, e.g. silver nanoparticles have long been proved to possess excellent sensory properties towards H_2O_2, and have been widely utilized to fabricate varying kinds of non-enzymatic H_2O_2 sensors.[14-16] Sensory response of the Ag NPs towards H_2O_2 is expected to be enhanced upon immobilizing onto the highly conductive substrates such as conducting polymers and CNTs, possibly due to the accelerated electron transfer process on the electrode-electrolyte interface.[17, 18] Therefore, in order to investigate the sensory properties of the as-synthesized PPy-Ag nanocomposites towards H_2O_2, and the possible interactions withthe metal nanostructures, a PPy-Ag modified graphite electrode (PPy-Ag/G) was fabricated and subject to the amperometric detection of H_2O_2.Figure 3A shows the as-obtained CVs of the PPy-Ag/G electrode with different H_2O_2 concentrations in PBS solution. A pair of redox peaks located at 0.1 V and -0.05 V, observed according to the CVs, which could be ascribed to the transitions of Ag^0/Ag(I), and Ag(I)/Ag^0, respectively.[19] On the other hand, a pair of broad anodic and cathodic waves, which center at -0.25 V and -0.45

V accordingly, is also shown on the CVs. However, the anodic wave at -0.25 V is possibly arisen from the oxidation of polypyrrole and the ingression of anions/expulsion of cations; while the cathodic wave at -0.45 V could be ascribed to the reduction of polypyrrole as well as the expulsion of anions/ingression of cations.[20, 21] The observation that both features of Ag NPs and polypyrrole are presented in the CVs thus indicating strong interaction between the nanodeposite (Ag NPs) and the polymer support (PPy),[19] possibly through the synergistic electronic interactions between Ag NPs and the conducting polymer support. Nonetheless, a continuous increase in the cathodic current density of the CVs could be clearly observed with the increasing H_2O_2 concentration, which indicates the notable electrocatalytic activities of the PPy-Ag towards the reduction of H_2O_2, possibly due to the synergistic amplification effect of the PPy-Ag interaction, along with the electrocatalytic properties of the Ag NPs towards H_2O_2.[15] Figure 3B shows the amperometric response of the PPy-Ag/G electrode upon successive addition of H_2O_2. The detection potential was set at -0.45 V, for most of the Ag NP-based sensory materials for H_2O_2 exhibit characteristic peak current around -0.45 V, and a relatively low over-potential could be attained for the detection of H_2O_2.[14-16] However, rapid response of the PPy-Ag/G electrode corresponding to each addition of H_2O_2 could be observed, as the amperometric current increases and reaches the steady state within 5s. The electrode also shows a linear response to H_2O_2 from 0.1-1.6 mM, with a correlation coefficient of 0.991 and a sensitivity value of 208.8 μA/mM, which are demonstrated by the calibration curve (Figure 3B: inset). The sensitivity is sufficiently high as it surpasses a plenty of other electroactive materials for H_2O_2 demonstrated before.[15, 22] Thus it could be inferred from the amperometric test result that the PPy-Ag/G electrode obtains notable sensory properties according to amperometric detection of H_2O_2, indicating

considerable application potential for the PPy-Ag nanocomposite as electrode material for the fabrication of H_2O_2 sensors.

It has been reported that the conducting polymer-metal composite could be converted to the nanocarbon-metal composite upon microwave irradiation.[23] Thermogravimetric Analysis (TGA) tests of the nanocomposites can further reflect the increment of carbon concentration from the microwave heat treatment. It is noted from both the EDX and TGA that, microwave assisted carbonization takes place and is able to increase the carbon mass percentage approach to almost 95%, which reflects the strategy and technological ease of direct fabricate carbon-metal nanocomposites.

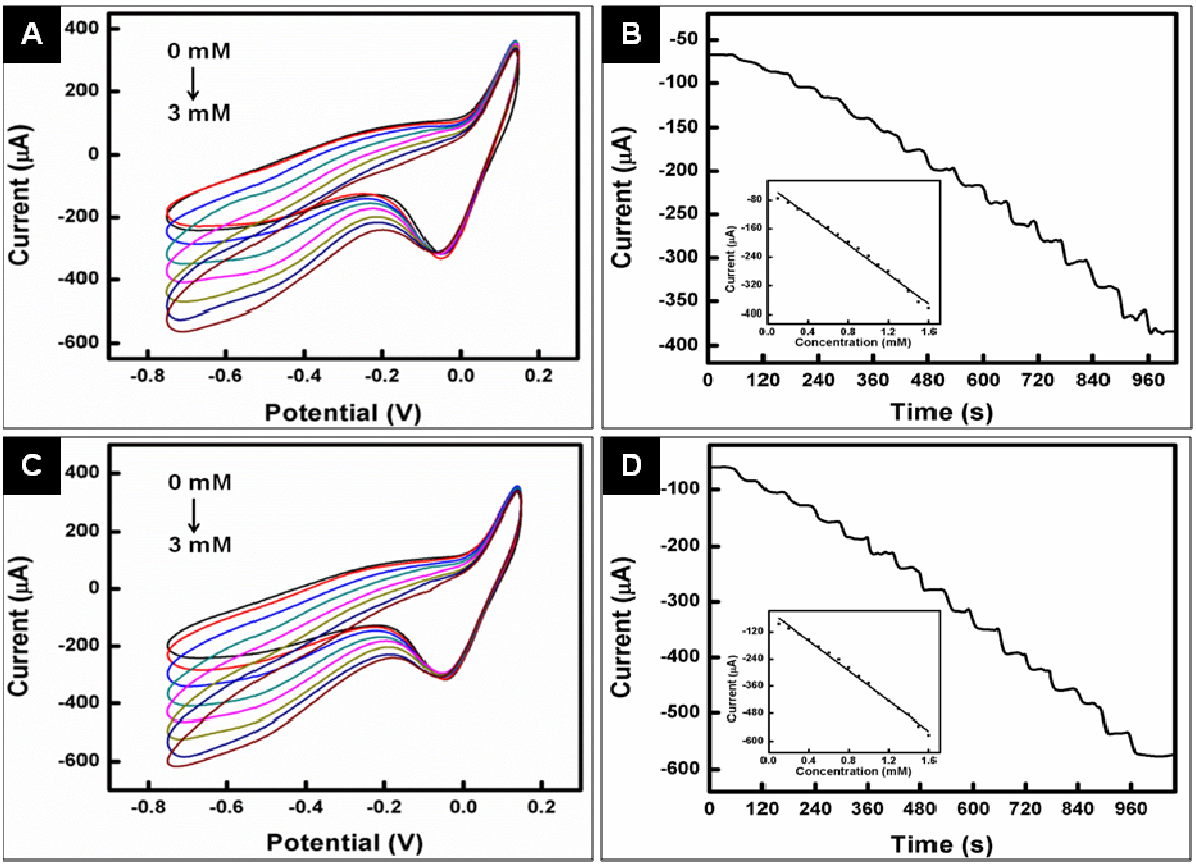

Figure 4.12. (A, C) Cyclic voltammograms (CVs) of PPy-Ag nanocomposite modified graphite electrode (PPy-Ag/G) and C-Ag/G electrode in 10 mM PBS solution in the absence and presence of H_2O_2 with different concentration (from top to bottom: 0, 0.1, 0.5, 1, 1.5, 2, 2.5, 3 mM). Scan reate: 20 mV/s. (B, D) Amperometric response of PPy-Ag/G electrode and C-Ag/G electrode upon successive addition of 0.1 mM (0.1-1.6 mM) in stirring 10 mM PBS solution. Applied potential: -0.45 V. Inset shows the corresponding calibration curves of the electrodes in the measured H_2O_2 concentration range.

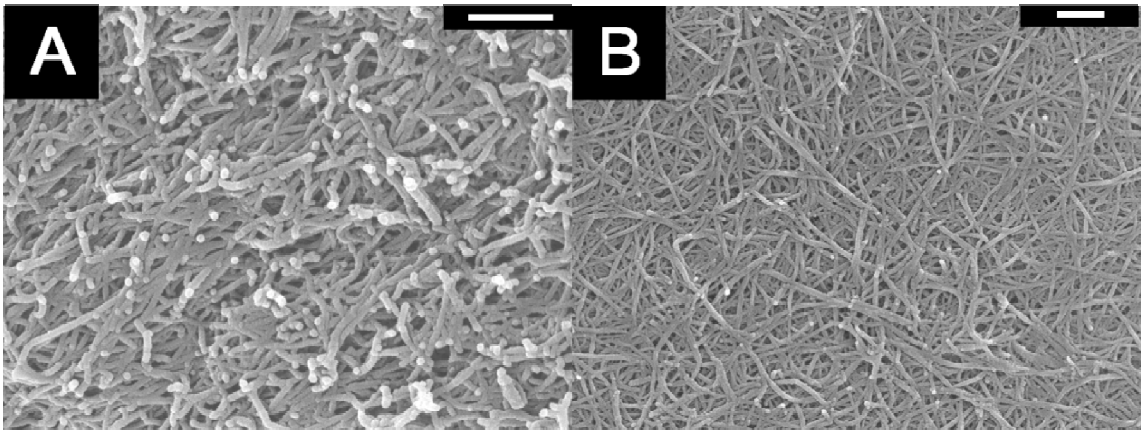

Figure 4.13. Microwave heated PPy/metal nanofiber composites: (a) $AgNO_3/V_2O_5$/pyrrole (0.02M); (b) $CuCl_2/V_2O_5$/pyrrole(0.02M).

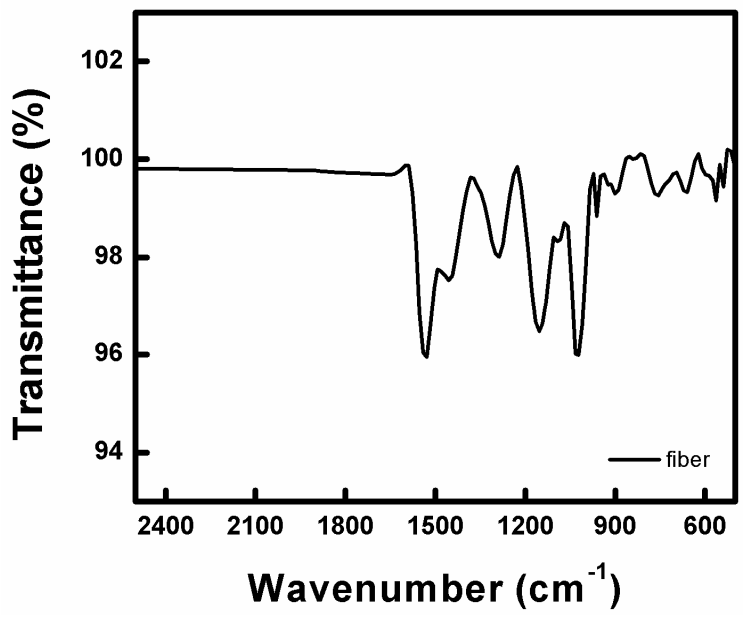

Figure 4.14. FTIR for PPy nanofiber.

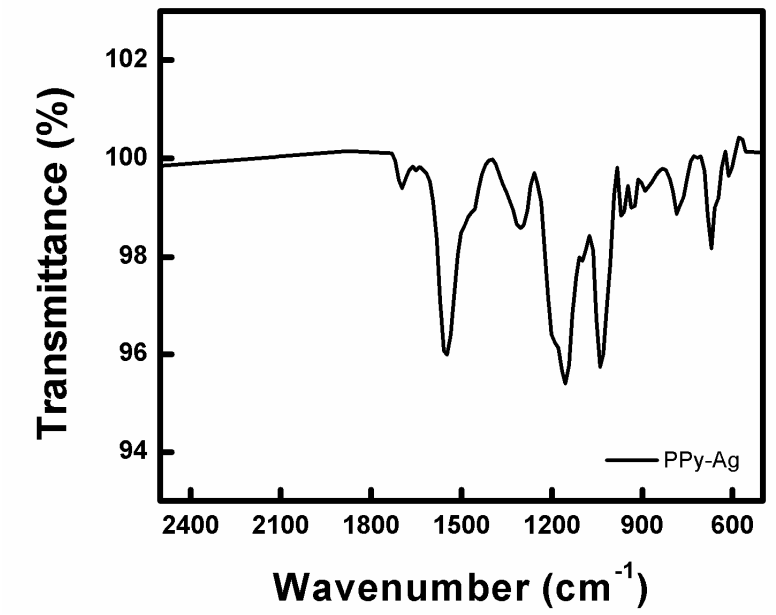

Figure 4.15. FTIR for PPy/Ag nanofiber composites

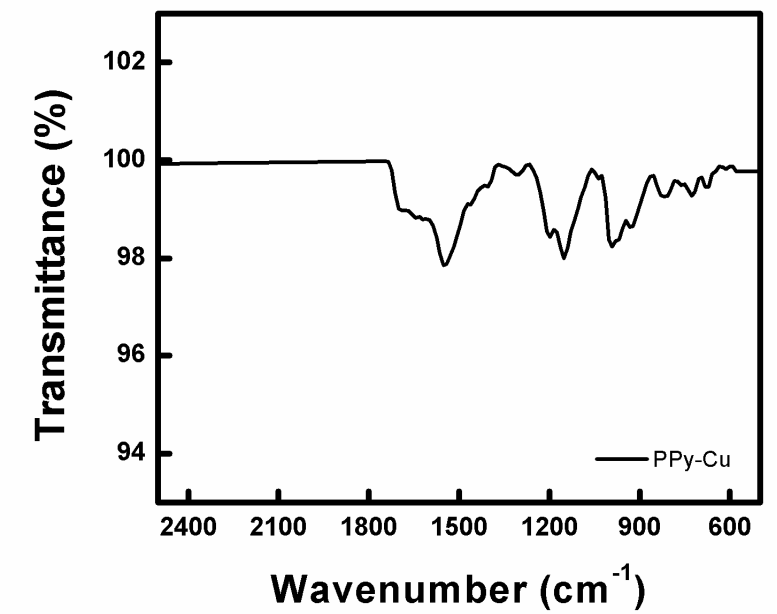

Figure 4.16. FTIR for PPy/Cu nanofiber composites

Table 4.2. EDX data of the nanocomposites made in transition metal systems

Systems	C	N	O	V	Ag / Cu	Total
V_2O_5/Pyrrole/$AgNO_3$ 0.02M	42.51	37.41	15.41	0.25	4.42	100
Microwaved V_2O_5/Pyrrole/ $AgNO_3$ 0.02M	85.54	0	0	1.18	13.28	100
V_2O_5/Pyrrole/$CuCl_2$0.02M	38.86	34.33	19.63	5.94	1.24	100
Microwaved V_2O_5/Pyrrole/$CuCl_2$ 0.02M	73.34	0	18.75	5.82	2.09	100

The conversion of conducting polymer support to nanocarbon support is supposed to enhance the overall performance of the nanocomposite, as nanocarbons (carbon nanotubes, carbon nanofibers, graphenes, etc.) generally obtain higher conductivity, stability, and processibility than conducting polymers.[24] In order to testify this speculation and evaluate the effect of microwave treatment, the PPy-Ag nanocomposite was subject to microwave irradiation with the method described previously.[23] The resulting electrochemical and sensory properties of this nanocarbon-Ag nanocomposite (C-Ag) were also measured in comparison with the PPy-Ag nanocomposite using a C-Ag modified graphite electrode (C-Ag/G). The as-obtained CVs for the C-Ag/G electrode in PBS with different H_2O_2 concentration could be viewed from Figure 3C. Compared to the ones of PPy-Ag/G electrode, a higher current density and a clearer peak separation could be observed for the C-Ag/G electrode, indicating accelerating electrode process of the C-Ag nanocomposite resulting from the enhanced conductivity and specific surface area of the nanocarbon support.[23] On the other hand, the amperometric response of the C-Ag/G electrode was also enhanced substantially compared to the PPy-Ag/G electrode. However, the electrode shows a linear response to H_2O_2 from 0.1-1.6 mM with a correlation coefficient of 0.994 and a sensitivity of 331.0μA/mM. Moreover, a decrease in noise could also be observed for

amperometric response of the C-Ag/G electrode. Nonetheless, the enhanced CV and sensory response of the C-Ag/G electrode could be unambiguously attributed to the relative higher conductivity and specific surface area of the nanocarbon support obtained after the microwave treatment, which thus enhances the C-Ag interaction through accelerated interfacial electron transfer process, similar to the case of carbon support platinum catalyst.[17, 18] The CV curve shape of C-Ag/G displays subtle changes compared with PPy-Ag, as the redox waves corresponding to PPy could still be observed. This phenomenon thus indicates the incomplete nanocarbon conversion upon the microwave treatment, only a small portion of the PPy chains have undergone the conversion whereas the large portion is still unaffected, as evidenced by the EDX analysis.

4.4. Conclusions

In summary, we have demonstrated for the first time (i) a novel concept of synthetic metal-noble metal displacement reaction; (ii) a facile, one-step approach to PPy/noble metal nanocomposites starting from monomer and noble metal salts; (iii) a concise displacement reaction between transition metals and synthetic metals (PPy) mediated by seeds V_2O_5 nanofiber and thus can afford to yield ultrathin conducting polymer-metal nanoparticle composite films; (iv) the "nanofiber seeding" method can be extended to make, in one step, conducting polymer nanofiber network deposited with noble metal nanoparticles; (v) PPy/Ag nanocomposites are excellent candidate to fabricate non-enzymatic H_2O_2 sensors; (vi) microwave heating assisted nano-carbonization leads to higher sensitivity could enhance the sensory properties of the nanocomposite to a significant extent. This study thus reveals the unprecedented application potential for the

novel nanostructured metal-polymer networks providing a number of noble pieces for toolbox of metallic nanoparicles/polymer composite fabrication and engineering, and will further impact on the futuristic electric composite materials structure and property development.

4.5. References

(1)Zhang, X.; Manohar, S. K. *J. Am. Chem. Soc.***2004**, *126*, 12714.

(2)Bailey, J. K.; Pozarnsky, G. A.; Mecartney, M. L. *J. Mater. Res.***1992**, *7*, 2530.

(3)Zhang, X.; Kolla, H. S.; Wang, X.; Raja, K.; Manohar, S. K. *Adv. Funct. Mater.***2006**, *16*, 1145-1152.

(4)Li, D.; Huang, J. ; Kaner, R. B. *Acc. Chem. Res.***2009**, *42*, 135.

(5)Yuan, J.; Muller, A. H. E. *Polymer***2010**, *51*, 4015.

(6)Peng, X.; Jin, J.; Ericsson, E. M.; Ichinose, I. *J. Am. Chem. Soc.***2007**, *129*, 8625.

(7)Peng, X.; Jin, J.; Ichinose, I. *Adv. Funct. Mater.***2007**, *17*, 1849.

(8)Huang, H.; Feng, X.; Zhu, J. *Nanotechnology***2008**, *19*, 7.

(9)Janata, J.; Josowicz, M. *Nat. Mater.***2003**, *2*, 19.

(10)de la Venta, J.; Pucci, A.; Pinel, E. F.; Garcia, M. A.; Fernandez, C. D. J.; Crespo, P.; Mazzoldi, P.; Ruggeri, G.; Hernando, A. *Adv. Mater.***2007**, *19*, 875.

(11)Yang, J.; Wu, J.; Wu, Y.; Wang, J.; Chen, C. *Chem. Phys. Lett.***2005**, *416*, 215.

(12)Duca, M.; Cucarella, M. O.; Rodriguez, P.; Koper, M. T. M. *J. Am. Chem. Soc.***2010**, *132*, 18042.

(13)Min, M.; Kim, C.; Lee, H. *J. Mol. Catal. A-Chem.***2010**, *333*, 6-10.

(14)Zhang, X.; Manohar, S. K. *J. Am. Chem. Soc.***2005**, *127*, 14156.

(15) Liu, Z.; Zhang, X.; Poyraz, S.; Surwade, S. P.; Manohar, S. K. *J. Am. Chem. Soc.***2010**, *132*, 13158.

(16) Wang, L.; Li, X.; Yang, Y. *React.& Funct. Polym.***2001**, *47*, 125.

(17) Pringle, J. M.; Winther-Jensen, O.; Lynam, C.; Wallace, G. G.; Forsyth, M.; MacFarlane, D. R. *Adv. Funct. Mater.***2008**, *18*, 2031.

(18) Feng, X.; Huang, H.; Ye, Q.; Zhu, J.; Hou, W. *J. Phys. Chem. C***2007**, *111*, 8463.

(19) Cao, H.; Xu, Z.; Sang, H.; Sheng, D.; Tie, C. *Adv. Mater.***2001**, *13*, 121.

(20) Zhang, J.; Shi, G.; Liu, C.; Qu, L.; Fu, M.; Chen, F. *J. Mater. Sci.***2003**, *38*, 2423.

(21) Hernandez, R. M.; Richter, L.; Semancik, S.; Stranick, S.; Mallouk, T. E. *Chem. Mater.***2004**, *16*, 3431.

(22) Liu, Z.; Liu, Y.; Poyraz, S.; Zhang, X. **2011**, *Chem. Commun.*, *47*, 4421.

(23) Zhang, X.; Manohar, S. K. *Chem. Commun.***2006**, 2477.

(24) Whang, Y. E.; Han, J. H.; Motobe, T.; Watanabe, T.; Miyata, S. *Synth. Met.***1991**, 45, 151.

(25) Antolini, E.; Gonzalez, E. R. *Appl. Catal.A-Gen.***2009**, *365*, 1.

(26) Rahim, M. A. A.; Hassan, H. B.; Hameed, R. M. A. *Fuel Cells***2007**, *7*, 298.

(27) Zhao, J.; Manthiram, A. *J. Electrochem. Soc.*,**2011**,*158*, B208.

(28) Wolfenstine, J.; Read, J.; Allen, J. L. *J. Power Sources* **2007**, *163*, 1070.

(29) Yu, X.; Ye, S. *J. Power Sources* **2007**, *172*, 133.

(30) Yu, X.; Ye, S. J. Power Sources **2007**, 172, 145.

Chapter 5

Microwave Initiated Ultrafast Carbon Nanotube Growth

5.1. Introduction

Carbon nanotubes (CNT) have drawn great deal of attention ever since Iijima discovered this new class of allotrope of carbon.[1] Due to its extraordinary mechanical, thermal and electrical properties, CNT has huge potential in the applications of composite materials,[2] smart structures,[3] chemical sensors,[4] energy storage[5] and nano-electronic devices.[6] However, the challenges remain in the high cost of CNT raw materials and the difficulty in its processing and applications. For example, vacuum or inert gas protection, high temperature and/or high energy density are always needed for the production of CNT, e.g., arc-discharge,[7] laser ablation[8] and chemical vapor deposition (CVD)[9] approaches, which make the cost of as-produced CNT remains high. In addition, strong van der Waals force induced poor solubility/dispersibility is another factor that restricts the application of CNT, especially in reinforcing composite materials.[10]

As an attempt to address the challenges mentioned above, some reports discussed to embed CNT into carbon fibers through conventional thermal heating process[11], and CVD methods [12], which can partially solve the dispersibility issue, but the reaction setup is still costly and complicated, and the process is time-consuming and energy inefficient due to the target-less volumetric heating.

The production of nanostructured carbon materials often requires high temperature,[40,41] high pressure[42] and high current[43]density processes, or in another words, it is an energy intensive process. The process temperature can be as high as 800-900ºC[40] in a thermal CVD approach, when producing sea urchin-like nanocarbons. Sometimes even higher temperature (> 1000ºC[41]) can be used to produce iron filled nanocarbon spheres. In HiPCo and arc discharge approaches to single walled carbon nanotubes, high pressure[44] and high current density[43] are always required. As a common practice, at this level of energy intensity, inert gas protection is always a must to prevent carbon elements being oxidized by the harsh experimental conditions. It's not very usual to see nanocarbon production under standard condition for temperature (20°C) and pressure (101.325 KPa, 1 atm), which is defined by National Institute of Standards and Technology (US). Due to its uniqueness of the heating process, microwave offers the opportunity to initiate the nanocarbonization process at room temperature, in the air with atmospheric pressure. Since microwave chemistry in dielectric heating to produce organic compounds[45] and inorganic nanomaterials[46] has been extensively reviewed and discussed, we will focus more in the studies about microwave initiated carbonization process by irradiating conducting materials, instead of insulating materials. Although the methodologies in this direction are still under investigation, with much fewer published reports, there is great opportunity and potential in leading to newly designed advanced materials, and novel manufacturing systems.

We use an affordable and scalable microwave approach for the direct growth of CNT on a wide range of substrates, including carbon fibers, glass fibers, Kevlar, fly ash, Kaolin, and Basalt fibers. The microwave initiated CNT growth will take only 5-15 seconds under the microwave irradiation at room temperature in the air, no need of any inert gas protection, and additional feed stock gases, usually required in CVD approach. To the best of our knowledge, this is the world's record speed for CNT growth, and probably the only approach that can be done in ambient condition.

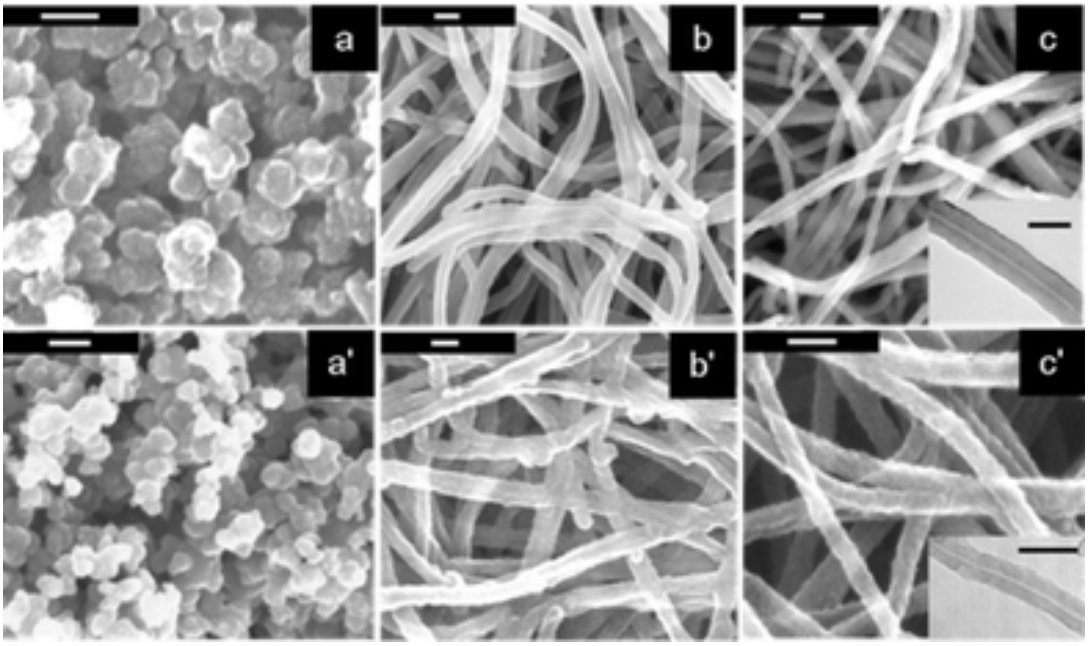

Fig. 5.1. Microwave synthesis of nanostructured carbon from doped polypyrrole. SEM images before (a,b,c) and after (a',b',c') microwave heating. Nanospheres (a/a'), Nanofibers (b/b'), Nanotubes (c/c'). Inset in c/c': TEM images showing nanotube with inner diameter. Scale: 100 nm.

As the skin depth is larger than the nano-dimension of the as-produced nanostructured conducting polymers, which also possess moderate conductivity (10^{-4}~10^{-2} Ω•m),[63] they can absorb microwave energy very efficiently without much

of reflection. This unique combination makes the nanostructured conducting polymers ideal precursors for rapid heating and conversion to nanocarbons. In our previous study, we have successfully demonstrated that conducting polypyrrole can be converted to graphitic carbon by microwave heating within 5 min.[33]

As shown in Figure 2, polypyrrole with granular, nanofibrillar and nanotubular morphologies were obtained through conventional synthesis, nanofiber seeding[60] and sacrificial template[62] approaches respectively. When irradiated with microwave, the conducting polypyrrole will be converted to nanocarbons, retaining the original morphologies of the precursors. During the microwave process, continuous sparks were observed due to electric discharge. It is the evidence of high electric field that has been generated by the microwave, between the tips or edges of the nanostructures. The high electric field leads to breakdown of the dielectric, i.e., air, and also the rapid temperature rise of the conducting polypyrrole.

Although started from room temperature, the conducting polypyrrole can be easily heated up to 800-1000ºC, or even higher, within a couple of seconds. Uniformity of the polypyrrole precursors in their dimensions and nanoscale features made it possible for homogeneous and fast heating, which resulted in quick nanocarbonization within a few minutes. The as-produced nanocarbons have a carbon composition well above 90%, which is comparable with the commercial activated carbons. Zoom-in images using high resolution transmission electron microscope (HRTEM) revealed the amorphous nature of the conducting polypyrrole precursor (Figure 3A), while after 3

min of microwave irradiation, graphitic carbon lattice was clearly shown (Figure 3B), which can be the evidence of this nanocarbonization process.

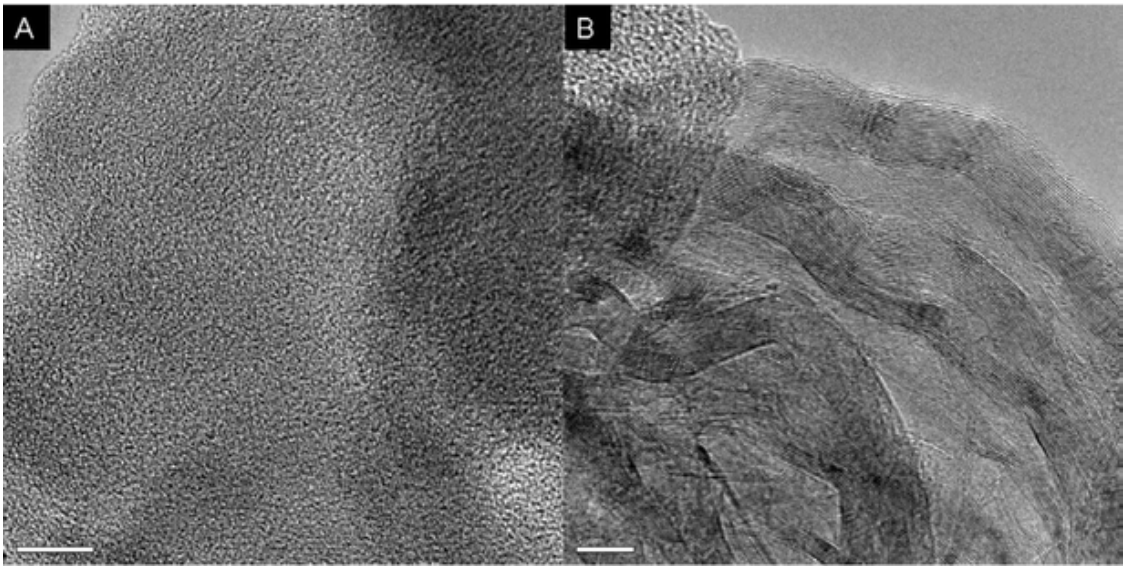

Fig. 5.2. Representative HRTEM images of polypyrrole.Cl nanospheres before (A) and after (B) microwave heating for 3 min. Scale: (A) 10 nm and (B) 5 nm.

The as-produced nanocarbons not only possess high purity, but also excellent thermal and electrochemical stabilities comparing to their conducting polymer precursors.Evidenced by thermogravimetric analysis (TGA) and cyclic voltammogram (CV) study, the nanocarbon started decomposing at much higher temperature comparing to its polypyrrole precursor, and the nanocarbon has almost no faradaic current during the CV process, i.e., there was no oxidation and reduction reaction took place whilesweeping the voltage.In addition to high quality nanocarbons, this approach can be used to convert conducting polymer-noble metal composites to nanocarbon supported noble metal composites, which possess better electrochemical catalytic properties.

The advantage of this microwave nanocarbonization process is obvious comparing to the conventional heating processes, which mainly involves time-consuming thermal/resistive heating process. Most of the thermal heating processes will take hours[1] or even days to complete the carbonization step, while the efficiency is also much lower than microwave heating.

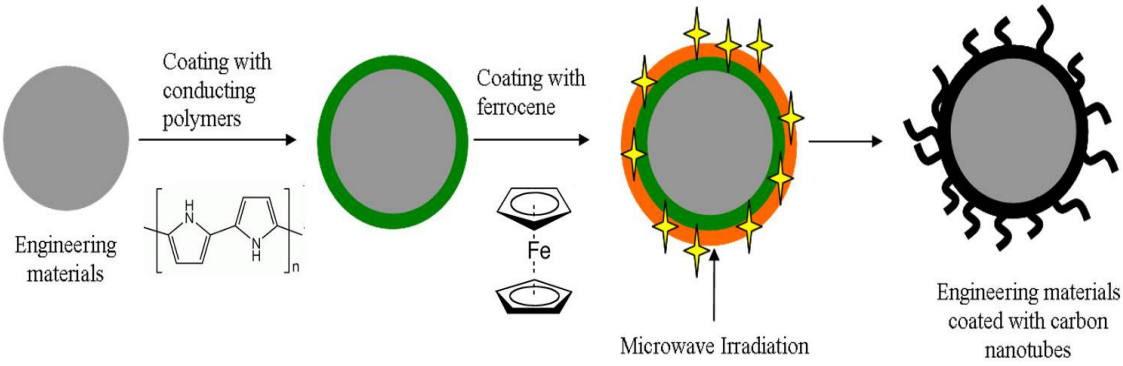

Scheme 5.1. Microwave initiated CNT growth on engineering materials

In a typical process, microwave Poptube precursors are prepared by decorating catalyst precursor, ferrocene,[13-15] on either stand-alone conductive materials (conducting polymers, ITO powders etc.) or conductive materials coated engineering materials (Scheme 1). Upon microwave irradiation to the Poptube precursors, the conductive materials will be heated to spark, arc and rapidly reach the temperature above 1100°C,[16,17] where the ferrocene will be decomposed to iron catalyst[18] and cyclopentadienyl, that could serve as the carbon source.

5.2. Experimental

5.2.1. Synthesis of Conductive Polypyrrole Coated Fly Ash

In a typical experiment, 1 g fly ash is dispersed in 60 mL 1M HCl under magnetically stirring for 10 min, pyrrole (0.24 M) was then added into the above dispersed glass fiber/HCl mixture suspension, keep stirring for 10 min, after that 0.03 M ammonium peroxydisulfate (APS) was added into the solution mixture and keep stirring for 4 hrs resulting in polypyrrole coated fly ash in the form of dark precipitates. The resulting black precipitate of polypyrrole coated fly ash was suction filtered, washed with copious amounts of aq. 1 M HCl (3 x 100 mL) and acetone (3 x 100 mL) and dried under freeze dry for 12 hrs. The yield of polypyrrole coated fly ash was ~1200 mg.

5.2.2. Synthesis of Conductive Polypyrrole Coated Glass Fiber

In a typical experiment, 1 g fine cut glass fibers (0.25mm average length each unit fiber) is dispersed in 60 mL 1M HCl under magnetically stirring for 10 min, pyrrole (0.24 M) was then added into the above dispersed glass fiber/HCl mixture suspension, keep stirring for 10 min, after that 0.03 M ammonium peroxydisulfate (APS) was added into the solution mixture and keep stirring for 4 hrs resulting in polypyrrole coated glass fiber in the form of dark precipitated polypyrrole coating on glass fibers. The resulting black precipitate of polypyrrole coated glass fiber was suction filtered, washed with copious amounts of aq. 1 M HCl (3 x 100 mL) and

acetone (3 x 100 mL) and dried under freeze dry for 12 hrs. The yield of polypyrrole coated glass fiber was ~1200 mg.

5.2.3. Synthesis of Conductive Polypyrrole Coated Glass Balloon

In a typical experiment, 1 g glass balloons (25 μm average diameter each unit balloon) is dispersed in 60 mL 1M HCl under magnetically stirring for 10 min, pyrrole (0.24 M) was then added into the above dispersed glass balloon/HCl mixture suspension, keep stirring for 10 min, after that 0.03 M ammonium peroxydisulfate (APS) was added into the solution mixture and keep stirring for 4 hrs resulting in polypyrrole coated glass balloon in the form of dark precipitated polypyrrole coating on glass balloon. The resulting black precipitate of polypyrrole coated glass balloon was suction filtered, washed with copious amounts of aq. 1 M HCl (3 x 100 mL) and acetone (3 x 100 mL) and dried under freeze dry for 12 hrs. The yield of polypyrrole coated glass balloon was ~1200 mg.

5.2.4. Solid state blending of conducting polymer coated fly ash with ferrocene

In a typical solid state powder blending experiment, polypyrrole coated fly ash was blended with same mass amount of ferrocene. 100 mg PPy coated fly ash was mixed with ferrocene granules, the mixture was sealed into a 10 mL plastic vial and rotated in speed mixer at the rotation speed of 3500 rpm for 5 min. The resulting mixture appeared to be dark yellow colored polymer coated fly ash with ferrocene.

5.2.5. Solid state blending of conducting polymer coated Glass Fiber with ferrocene

In a typical solid state powder blending experiment, polypyrrole coated glass fiber was blended with same mass amount of ferrocene. 100 mg PPy coated glass fiber was mixed with ferrocene granules, the mixture was sealed into a 10 mL plastic vial and rotated in speed mixer at the rotation speed of 3500 rpm for 5 min. The resulting mixture appeared to be dark yellow colored polymer coated glass fiber with ferrocene mixture.

5.2.6. Solid state blending of conducting polymer coated Glass Balloon with ferrocene

In a typical solid state powder blending experiment, polypyrrole coated glass balloon was blended with same mass amount of ferrocene. 100 mg PPy coated glass balloon was mixed with ferrocene granules, the mixture was sealed into a 10 mL plastic vial and rotated in speed mixer at the rotation speed of 3500 rpm for 5 min. The resulting mixture appeared to be dark yellow colored polymer coated balloon with ferrocene mixture.

5.2.7. Solid state blending of ITO nanopowder with ferrocene

In a typical solid state powder blending experiment, ITO nanopowder was blended with same mass amount of ferrocene. 100 mg ITO nanopowder was mixed with ferrocene granules, the mixture was sealed into a 10 mL plastic vial and rotated

in speed mixer at the rotation speed of 3500 rpm for 5 min. The resulting mixture appeared to be green-yellow colored ITO with ferrocene mixture.

5.2.8. Solid state blending of polypyrrole nanoclip with ferrocene

In a typical solid state powder blending experiment, polypyrrole nanoclip was blended with same mass amount of ferrocene. 100 mg polypyrrole nanoclip was mixed with ferrocene granules, the mixture was sealed into a 10 mL plastic vial and rotated in speed mixer at the rotation speed of 3500 rpm for 5 min. The resulting mixture appeared to be dark colored polypyrrole nanoclip with ferrocene mixture.

5.2.9. Microwave assisted of carbon nanotubes ultrafast growth from polypyrrole coated fly ash and ferrocene mixture heating

150 mg as-spinned polypyrrole coated fly ash and ferrocene mixture were placed in glass vials and then heated in a conventional microwave oven for 15 s. There was sharp sparking associated with light flame which appeared on mixture sample. Microwave heating is associated with dark smoke, which is attributed to the loss of backbone nitrogen atoms and dopant ions (Cl-). The yield product appeared to be dark colored soft carbon materials and fly ash residuals.

5.2.10. Microwave assisted of carbon nanotubes ultrafast growth from polypyrrole coated glass fiber and ferrocene mixture heating

150 mg as-spinned polypyrrole coated glass fiber and ferrocene mixture were placed in glass vials and then heated in a conventional microwave oven for 15 s. There was sharp sparking associated with light flame which appeared on mixture sample. Microwave heating is associated with dark smoke, which is attributed to the loss of backbone nitrogen atoms and dopant ions (Cl^-). The yield product appeared to be dark colored soft carbon materials with glass fiber residuals.

5.2.11. Microwave assisted of carbon nanotubes ultrafast growth from polypyrrole coated glass balloon and ferrocene mixture heating

150 mg as-spinned polypyrrole coated glass balloon and ferrocene mixture were placed in glass vials and then heated in a conventional microwave oven for 15 s. There was sharp sparking associated with light flame which appeared on mixture sample. Microwave heating is associated with dark smoke, which is attributed to the loss of backbone nitrogen atoms and dopant ions (Cl^-). The yield product appeared to be dark colored soft carbon materials with glass balloon residuals.

5.2.12. Microwave assisted of carbon nanotubes ultrafast growth from ITO and ferrocene mixture heating

150 mg as-spinned ITO nanopowder and ferrocene mixture were placed in a glass vials and then heated in a conventional microwave oven for 10 s. There was

sharp sparking associated with light flame which appeared on mixture sample. Microwave heating is associated with dark smoke. The yield product appeared to be yellow colored soft materials with ITO residuals.

5.2.13. Microwave assisted of carbon nanotubes ultrafast growth from polypyrrole clip and ferrocene mixture heating

150 mg as-spinned polypyrrole nanoclip and ferrocene mixture were placed in a glass vials and then heated in a conventional microwave oven for 10 s. There was sharp sparking associated with light flame which appeared on mixture sample. Microwave heating is associated with dark smoke, which is attributed to the loss of backbone nitrogen atoms and dopant ions (Cl-). The yield product appeared to be dark colored soft carbon materials with polypyrrole residuals

5.2.14. Fracture test sample preparation

To demonstrate the applicability of above method, carbon nanotubes were grown on glass micrballoons (Fig. 6.1) and used as filler to strengthen the mechanical characteristics of epoxy based conventional syntactic foam. The amino-silane (γ-aminopropyltrimethoxysilane) treated glass microballoons (XLD3000, from 3M Corporation, USA; true density 230 kg/m^3 and average diameter 30 microns) were employed for this purpose. The carbon nanotube grown microballoons were infused into the low viscosity epoxy (Epo-Thin, from Beuhler Inc., USA; Bisphenol-A resin and Amine based hardener; densities 1130 kg/m^3 and 961 kg/m^3, respectively) to

make a novel nanocomposite, called nano syntactic foam. To carry out the comparative static fracture study, syntactic foam (containing 15% microballoons by volume) and nano syntactic foam (containing equal amount of carbon nanotube grown microballoons as in case of syntactic foam) sheets were cast separately. Cast sheets were machined into test specimens of dimensions 76.2 mm X 22.0 mm X 8.7 mm. An edge notch of nominal length of 4.4 mm was introduced at mid span of each specimen using a high speed diamond impregnated circular saw. The tip of notch was sharpened using a razor blade.

Appendix: three-point bending test

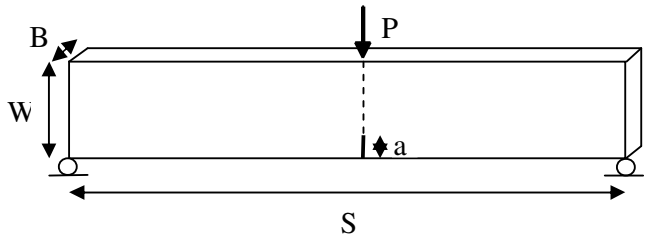

5.3. Results and Discussion

The SEM images revealed very different morphologies of the CNTs made from conductive

polypyrrole.Cl powder (PPy.Cl) and ITO nanopowders (Figure 5.3). Spaghetti-like, hollow CNTs were observed (Figure 5.3D), when conducting PPy.Cl was used as the heating layer,

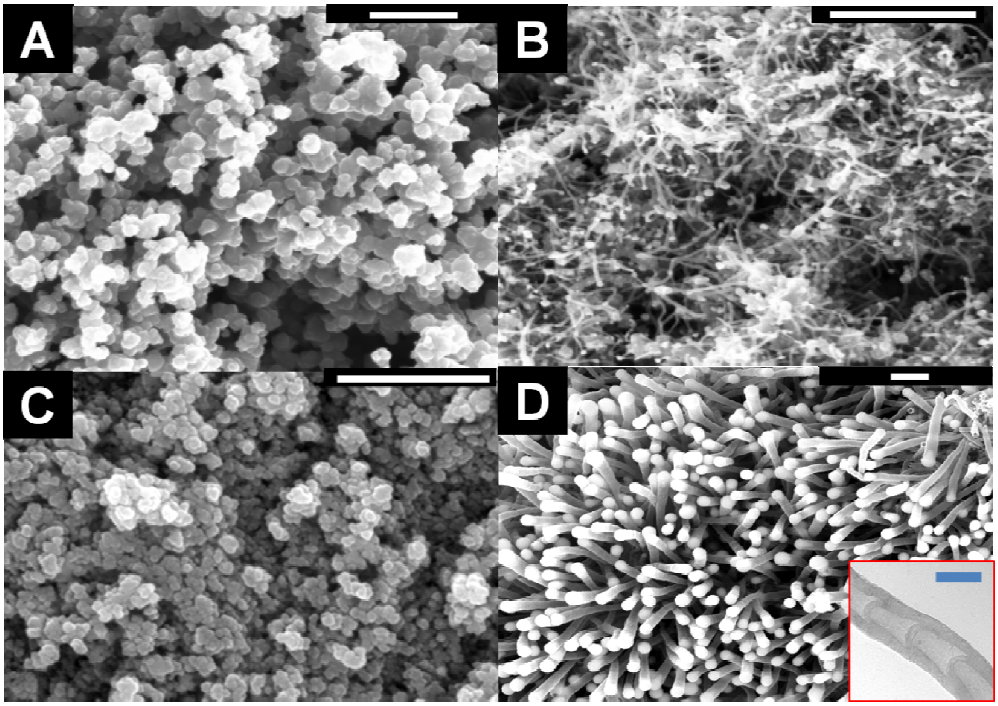

Figure 5.3. SEM images of (A) granular PPy.Cl; (B) CNTs grown on PPy.Cl granules; (C) ITO nanopowders; and (D) CNTs grown on ITO nanopowders (scale bar: 1 μm), inset: the TEM image of an individual CNT grown on ITO nanopowders (scale bar: 100 nm)

with outer diameter in the range of 30-50 nm. However, rod-like CNTs with bamboo-shaped inner hollow structures were obtained when ITO nanopowders were used as the heating layer (Figure 5.3D and the inset), having outer diameter in the range of 150-200 nm.

CNTs were observed (Figure 5.3B), when conducting PPy.Cl was used as the heating layer, with outer diameter in the range of 30-50 nm. However, rod-like CNTs with bamboo-shaped inner hollow structures were obtained when ITO nanopowders were used as the heating layer (Figure 5.3D and the inset), having outer diameter in the range of 150-200 nm.

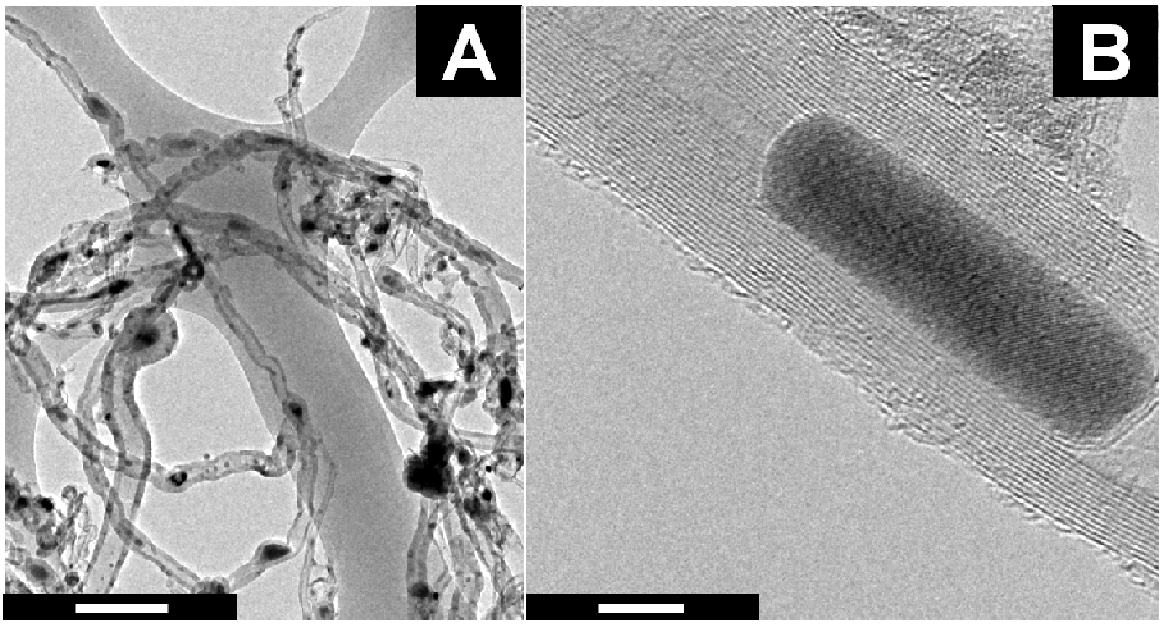

Figure 5.4. (A) TEM image of CNTs grown on PPy.Cl granules (scale bar: 200 nm); and (B) HRTEM of individual CNT with trapped Fe catalyst particle (scale bar: 5 nm)

The nature of the conducting layers could play significant role in controlling the morphology of the CNTs, e.g., the crystallinity and conductivity of the heating layers could affect the crystallinity and dimension of the iron catalyst nanoparticles. The multi-walled nature of the CNTs was evidenced by high resolution TEM (HRTEM, Figure 5.4B), confirming the CNTs are composed of ~20 layers of coaxially folded grapheme sheets.

Besides the stand-alone conductive materials such as PPy.Cl or ITO nanopowders, these multi-walled CNTs (MWNT) can also grow on a variety of engineering materials, which are either pre-coated with the conductive materials or intrinsically conductive such as carbon fibers. Actually, MWNTs were successfully grown on PPy.Cl coated fly ash powders, glass fibers, Kevlar, Basalt fibers, commercial 3M glass microballoons and carbon fibers through this Microwave Initiated Poptube (MIP) approach, using ferrocene and its derivatives as the catalyst and carbon source combo (Figure 3 and Figure S3 in supporting information). In this aspect, Poptube approach can be considered as a "Universal" method due to the diversity of the surfaces this method can apply.

With an attempt to see the scalability of the Poptube process, we carried out experiments with powder and fabric materials. Conducting PPy.Cl coated fly ash and glass fiber cloth were selected as the substrate materials. We could easily produce 10g powder of the fly ash-CNT nanocomposites using this Poptube approach within 10 minutes in the lab (Figure 6.3A inset), and make CNT coated glass fiber fabrics with dimension at 1 inch × 1 inch (Figure 6.3B inset), which depends on the size of the container in the microwave oven.

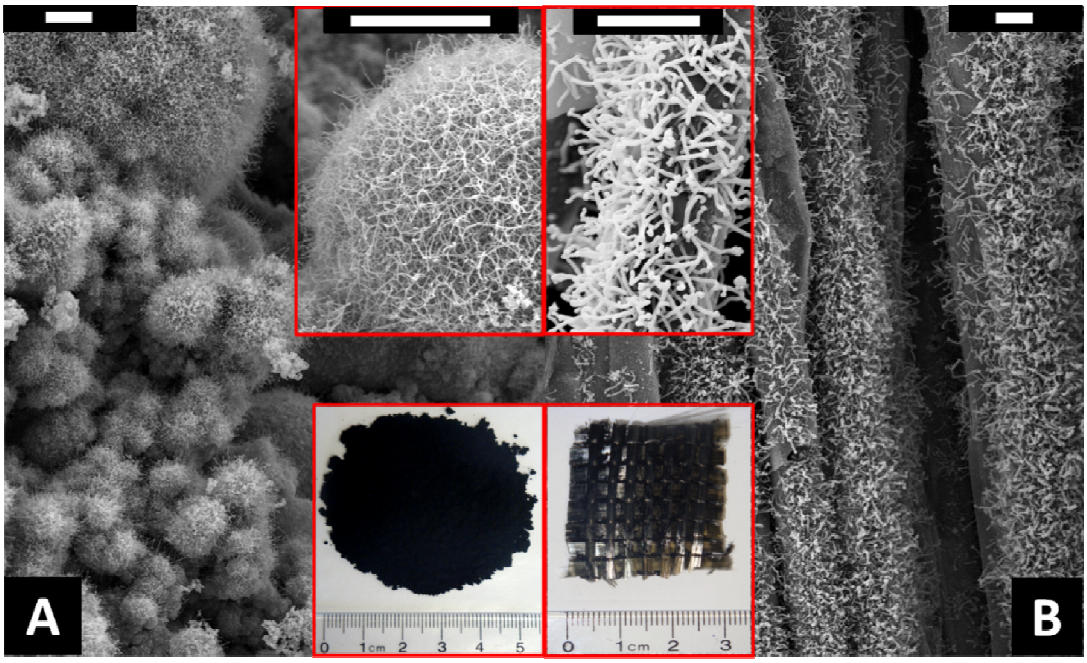

Figure 5.5. SEM images of as produced CNTs on (A) fly ash, insets: (top) zoom-in SEM image; (bottom) digital picture of 10 g fly ash coated with CNTs; and (B) glass fiber fabrics, inset: (top) zoom-in SEM image; (bottom) digital picture of 1 inch × 1 inch glass fiber fabric coated with CNT (scale bar: 5 µm)

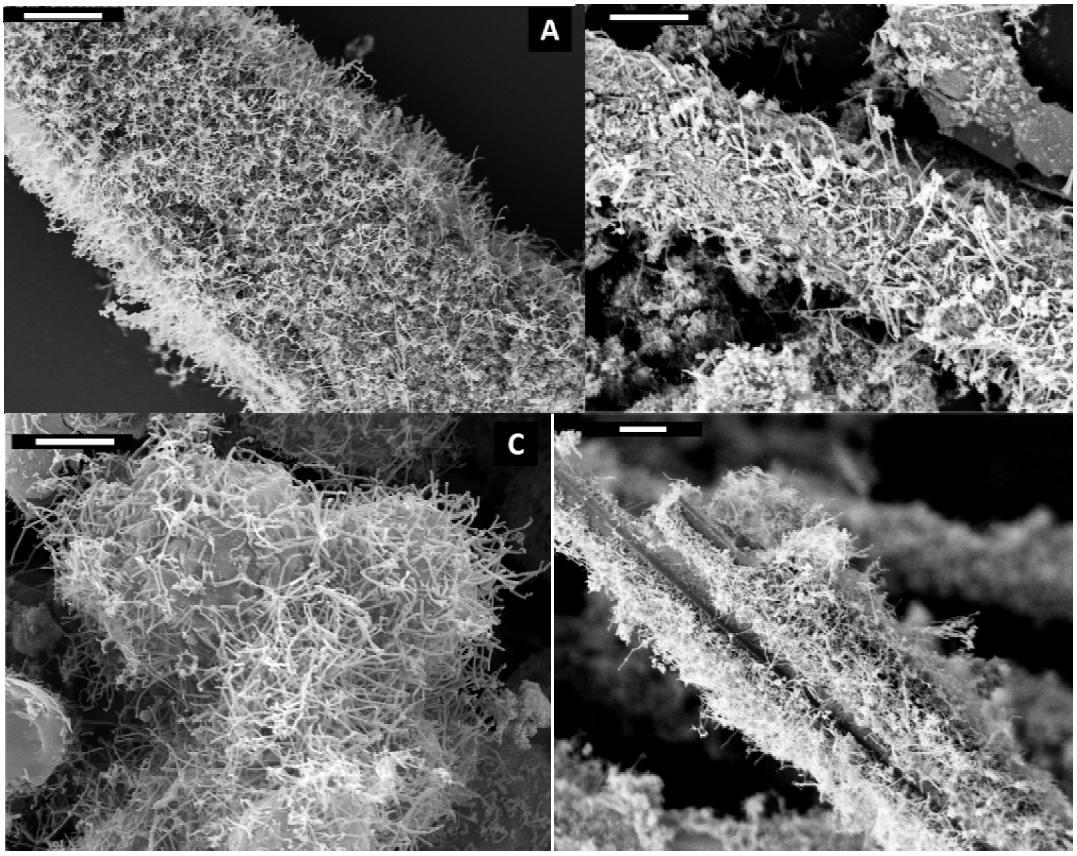

Figure 5.6. SEM images of CNT coated (A) Kevlar fiber, (B) Basalt fibers, (C) commercial 3M glass microballoons, and (D) carbon fibers

The mechanism of the CNT growth is still unclear, although a tip-growth model could be proposed for this Poptube process. This is confirmed by the electron microscope images, since most of the catalyst particles are either at the tip or middle part of the carbon nanotubes, indicating the CNT growth is following the tip-growth mode instead of base-growth mode.[19]

These CNT-decorated engineering materials can be used as multifunctional fillers into polymer matrix, or construction materials to build intelligent structures, in order to enhance the electrical and thermal conductivity and mechanical strength. To

demonstrate the applicability of this strategy, CNT decorated glass microballoons (Figure 6.4 inset) were used as filler to enhance the mechanical characteristics of epoxy based conventional syntactic foam (SF).[20] The CNT grown amino-silane treated glass microballoons were infused into the low viscosity epoxy resin to make a novel nanocomposite, called nano-syntactic foam (nano-SF). Static fracture studies were carried out for conventional SF and nano-SF, containing 15 vol. % undecorated/decorated microballoons respectively.

The three-point bending tests revealed an enhancement for the nano-SF in terms of critical fracture toughness and cross head displacement at ~17.0% and ~7.5%, respectively, compared to conventional SF. To assure the repeatability of experimental results, three specimens of each composite were tested under identical conditions. The results were repeatable within the error range of ~4.0%. This finding confirmed that direct growth of CNT will assist the improvement of the mechanical characteristics such as static toughness.

The three-point bending tests were performed at room temperature using Instron 4465 testing machine, under displacement control mode and a crosshead speed of 0.002 mm/sec was maintained during the tests. The load-displacement behavior (Fig. 2) remains linear until fracture, which proposes the failure to be brittle for syntactic as well as nano syntactic foams. The critical fracture toughness $(K_I)_{cr}$ at failure was computed using Eq. 1 [2].

$$K_I^{cr} = \frac{P_{cr} S}{B W^{3/2}} \left[2.9\left(\frac{a}{W}\right)^{1/2} - 4.6\left(\frac{a}{W}\right)^{3/2} + 21.8\left(\frac{a}{W}\right)^{5/2} - 37.6\left(\frac{a}{W}\right)^{7/2} + 38.7\left(\frac{a}{W}\right)^{9/2} \right]$$

(1)

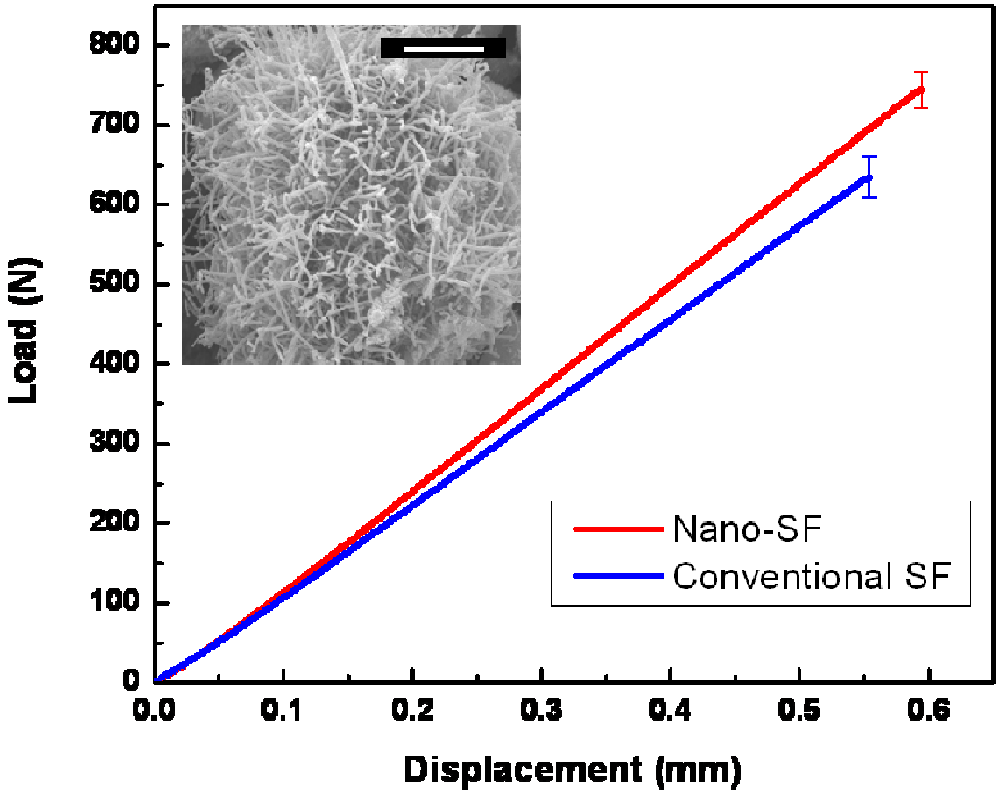

Figure 5.7. Load-displacement response for conventional SF and nano-SF. Inset: SEM image of the CNT decorated glass microballoon, scale bar: 10 µm)

where, $(K_I)_{cr}$ is critical fracture toughness for mode I fracture, P_{cr} is critical load at failure, a is notch length, B is thickness, S is span length and W is Width. The $(K_I)_{cr}$ values for syntactic and nano syntactic foam are 2.001± 0.050 MPa√m (at ultimate cross head displacement of 0.554± 0.024 mm) and 2.346± 0.064 MPa√m (at ultimate cross head displacement of 0.595± 0.030 mm) respectively. The introduction of carbon nanotube grown microballoons enhanced the critical fracture toughness and cross head displacement at fracture by ~17.0% and ~7.5%, respectively, compared to syntactic foam. To assure the repeatability of experimental results, three specimens of

each composite were tested under identical conditions. The results were repeatable within the error range of ~4.0%.

The length and the coverage density of the CNT on the conductive surfaces can be manipulated by either multi-step growth, or the addition of small organic molecules, such as hexane and pyridine.Multi-step growth is to repeat the PopTube process to the as-produced CNT coated engineering materials to enhance the CNT coverage density and length, which is confirmed by the SEM images (Fig. 5A and

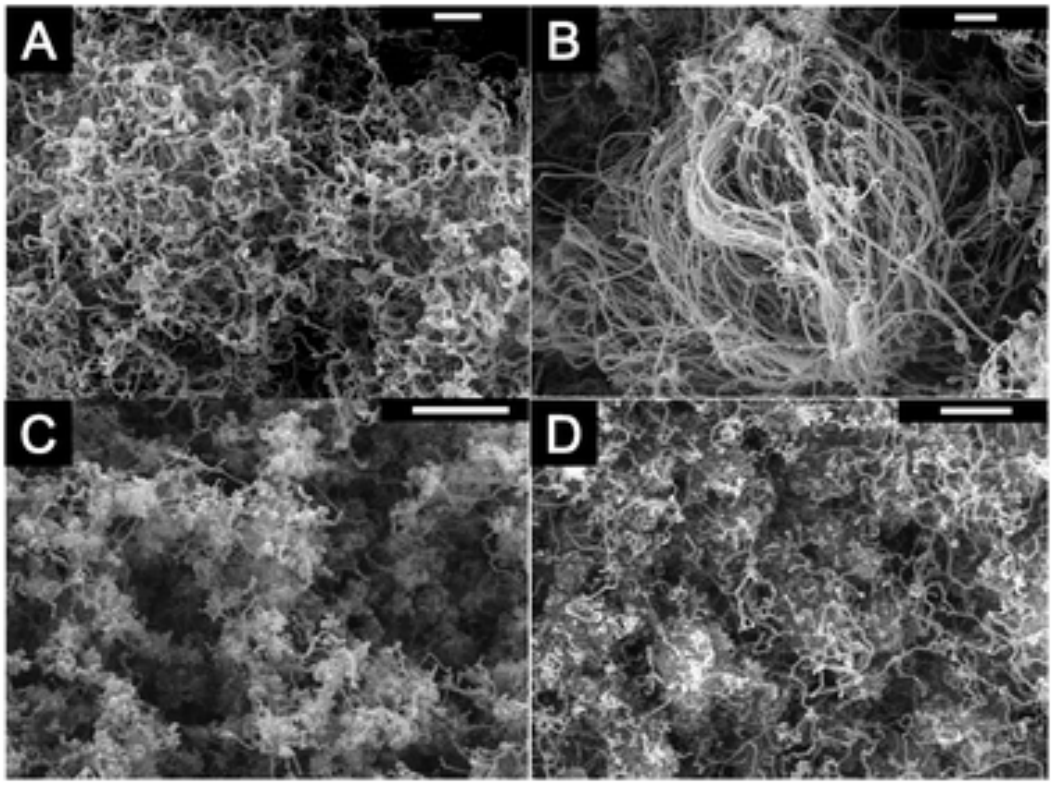

Figure 5.8. SEM images of CNT coated (A) polypyrrole coated fly ash via two step CNT growth method, (B) polypyrrole coated fly ashvia three step CNT growth method, (C) graphite powder and (D) graphite powder with addition of hexane(scale bar: 1μm) (Reproduced from ref. 70 with permission of RSC.)

B).The addition of hexane or other small molecules to improve the quality and length of CNT was reported previously using CVD approaches.[73,74]We have confirmed that this strategy is suitable for the microwave approach as well.

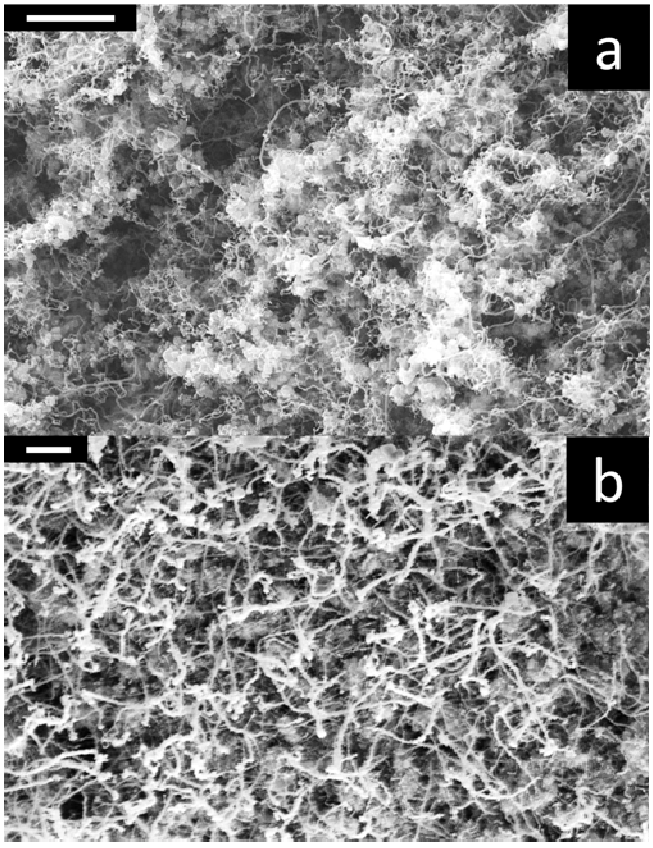

Figure 5.9. SEM images of CNTs made from polypyrrole coated substrates with (a) nickelocene, and (b) cobaltocene precursors (scale bar:

Besides high efficiency and low-cost, this PopTube approach can be considered as a "universal" method, in terms of the selection of organometallic precursors and the engineering material substrates on which CNT could grow. We have successfully demonstrated a variety of metallocenesas the precursors and a series of engineering materials as the substrates. As shown in Fig. 6A and B, cobaltocene and nickelocene were also selected as precursors and yielded similar results as ferrocene did. The substrates we have tried so far include polypyrrole coated insulating engieering materials such as fly ash powders, glass fibers, Kevlar, Basalt fibers, Kaolin powders, and glass microballoons, and conductive materials such as ITO, carbon fibers and graphite powders. PopTube approach opens a new era of nanoscale engineering of carbon materials, and will lead to significant change in future nanocarbon manufacturing systems, or even to the nanomaterials in general, such as nanostructured metal oxides and sulphides.

5.4. Conclusions

Described for the first time (i) ultrafast microwave approach to CNT growth in the air at room temperature within 5-15 seconds; (ii) CNTs can be directly grown on a wide selection of engineering materials including glass fibers, carbon fibers fly ash and glass microballoons etc.; (iii) the incorporation of CNT decorated glass microballoons enhanced the toughness of syntactic foam. This novel Poptube approach also provides a possible solution for the existing challenges in CNT applications, such as high cost, low dispersibility and small scale production. In addition, due to the high-efficiency and

selective heating of microwave irradiation, this Poptube method can be considered as a "green and sustainable" technology.

There are many advantageous features of using microwave technology for the manufacturing of nanostructured carbon materials, i.e., high efficiency in heating process, simplicity of the instrumentation and rapid carbonization reactions, which helps to save tremendous amount of time and energy. Or in other words, it will produce nanocarbons with much lower cost. Of course, there are some major hurdles preventing microwave technology producing nanocarbons with commercial-scale, well controlled size and shape.

As have seen in many of the previous reports including ours, the majority of the processes is still batch production, and the microwave heating of the conductive materials will raise the temperature to red hot (> 1000 °C) within a couple of seconds. Therefore, the existing challenges for the microwave initiate nanocarbonization include: (i) the manufacturing scale of the nanocarbons is not high enough; and (ii) the uniformity in size and shape of the nanocarbons remains at relatively low level.

To make nanocarbons with consistent quality for the real world applications, such as energy, composite or even construction industries, several steps have to be made to advance the nanocarbon industry.The first and critical step is to make continuous, instead of batch mode, manufacturing of nanocarbons. Due to the requirements of inert gas/vacuum protection and/or high temperature or current densityin the well-developed existing

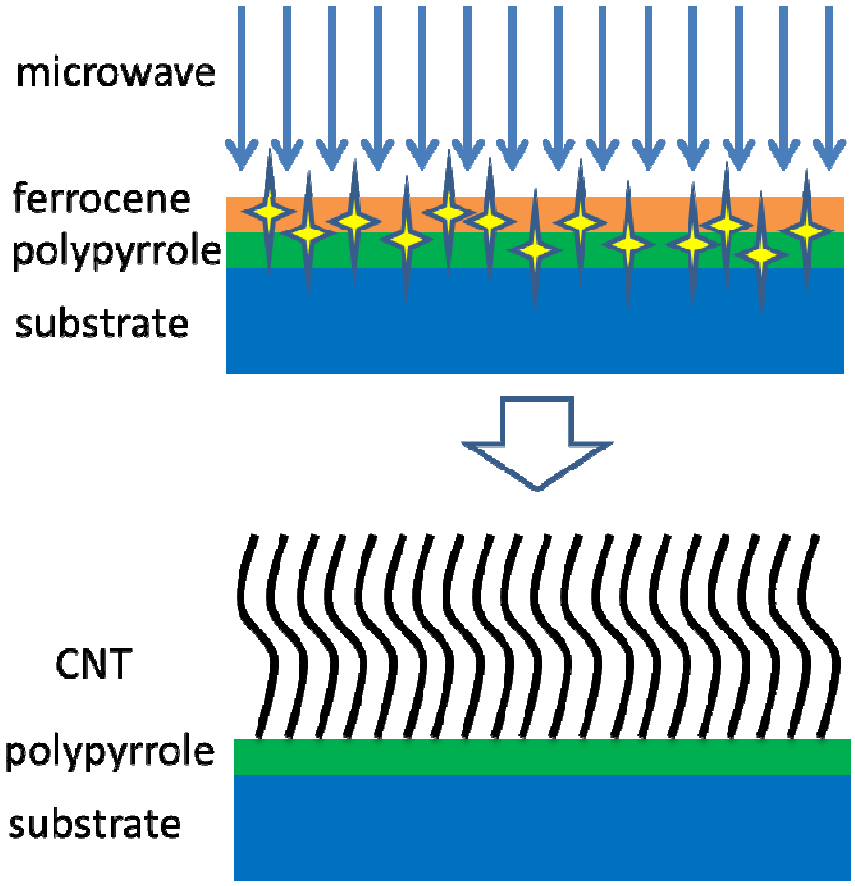

Scheme 5.2. Microwave initiated CNT growth on conductive surfaces

approaches, such as CVD, arc-discharge and conventional thermal heating methods, it is necessary for these systems to be nicely sealed and insulated, and makes it difficult to establish a continuous mode production in these systems. While microwave related techniques will take the advantages that the microwave oven is relatively simple in design, and some of the reactions can be done in the air, as mentioned in the PopTube and microwave arcing approaches. A continuous microwave process for nanocarbon manufacturing will not only benefit the fundamental scientific researches, but also

pave the road towards large-scale, commercializable products for the future composite, catalyst, energy and construction industries.

Another crucial step is to manipulate the shape and size of the as-produced nanocarbons. There are many different attempts in the existing methods, especially CVD method, to control the length, diameter and helicity of the nanocarbons to fit different application purposes. These attempts include addition of the small molecules, control of the catalyst size and crystalline structures, changing reaction parameters such as temperature and feeding stock ratio etc. All of these previous successes will be readily adapted in the microwave system. Actually, hexane has been confirmed to be able to improve the length of the CNTs and their coverage on the substrates.[70] It can be envisioned that large-scale production and better quality control can be achieved for the manufacturing of nanocarbons in the near future.

5.5 References

(1) Iijima, S. *Nature (London, United Kingdom)* **1991**, *354*, 56-8.

(2) Dalton Alan, B.; Collins, S.; Munoz, E.; Razal Joselito, M.; Ebron Von, H.; Ferraris John, P.; Coleman Jonathan, N.; Kim Bog, G.; Baughman Ray, H. *Nature* **2003**, *423*, 703.

(3) Rakesh, L.; Howell, B. A.; Chai, M.; Mueller, A.; Kujawski, M.; Fan, D.; Ravi, S.; Slominski, C. *Nanomedicine (London, U. K.)* **2008**, *3*, 719-739.

(4) Kong, J.; Franklin, N. R.; Zhou, C.; Chapline, M. G.; Peng, S.; Cho, K.; Dailt, H. *Science (Washington, D. C.)* **2000**, *287*, 622-625.

(5) Baughman, R. H.; Zakhidov, A. A.; de Heer, W. A. *Science* **2002**, *297*, 787-792.

(6) Rinzler, A. G. *Nat. Nanotechnol.* **2006**, *1*, 17-18.

(7) Journet, C.; Maser, W. K.; Bernier, P.; Loiseau, A.; Lamy de la Chapells, M.; Lefrant, S.; Deniard, P.; Lee, R.; Fischer, J. E. *Nature (London) FIELD Full Journal Title:Nature (London)* **1997**, *388*, 756-758.

(8) Fischer, J. E.; Dai, H.; Thess, A.; Lee, R.; Hanjani, N. M.; Dehaas, D. L.; Smalley, R. E. *Physical Review B: Condensed Matter* **1997**, *55*, R4921-R4924.

(9) Baykal, B.; Ibrahimova, V.; Er, G.; Bengue, E.; Tuncel, D. *Chem. Commun. (Cambridge, U. K.)* **2010**, *46*, 6762-6764.

(10) Abusch-Magder, D.; Someya, T.; Wang, J.; Laskowski, E.; Dodabalapur, A.; Bao, Z.; Tennant, D. M. *Los Alamos National Laboratory, Preprint Archive, Condensed Matter* **2002**, 1-15, arXiv:cond-mat/0210332.

(11) Fraczek-Szczypta, A.; Bogun, M.; Blazewicz, S. *Journal of Materials Science* **2009**, *44*, 4721-4727.

(12) Zhao, J.; Liu, L.; Guo, Q.; Shi, J.; Zhai, G.; Song, J.; Liu, Z. *Carbon* **2008**, *46*, 380-383.

(13) Gui, X.; Wei, J.; Wang, K.; Cao, A.; Zhu, H.; Jia, Y.; Shu, Q.; Wu, D. *Advanced Materials (Weinheim, Germany)* **2010**, *22*, 617-621.

(14) Li, Y.-L.; Kinloch, I. A.; Windle, A. H. *Science (Washington, DC, United States)* **2004**, *304*, 276-278.

(15) Shiozawa, H.; Pichler, T.; Grueneis, A.; Pfeiffer, R.; Kuzmany, H.; Liu, Z.; Suenaga, K.; Kataura, H. *Advanced Materials (Weinheim, Germany)* **2008**, *20*, 1443-1449.

(16) Hsin, Y.-L.; Lin, C.-F.; Liang, Y.-C.; Hwang, K. C.; Horng, J.-C.; Ho, J.-a. A.; Lin, C.-C.; Hwu, J. R. *Adv. Funct. Mater. FIELD Full Journal Title:Advanced Functional Materials* **2008**, *18*, 2048-2056.

(17) Zhang, X.; Manohar Sanjeev, K. *Chemical communications (Cambridge, England)* **2006**, 2477-9.

(18) Anisimov, A. S.; Nasibulin, A. G.; Jiang, H.; Launois, P.; Cambedouzou, J.; Shandakov, S. D.; Kauppinen, E. I. *Carbon FIELD Full Journal Title:Carbon* **2009**, *48*, 380-388.

(19) Ci, L. J.; Zhao, Z. G.; Bai, J. B. *Carbon FIELD Full Journal Title:Carbon* **2005**, *43*, 883-886.

(20) Kim, H. S.; Oh, H. H. *J. Appl. Polym. Sci.* **2000**, *76*, 1324-1328.

Chapter 6

Conclusions

In summary, five individual projects projected from the center subject “electric conducting nanomaterials” have been established to present the novel and timely synthesis of nanostructured conducting polymer and achieve well confined 0D (nanosphere), 1D (nanofibers), 2D (nanolips) and 3D (networks) growth orientations. Also, microwave irradiation as common practice in our daily life, has been rediscovered as a novel fabrication approach to initiate ultrafast carbon nanotube growth.

It is experimentally established that the nano-feature has proliferated unique performance of conducting materials with the reinforcement of chemical, physic and biological properties compared to the one in bulk state.

Conducting polymer nanoclips has six-fold increment in specific capacitance than bulk polymers, which can be applied as next generation energy storage device.

Polypyrrole based nanomaterials and nanocomposites can be achieved synthetically by concise seeding methods in various medium, which can afford to yield multifunctional nanocomposites and serve as toolbox for the flexible electrochemistry sensory electrodes fabrications.

Microwave initiated ultrafast carbon nanotube growth, as a simple and novel approach, provides a possible solution for the existing challenges in CNT applications, such as high cost, low dispersibility and small scale production. In addition, due to the high-efficiency and selective heating of microwave irradiation, this Poptube method can be considered as a “green and sustainable” technology.